UNIVERSITY OF LONDON THESIS

Degree PhD Year 2005 Name of Author CHANG

Regulation of Viability in Corneal Endothelial Cells

Giulia Chan

Division of Cell Biology
Institute of Ophthalmology
University College London
11-43 Bath Street
London EC1V 9EL

Thesis submitted to the University of London for the degree of Doctor of Philosophy

December 2004

ProQuest LLC
789 East Eisenhower Parkway
P.O. Box 1346
Ann Arbor, MI 48106-1346

Abstract

The major cause of corneal opacity and resultant visual loss is a critical decrease in corneal endothelial cell density. Due to the fact that corneal endothelial cells do not generally proliferate, cell densities gradually decrease in the corneal endothelium with age. Before we can begin to aid patients with decreasing endothelial cell densities, by inhibiting cell death or stimulating cell proliferation, it is necessary to understand the basic cell signalling that underlies these processes. As human tissue is difficult to obtain, a representative animal model of corneal endothelium was devised. Analysis of cell morphology and expression of α1 type VIII collagen were used to verify that primary cells derived from an explant model of mouse corneal cells were endothelial. A range of phenotypic and functional cellular features were also analysed to assess the usefulness of primary mouse corneal endothelial cultures as a model for human corneal endothelium. These included tight junction protein localization, proliferative responses to growth factor stimulation and ERK1/2 activation following growth factor stimulation. From these analyses, it was shown that primary mouse corneal endothelial cultures provide a representative model of the human corneal endothelium.

A similar comparison was also made between primary mouse corneal endothelial cultures and an SV40 transformed mouse corneal endothelial cell line. Studies revealed significant differences in propensity to proliferate, junctional integrity, ERK1/2 activation, expression of apoptotic proteins and sensitivity to staurosporine-induced apoptosis between primary cells and the SV40 transformed cell line, suggesting that the SV40 transformed cell line is a less appropriate model for primary mouse corneal endothelial cells.

In conclusion, the derivation and characterisation of mouse primary corneal endothelial cells provides a better model of the corneal endothelium, that offers greater understanding of cellular responses and which may eventually lead to the development of alternative therapies for primary corneal endotheliopathies.

Acknowledgements

I would like to thank my two supervisors Prof. Steve Moss and Dr. Frank Larkin for giving me the opportunity to do my Ph.D. at the Institute of Ophthalmology and for their guidance along the way. This project would not have been possible without funding from Mr.& Mrs. Frankenburg, who funded my studentship, Fight for Sight, the charity responsible for allocating the studentship and the Overseas Research Studentship, for helping with my tuition fees. Additional funding from the Bogue fellowship and the kindness of Dr. Nancy Joyce and her lab were instrumental to the work in human tissue.

Thanks also to everyone in the Department of Cell Biology, who have been so supportive and helped to make my time at the Institute so wonderful, especially Chris, Dr. Karl Matter and Dr. Marisu Balda, who always made themselves available to help answer any questions I had. The Metro crossword, coffee mornings, pub lunches, etc... have meant that I have learnt so much more than science from my time at the Institute.

Last but not least, thanks to my family at home in Canada, who have supported me through everything I've ever wanted to do.

Table of Contents

List of Figures

List of Tables

List of Abbreviations

AD	Autosomal Dominant
AGE	Advanced Glycation End products
AJ	Adherens Junction
AR	Autosomal Recessive
ATPase	Adenosine Triphosphatase
BH	Bcl-2 Homology
BIR	Baculovirus Inhibitor of apoptosis proteins Repeat
bp	base pairs
BSE	Bovine Spongiform Encephalopathy
CAR	Coxsackie- and Adeno-virus Receptor
CARD	Caspase-Associated Recruitment Domain
CDK	Cyclin-Dependent Kinase
CHED	Congenital Hereditary Endothelial Dystrophy
CKI	Cyclin-dependent Kinase Inhibitor
DD	Death Domain
DED	Death Effector Domain
ECM	Extracellular Matrix
EDTA	Ethylenediaminetetraacetic Acid
EGF	Epidermal Growth Factor
ER	Endoplasmic Reticulum
ERK	Extracellular signal Regulated Kinase
ESAM	Endothelial cell-Selective Adhesion Molecule
FCS	Fetal Calf Serum
FGF-2	Fibroblast Growth Factor-2
GAG	Glycosaminoglycan
HGF	Hepatocyte Growth Factor
IAP	Inhibitor of Apoptosis Proteins
ICE	Iridocorneal Endothelial
IGF	Insulin-like Growth Factor

IL	Interleukin
JAM-A	Junctiona Adhesion Molecule-A
kDa	kilodaltons
LPS	Lipopolysaccharide
NC1	non-triple helical domain
NF-κB	Nuclear Factor-κB
MAGUK	Membrane-Associated Guanylate Kinase
MAPK	Mitogen Activated Protein Kinase
MDCK	Madine-Darby Canine Kidney
MEK	Mitogen Activated Protein Kinase Kinase
PAF	Platelet Activating Factor
PAGE	Polyacrylamide Gel Electrophoresis
PBS	Phosphate Buffered Saline
PCR	Polymerase Chain Reaction
PDGF BB	Platelet-Derived Growth Factor BB
PDZ domain	Postsynaptic density protein/Disc large-A/ZO-1 domain
PI3 kinase	Phosphatidylinositol 3 kinase
PI3P	Phosphatidylinositol 3 Phosphate
PKA	Protein Kinase A
PKC	Protein Kinase C
PLC	Phospholipase C
PPD	Posterior Polymorphous Dystrophy
RAGE	Receptor for Advanced Glycation End products
RT-PCR	Reverse Transcriptase Polymerase Chain Reaction
SH3 domain	Src homology 3 domain
SOD	Superoxide Dismutase
SPARC	Secreted Protein, Acidic and Rich in Cystein
SV40	Siminian virus 40
TGF	Transforming Growth Factor
TJ	Tight Junction
TNF	Tumor Necrosis Factor

ZO	Zonula Occludin
ZONAB	ZO-1-associated Nucleic Acid Binding protein

Chapter 1: Introduction

1.1 The cornea

The cornea is a multicomponent, transparent, avascular tissue with a smooth surface and uniform curvature, found at the anterior of the eye. The structure of the cornea sheds light on the diverse functions of the tissue, which include transparency, light refraction, containment of intraocular pressure and protection from the external environment (Bron et al., 2001). The specialized organisation of the cornea allows it to perform all these functions in the absence of blood vessels.

The main function of the cornea is optical as it forms the principal refractive surface, accounting for 70% (40-45 diopters) of the total refractive power of the eye. Refraction is accomplished through the regular curvature of the cornea and the optically smooth overlying tear film. Most of the total refraction within the eye takes place at the surface of the cornea at the tear/air interface (Bron et al., 2001). Deeper into the middle of the cornea lies the corneal stroma. The collagenous base of the corneal stroma allows the cornea to provide resistance to ocular pressure and also provides a protective layer. Closeness, regularity and the homogeneity of the packing of the collagen fibrils within the corneal stroma are also responsible for corneal transparency (Waring, III et al., 1982; Bron et al., 2001; Meek and Boote, 2004). The perpendicular packing of the collagen fibrils within the stroma is maintained by regulation of corneal hydration. Stromal water content is controlled by pump actions of the corneal endothelium, preventing stromal swelling and corneal clouding (Waring, III et al., 1982; Kenney et al., 1986; Bron et al., 2001).

The curvature of the cornea is slightly greater than that of the sclera so as to produce a slight furrow between the cornea and the sclera, the sulcus sclerae (Bron et al., 2001). The overlying tear film aids in the identification of this furrow within the living eye. The overlapping sclera may be greater above and below the cornea than it is laterally, helping to explain the elliptical, frontal appearance

of the cornea. The horizontal meridian of the cornea is slightly greater than the vertical meridian. The central third of the cornea is typically referred to as the optical zone and is almost spherical, and the peripheral cornea becomes progressively flatter as it encounters the sclera (Arffa, 1997; Bron et al., 2001). This results in a variance of the radius of curvature between the anterior and posterior sections of the cornea, with the anterior surface having a greater radius of curvature. Overall, the surface area of the cornea composes one-sixth the surface area of the entire eye globe, with that of males being slightly larger than females (Bron et al., 2001).

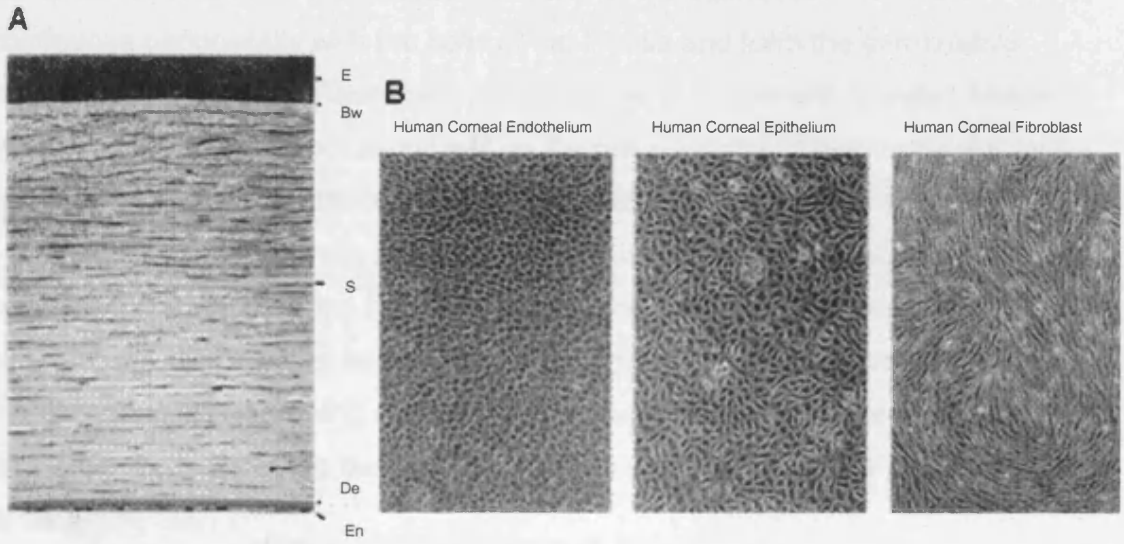

Figure 1.1 Cell types of the human cornea. Cross section of the cornea (A) reveals outer, epithelial cell layers (E), Bowman's layer (Bw), the stroma (St), which makes up the majority of the tissue, Descemet's membrane (De) and the endothelial cell monolayer (En). The morphology of each of the corneal cell types is distinct in cell culture conditions (B). Both endothelial and epithelial cells form monolayers of polygonal cells, however, their appearances are distinguishable. Corneal fibroblasts are elongated and form a swirling pattern in culture. (images from: Joyce 2003. Proliferative capacity of the corneal endothelium. Prog.Retin.Eye Res. 22:361&380)

There are 5 major tissue layers that make up the cornea beneath the precorneal film (Figure 1.1). Each of these layers is further detailed below.

i. Epithelium
ii. Bowman's layer
iii. Stroma
iv. Descemet's membrane
v. Endothelium

1.1.1 Corneal epithelium

The corneal epithelium is stratified, squamous and non-keratinized. The epithelium is continuous with the conjunctiva at the corneal limbus and is composed of three types of cells, typically forming five or six layers of nucleated cells. Basal cells form the deepest cell layer of the epithelium. They are continuous peripherally with the cells of the limbus and form the germinative layer of the epithelium. Basal cells are columnar in shape with rounded heads and flat bases, and perfect alignment on the basal lamina. Their nuclei are oval and oriented parallel to the cells' long axis (Pfister and Burnstein, 1977).

'Wing' or 'umbrella' cells make up the next layers of the epithelium. These polyhedral cells sit atop the basal cells and send processes between them (Bron et al., 2001). Their nuclei lie parallel to the surface and there is extensive interdigitation between wing cells with numerous desmosomal attachments. The closer the wing cell to the basal layer the more columnar in shape the cell tends to be (Arffa, 1997).

The most exterior two or three cell layers are also polyhedral and become wider and flattened towards the surface. Surface cells have the largest surface area, with cells at the periphery having the greatest surface area. Their flattened nuclei typically project backwards, leaving the surface smooth (Arffa, 1997; Bron et al., 2001). Superficial cells attach to each other by straight cell boundaries but have numerous microprojections and an extensive fibrillar glycocalyx on the surface membrane. These aid in the adherence of tear film to the glycocalyx (Arffa, 1997). Tight junctions along the circumference of contiguous cells prevent the passage of substances into the intercellular spaces (Ban et al., 2003).

Epithelial cells tend to be actively metabolising cells and as such contain organelles typical of active cells. Mitochondria are small and scarce in the basal cell layer, which is primarily germinative, but are more abundant in the wing and middle cell layers. The Golgi apparatus and rough endoplasmic reticulum of corneal epithelial cells are relatively small (Pfister and Burnstein, 1977). Electron-dense tonofibrils form a cytoplasmic meshwork within the cells similar to other epithelia composed of cytokeratins. Wing and basal cells possess numerous tonofibrils and basal cells also contain anchoring filaments which pass through the hemidesmosomal structures and inserted directly into the underlying basal lamina. Plasma membranes of contiguous cells interdigitate with their neighbours with an intervening space of no more than 20nm. Desmosomes form the majority of junctions between epithelial cells, presumably because they are labile so as to allow movement over time as the cells migrate to the surface of the cornea (Arffa, 1997; Bron et al., 2001). Superficial cells are the only cell layers to show tight junctions. The most superficial of these are hexagonal and firmly attached to each other by straight cell boundaries (Ban et al., 2003). These cells also show surface microvilli, which may serve to stabilize deep precorneal tear film. The density of microvilli has been shown to be variable by scanning electron microscopy with cells of darker appearance proposed to be older and ready to desquamate (Sellheyer and Spitznas, 1988).

Occasionally, dendritic cells have also been noted within the superficial layers of the corneal epithelium. These members of the immune recognition system are thought to be responsible for the processing and presentation of foreign antigens to lymphocytes (Arffa, 1997; Bron et al., 2001). The majority of these cells remain along the periphery of the cornea and only migrate into the central corneal region in response to disease.

The basal lamina or basement membrane lies beneath and is produced by the basal layer of epithelial cells. Its composition makes it an irregular zone with a posterior lamina densa and a superficial lamina lucida. These two zones can be distinguished ultrastructurally. The components of the basal lamina are similar to those of skin, containing type IV collagen, laminin, fibronectin, fibrin and

bullous pemphigoid antigen (Arffa, 1997; Bron et al., 2001). Basal epithelial cells are anchored to the lamina by the hemidesmosome, which consists of an electron-dense attachment plaque. Electron-dense anchoring fibrils, composed of type VII collagen, form narrow bundles and insert into the subjacent stroma or Bowman's layer to terminate in anchoring plaques, composed of type IV and type VII collagen (Arffa, 1997; Bron et al., 2001). This arrangement allows for the tight adherence of the basal epithelium to the cornea.

Epithelial cell migration occurs centripetally across the corneal surface. Basal and wing cells slide toward the central cornea, as well as towards the surface, where desquamation occurs (Arffa, 1997). Thoft and Friend (1983) proposed that the higher mitotic rate and lower superficial cell slough rate in the corneal periphery relative to the central cornea was responsible for the centripetal sliding of basal epithelial cells. Epithelial stem cells are located in the limbal region and are thought to give rise to a transient amplifying cell population, which move centrally and become fully differentiated (Arffa, 1997; Chung et al., 1999). The rate of migration of cells is believed to be quite slow with migration from the limbus to the central cornea taking up to a year (Bron et al., 2001). During wound healing, the opposite effect is noted. Epithelial cells distal to the wound enhance their proliferative rate, however, cells migrating to cover the wound decrease their proliferation to almost zero (Chung et al., 1999). Of all the cells that make up the cornea, the epithelial cells are the only ones which are known to be actively continually cycling.

1.1.2 Bowman's layer (anterior limiting lamina)

Bowman's layer is a narrow, acellular zone, 8-14μm in thickness. Though the layer appears homogeneous, electron microscopy reveals a randomly arranged meshwork of short collagen fibrils in a ground substance. Collagen fibril diameter in Bowman's layer is smaller than in the stroma but in the posterior region, the fibrils become progressively larger in diameter and more ordered to blend and interweave with the fibrils of the anterior stroma (Jacobsen et al., 1984). The compacted arrangement lends strength to this region of the cornea.

Bowman's layer is relatively resistant to trauma, mechanical and infective, but once it is destroyed it is not renewed. A thin layer with a structure similar to Bowman's layer is formed during wound healing but it does not regain its original thickness (Arffa, 1997). Bundles of stromal lamellae randomly insert into the Bowman's layer, as do unmyelinated nerves in transit to the epithelium (Bron et al., 2001). At normal or raised intraocular pressure, Bowman's layer is under tension and appears smooth. When surface tension is relaxed, however, a series of convex ridges can be generated at its surface. The ridges correspond to the stromal bundles inserted into Bowman's layer which form a polygonal pattern (Jacobsen et al., 1984).

Bowman's layer was previously thought to be a specialized corneal membrane but is now recognized as a modified region of the anterior stroma. While the smooth, anterior surface borders the basal lamina of the epithelium, the posterior surface meshes into the corneal stroma.

1.1.3 Corneal stroma (substantia propria)

The stroma constitutes approximately 90% of the entire cornea. It is typically 500μm thick and consists of regularly arranged lamellae of collagen bundles, 200-300 centrally and 500 in the periphery (Meek and Boote, 2004). The collagen bundles lie in a proteoglycan ground substance and interspersed between the collagen bundles lies a small population of cells known as keratocytes. Lamellae of the stroma are arranged in layers parallel to each other and with the corneal surfaces. Generally, they run from limbus to limbus although in the anterior third of the stroma, there is interweave with the fibrils of the Bowman's layer (Jacobsen et al., 1984; Meek and Boote, 2004). Deeper in the stroma, lamellae form strap-like ribbons which run at almost right angles to those in consecutive layers (Müller et al., 2004).

Each stromal lamella comprises a band of collagen fibrils arranged in parallel. This banding pattern is most apparent by negative staining following the removal of proteoglycan (Bron et al., 2001). Cross-section reveals that the individual fibrils are composed of subunits of very fine fibrils (Arffa, 1997). Fibrils of type I

collagen are the most common within the stroma but type V and type VI collagen comprise 10% and 25% respectively of the total. It is also thought that type III collagen may be present in small amounts (Arffa, 1997). Collagen in the stroma is fairly stable with little annual turnover. It is the precise ordering of the collagen fibrils within the cornea which is responsible for corneal transparency.

As previously mentioned, stromal collagens are contained within a ground substance composed primarily of proteoglycans. Proteoglycans are a type of glycoprotein composed of non collagenous protein chains with covalently bound oligosaccharides and glycosaminoglycan (GAG) side chains. The primary GAGs of the corneal stroma are keratan sulphate and chondroitin sulphate in approximately 3:1 ratio (Muller et al., 2004). Decorin is the core protein that contains the chondroitin /dermatan sulphate chains, while lumican is the core protein containing keratan sulphate. These ground substances are thought to play a role in maintaining the regular arrangement of the collagen fibrils, as both decorin and lumican inhibit fibril diameter growth. Even during stromal swelling and oedema, individual collagen fibril size does not change but the volume of ground substance increases, thus increasing the space between collagen fibrils (Danielson et al., 1997; Song et al., 2003).

The predominant cell population of the corneal stroma is the keratocytes, which occupies between 2.5-5% of its volume. Keratocytes are responsible for the synthesis of stromal collagen and proteoglycan during development, and maintenance thereafter (Bron et al., 2001). They are large, thin, flattened cells that run parallel to the corneal surface. Viewed from the corneal surface, the cells appear with many tangential projections extending out of the cell body in stellate fashion. Keratocytes are dispersed throughout the entire cornea, predominantly between the stromal lamellae, with only occasional keratocytes found within lamellae (Møller-Pedersen and Ehlers, 1995). Stellate processes extend between the lamellae and frequent contacts are made with other keratocytes in the same horizontal plane. Contacts are made between keratocytes with a 20nm gap or with the formation of maculae occludentes, adherens or gap junctions (Watsky, 1995). Connections between keratocytes in

adjacent planes do not occur. Within the cell, there is a long, flattened nucleus surrounded by a complement of organelles that are few in number and sparsely distributed. The rough endoplasmic reticulum and Golgi are normally limited but become extensive in activated keratocytes of injured corneas (Arffa, 1997; Bron et al., 2001). Correspondingly, the cytoplasmic processes of the cells are reduced during injury. Stromal repair following small injuries involves keratocyte activation, migration and transformation into fibroblasts, and as a by product scar tissue is generated. The remodelled or scar tissue typically involves the laying down of collagen fibrils without regularity. Collagen fibrils deposited during injury also tend to be larger than normal. Remodelling of the scar tissue involves the thinning of the fibrils and reformation of the lamellae over a number of months to increase transparency (Bron et al., 2001).

There are three additional cell types that are occasionally encountered in the corneal stroma; lymphocytes, macrophages and very rarely polymorphonuclear leukocytes (Arffa, 1997; Bron et al., 2001; Hamrah et al., 2003). These can either enter from tear fluid before surface defects are covered by an epithelial plug, or, in larger wounds, from rapid vascular responses.

1.1.4 Descemet's membrane (posterior limiting layer)

Descemet's membrane is a thick basal lamina produced by the corneal endothelium. Schwalbe's ring marks the termination of Descemet's membrane peripherally (Arffa, 1997). By electron microscopy, it is evident that Descemet's membrane is composed of an anterior banded zone and a posterior homogeneous zone. The anterior third is produced in utero and is therefore oldest, while the posterior region is produced after birth and thickens with age. Continual production of Descemet's membrane means that thickness of the membrane accordingly changes with age; from 3-4μm at birth to 5μm in childhood and 10-12μm in adults. Though the entire membrane appears homogeneous, the laminated structure demonstrates differences in the postnatal component. The membrane is known to be composed of type IV collagen, type VIII collagen and fibronectin but there is also a large glycoprotein and

proteoglycan content (Waring, III et al., 1982). Unlike Bowman's layer, it is sharply defined and forms a resistant sheet along the back of the stroma, which is easy to distinguish from the stroma along a plane of separation. Also unlike Bowman's layer, there is a strong regenerative capacity following injury such that the fresh basal lamina is structurally identical to that surrounding it, while Bowman's is replaced by disorganized, fibrillar scar tissue (Arffa, 1997; Bron et al., 2001). During some pathologic conditions, metallic substances can be deposited in the membrane or there is an excessive production of abnormal basal lamina, containing type I collagen, such that the membrane becomes thickened and warts of matrix can be formed. With these multiple layers, Descemet's membrane can provide a morphologic record of previous episodes of disease (Arffa, 1997; Bron et al., 2001).

The posterior two thirds of Descemet's membrane, which are secreted after birth, consist of a homogeneous fibrillogranular material (Bron et al., 2001). The area closest to the endothelial cell layer is formed last and is attached to the endothelia by hemidesmosomes. With age, there may be polymerization of collagens to produce bands of long-spacing collagen may be found in Descemet's membrane. Focal overproduction of the basal laminar material produces peripheral excrescences called Hassal-Henle warts (Tuft and Coster, 1990). While these are considered normal in the aged cornea, they resemble warts of the central cornea, known as cornea guttata, which are associated with corneal abnormalities and an increase in endothelial permeability. Excrescences of cornea guttata also increase in number with age (Tuft and Coster, 1990).

1.1.5 Corneal endothelium

The corneal endothelium is a monolayer of hexagonal, cuboidal cells that lie posterior to Descemet's membrane. The lateral borders of the cells are markedly convoluted, producing complex interdigitation with neighbouring cells. Both the basal and apical membranes are relatively flat. Like the epithelium, the endothelium is attached to its basement membrane by modified hemidesmosomes. These are found in numerous focal areas of increased

density and are thought to be derived from the absorption of pinocytotic vesicles. Lateral membranes of contiguous cells are very interdigitated at the posterior plane. These interdigitations fold over one another, to form a marginal fold at the apical surface (Bron et al., 2001). For the majority of its length, the lateral intercellular space at these interdigitations is approximately 20nm. The cells are bound together by cell junctions and junctional complexes, including tight junctions and gap junctions on the posterior third and the apical interface (Waring, III et al., 1982). At the gap junctions the membrane separations are close to approximately 2nm, while at the tight junctions there effectively membrane fusion (Williams and Watsky, 2002).

The appearance of the corneal endothelial monolayer changes slightly with age. At birth, the corneal endothelium exists at a density of approximately 3000 cells/mm^2 arranged in a continuous monolayer of 4 to 6μm thick. The youthful endothelium has an uninterrupted uniform paving-stone mosaic appearance with cells approximately 20μm in diameter and a surface area of approximately 250μm^2 (Waring, III et al., 1982). Typically, the cells are fairly evenly distributed over the surface of the cornea, with a slightly higher density of cells at the periphery (Schimmelpfennig, 1984; Holley et al., 2000). Endothelial cells also become more irregular in shape and tend to have more cilia closer to the periphery (Waring, III et al., 1982; Schimmelpfennig, 1984; Holley et al., 2000). In addition, cells cultured from the periphery of the cornea were found to have less tight cell-cell attachments and proliferate more readily (Bednarz et al., 1998). The observed differences between the endothelial cell population at the centre versus those at the periphery have prompted some researchers to suggest that the periphery may contain a progenitor cell population for the endothelium (Joyce, 2003).

The posterior surface of the cell membrane shows 20 to 30 microvilli per cell. Other than increasing the absorptive surface area, their function remains unknown (Collin and Barry Collin, 2004). Cilia rarely occur and are directed into the anterior chamber, related to a pair of centrioles in the posterior of the cytoplasm. Cilia tend to be more frequent towards the periphery of the cornea.

This may represent the median of a continuum of cells from the corneal endothelium to the trabecular meshwork (Bron et al., 2001). The plasma membranes of these cells have also been noted to have inward vesiculations that form pinocytic vesicles, and while these are infrequent, the possibility of increased pinocytic activity in response to increased particulate matter in the anterior chamber has been demonstrated (Bron et al., 2001). These vesicles have been noted to transfer particulate matter from the anterior chamber to anterior intercellular spaces or the inner surface of Descemet's membrane and appear as small pits on the apical surface of the endothelial monolayer (Waring, III et al., 1982).

The subcellular organization of corneal endothelial cells is consistent with the highly metabolically active state of these cells. Nuclei are large and oblong in shape causing low, flat bulges on the apical surface of the monolayer. There are large numbers of mitochondria distributed throughout the cell, though mitochondria tend to be concentrated around the nucleus (Waring, III et al., 1982). The Golgi apparatus is also found in a perinuclear location, facing the anterior chamber. There is an extensive endoplasmic reticulum and free ribosomes. A terminal web of actin lies close to the posterior membrane and is thought to be connected with the tight junctions, joining the cell monolayer together (Bron et al., 2001).

Maintenance of corneal transparency, by regulation of corneal hydration, is the major function of the corneal endothelial monolayer. The leaky barrier is balanced by the pumping action of the endothelial cells. The leaky barrier also allows essential nutrients to pass from the aqueous humor to supply the cellular needs of the other corneal layers. Oxygen derived from aqueous also supplies the endothelium and the posterior stroma with all their needs (Bron et al., 2001).

1.2 Development of the corneal endothelium

The human eye is derived from a number of different embryological tissues, including surface ectoderm, neural ectoderm, neural crest and mesodermal

mesenchyme. This dispersed population of tissues are all originally derived from the mesoderm or neural crest (Tuft and Coster, 1990). At approximately 40 days of human gestation (18mm stage), mesenchymal cells separate from the rim of the optic cup and spread along the newly invaginated lens vesicle. These cells eventually differentiate into the corneal and trabecular endothelium (Waring, III et al., 1982). At this point, the cornea consists of a superficial squamous cell layer, a basal, cuboidal epithelial cell layer, a primary stroma and a double layer of flattened endothelial cells (Bron et al., 2001). Subsequently, two additional waves of mesenchymal cells migrate to the centre; presumptive corneal keratocytes anterior to the endothelium and presumptive iris stromal cells posterior to that (Waring, III et al., 1982). Chromatin studies in birds suggest that this tissue is derived from the neural crest rather than mesoderm, possibly explaining discrepancies between behaviours of corneal endothelium and vascular endothelium, which originates from mesoderm (Johnston et al., 1979; Waring, III et al., 1982). Immunofluorescence staining of neuron-specific enolase in human keratocytes and endothelium has also demonstrated their origin to be from the neural crest (Adamis et al., 1985; Bron et al., 2001).

By the third month of gestation (63mm stage), the endothelium in the central cornea has become a single, flattened layer of cells resting on an interrupted basal lamina (Bron et al., 2001). At this point, the basal lamina has separated into two zones dependent upon their proximity to the endothelial cell layer. The lamina densa is closer to the corneal stroma and forms an electron dense band while the lamina lucida, adjacent to the corneal endothelium, forms an electron-lucent zone (Bron et al., 2001). The secretion of Descemet's membrane, by the embryonic endothelium, begins primarily in the fourth month of gestation. Further differentiation and growth of Descemet's membrane is accomplished through a series of sequential secretions, which form a multilayered structure (Bron et al., 2001). The process is rapid with only one layer at three months gestation, to 10 layers at six months and 30-40 layers at birth (Waring, III et al., 1982; Bron et al., 2001). In the third trimester, cross-linking bridges bind the adjacent layers together and aid in the compaction of this portion of matrix, to

form Descemet's membrane (Bron et al., 2001). Because of the unique pattern of interconnected nodes in this zone, as seen by transmission electron microscopy, it is named the 'fetal' banded zone of Descemet's membrane (Waring, III et al., 1982; Arffa, 1997; Bron et al., 2001). This 'fetal' region of Descemet's membrane is approximately 3μm in thickness at birth and remains that thickness throughout life (Waring, III et al., 1982; Bron et al., 2001).

Deposition of Descemet's membrane in the fourth month of gestation corresponds with the onset of production of aqueous humour by the ciliary processes. In order to maintain the water balance of the developing cornea, the apices of the endothelial cells join by zonulae occludentes, also known as tight junctions (Bron et al., 2001). Immature tight junctions begin to develop at the eighth week of gestation but only begin to mature with the formation of aqueous humor (Bron et al., 2001). By the fifth month of gestation, the tight junctions have matured substantially and are similar to those at birth (Bron et al., 2001). By the sixth month of gestation, Descemet's membrane is clearly demarcated and the stroma consists of an immature matrix including collagen fibrils and active keratocytes (Bron et al., 2001).

In the newborn, the cornea is relatively quite large with a steeper curvature than the cornea of adults (Arffa, 1997). Premature babies have smaller corneas and the steepness of curvature is even greater than that of full term newborns (Bron et al., 2001). While the peripheral cornea is consistently thicker than the central cornea throughout life, corneal thickness at birth is slightly higher than that of adults (Arffa, 1997). Continual growth and flattening continues with age and the cornea approaches adult measurements following the first year of life (Arffa, 1997).

After birth, there is a negligible amount of cell proliferation to maintain corneal endothelial cell densities. As the tissue ages, some cells within the monolayer die and spaces are filled predominantly by cell enlargement and cell spreading. The appearance of the monolayer, therefore, shifts from a homogeneous population of hexagonal cells to a heterogeneous population of irregular sized and shaped cells. The enlargement of the cells is termed polymegathism and the

irregular cell shape termed pleomorphism. When the cell density falls below 500cells/mm^2, endothelial cell function is compromised and the monolayer can no longer perform its barrier function. The result is stromal swelling, leading to corneal opacification.

1.3 Corneal endothelial barrier function

Corneal hydration is controlled solely by the corneal endothelial cell monolayer and plays a major role in the maintenance of corneal thickness and transparency. However, the mechanisms that control corneal endothelial barrier function remain unclear. The pump-leak hypothesis is generally accepted as the basic model of water balance between the cornea and the aqueous humor (Figure 1.2). In its original formulation, Maurice (1951) suggested the swelling pressure of the stroma was balanced by an excess of ions in the aqueous humor. Ionic excess was maintained by active transfer of one of the major ions, Na^+, K^+, Cl^- or HCO_3^-, to create a difference in electrical potential across the endothelium. Ions of opposite charge would be in electrochemical equilibrium across the layer (Maurice, 1951). The two principal elements of the hypothesis are the leak of the aqueous fluid into the stroma, driven by stromal swelling pressure controlled by the ionic permeability of the endothelium, and the pump which moves fluid out of the stroma, also located in the endothelium (Maurice, 1951).

One of the remaining debatable elements of this hypothesis is whether corneal thickness is passively or actively regulated. With passive regulation, the pumps would continually operate at maximum capacity and swelling pressure would increase as the cornea thins until the pumps are balanced. Active regulation would involve a sensing mechanism to reduce pump activity as corneal thickness approaches a physiologically normal value (Fischbarg & Maurice, 2004).

Maintaining the balance of stromal swelling is a complex process and is broken down into a number of components, which are further detailed below.

These include stromal swelling pressure, endothelial monolayer permeability, endothelial pumps, thickness regulation and endothelial cell junctions.

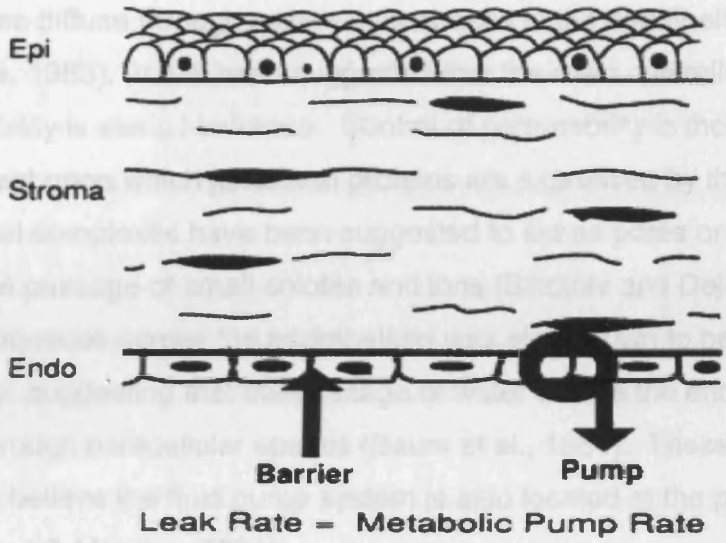

Figure 1.2 Schematic representation of corneal endothelial barrier function. Leakage of fluid from the aqueous humor into the corneal stroma is balanced by pumps on the corneal endothelium. It remains unclear whether this regulation is under active or passive controls. (image from: Waring III et al. 1982. The corneal endothelium. Normal and pathologic structure and function. Ophthalmology. 89:545)

1.3.1 Swelling pressure and leak

Swelling pressure created by the stroma is described by the Donnan effect, which suggests the existence of swelling pressure in a charged gel results from the ionic imbalances that it creates. Hodson and Earlam (1993) demonstrated a good correlation between the swelling pressure and the fixed charge density in the stroma. Fixed negative charge in the stroma has been attributed to different molecules by different groups. Hodson et al. (1992) suggest that this negative charge arises from the relative amounts of Cl^- in stromal tissue versus the aqueous humor. Another school of thought suggests that the principal source of the negative charge of the stroma arises from resident glycosaminoglycan molecules (Scott & Bosworth, 1990). Support for this latter theory is demonstrated by Maurice & Monroe (1990), who showed digestion of individual glycosaminoglycans reduced swelling pressure according to their concentration.

1.3.2 Endothelial monolayer permeability

Comparisons of the permeability of small solvents indicate that these molecules diffuse through paracellular spaces in the endothelial cell monolayer (Maurice, 1985). It has been suggested that the main controlling factor of permeability is steric hindrance. Control of permeability is thought to be dependent upon which junctional proteins are expressed by the endothelium, as junctional complexes have been suggested to act as pores or channels which allow the passage of small solutes and ions (Bazzoni and Dejana, 2004). The flow of aqueous across the endothelium was also shown to be proportional to its viscosity, suggesting that the passage of water across the endothelium takes place through paracellular spaces (Baum et al., 1984). These results have led some to believe the fluid pump system is also located at the paracellular space (Fischbarg & Maurice, 2004).

1.3.3 Endothelial cell pumps

Early investigations implicated the bicarbonate ion as the prime molecule of the endothelial fluid pump (Hull et al., 1977; Hodson & Miller, 1976). Results from more recent studies, however, suggest some inconsistencies. Some studies have even questioned the importance of the bicarbonate ion to pump function, instead suggesting that the differences noted with alterations in concentration of bicarbonate ion are not due to the ion itself but rather pH changes (Kuang et al., 1990; Doughty & Maurice, 1988). In the most recent model of electro-osmotic fluid pumping, bicarbonate plays a partial role in fluid transport. The remaining fluid pump is thought to be maintained by sodium recirculation via apical Na^+ pumps (Sanchez et al., 2002). A further challenge to the most recent theory remains with suggestions by Doughty (1991), who reports differences in pump behaviour according to whether bicarbonate concentrations are varied on the apical or basolateral side of the endothelium. Clearly, there is no consensus as to which pumps are vital for endothelial pump function and more research is needed.

1.3.4 Thickness regulation

The active model of the pump-leak hypothesis would require a set of receptors or sensors in the corneal stroma to assess the hydration of the tissue, another set to regulate the activity of the corneal endothelial pumps and a mechanism to link the two sets (Fischbarg & Maurice, 2004). As yet, no such receptor sets have been found, however, a number of putative receptors, which could alter pump rate have been determined.

The muscarinic acetylcholine receptor has been characterized and localized in the corneal endothelium (Lind & Cavanagh, 1995). While there is no evidence for a role for this receptor in fluid transport in the corneal endothelium, acetylcholine has been linked to increased fluid transport in other systems and may have a similar role in the corneal endothelium. Additionally, the abundance of acetylcholine in the cornea has also never been adequately explained.

The adenosine receptor has also been suggested to play a role in regulation of endothelial permeability. This suggestion is supported by studies in bovine corneal endothelium (Walkenbach & Chao, 1985; Walkenbach & LeGrand, 1982). Stimulation of the adenosine receptor was shown to activate adenyl cyclase and the resultant increase in cAMP also increased net endothelial fluid transport (Riley et al., 1996). These pathways are thought to converge with the activation of protein kinase A (PKA) (Fischbarg & Maurice, 2004).

Perhaps the most compelling evidence to date is that of platelet activating factor (PAF), which has been shown to inhibit fluid transport in a dose-dependent, saturable manner (Zhu et al., 1996). PAF stimulation in other systems has been shown to stimulate calcium mobilization and activation of protein kinase C (PKC). It is possible that the PKA and PKC pathways provide competitive regulation of endothelial pump control (Fischbarg & Maurice, 2004).

In addition to receptors, the corneal endothelium has been found to contain a number of water channel proteins. The role of these water channels is unclear as they do not appear to be evenly distributed across the monolayer. It has been suggested that certain cells, requiring rapid water passage through their membranes, contain these water channels while others do not (Fischbarg &

Maurice, 2004). Of additional interest is the fact that when water channels are present on the plasma membrane, they appear to cover the entire surface of the endothelial cell membrane (Li et al., 1999). However, these channels are more likely to play only a minor role in the regulation of water flow, as aquaporin knockout mice appear to have transparent corneas with fairly normal flow (Kuang et al., 2003).

1.3.5 Cell junctions

Endothelial cells adhere to one another at junctional structures. These are formed by homophilic cell-cell adhesion of transmembrane adhesive proteins. Stabilization of the junction is achieved through binding of specific intracellular partners to both the transmembrane proteins and the actin cytoskeleton. There are two major types of junctions described in both endothelial and epithelial cells; adherens junctions (AJs) and tight junctions (TJs). Both cell types also form gap junctions, which mediate cell-to-cell communication by allowing intercellular passage of ions and low molecular weight molecules (Simon and Goodenough, 1998). In addition to the aforementioned junctions, epithelial cells also form desmosomes but these are lacking in the endothelium (Bazzoni and Dejana, 2004). The organization of junctional complexes in a polarized cell is illustrated in Figure 1.3. Generally, junctions in the epithelium are better organized and more clearly defined than those in the endothelium, which occasionally displays mixing of the AJ and TJ. In the endothelium, the development of the mature junction is also a longer process than in the epithelium, with fully mature junctions only reached late in development. In general, junctions are not completely differentiated in the embryo (Bazzoni and Dejana, 2004).

Junctions are dynamic structures and organization of the endothelial monolayer follows a number of different steps to maturation. Evidence from epithelial cells suggests that adhesive membrane proteins of AJ and TJ form adhesion complexes at sites of cell-cell contact, which then organize into zipper

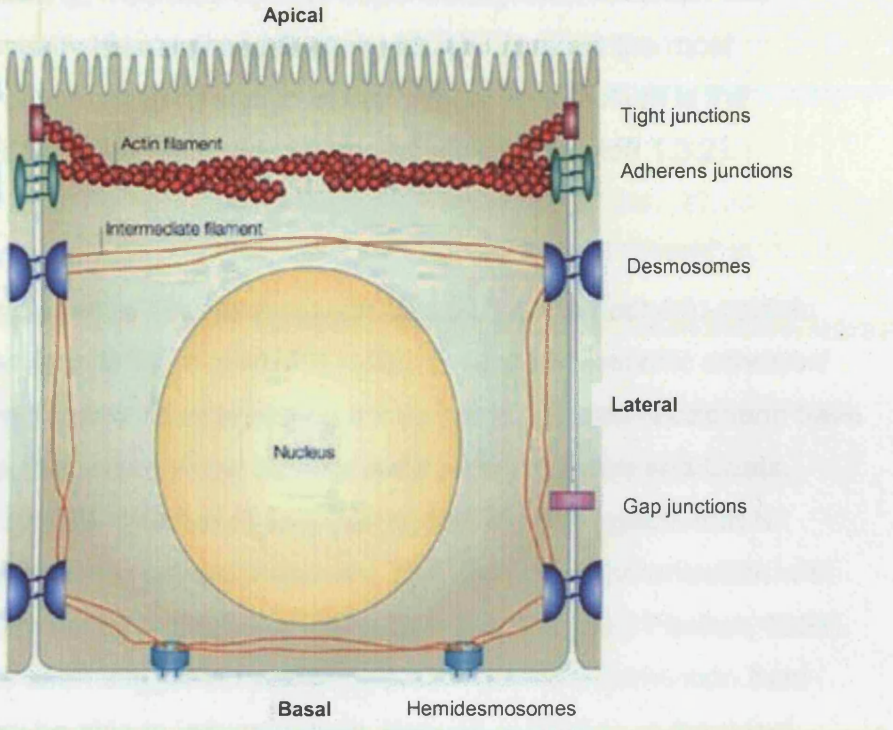

Figure 1.3 Epithelial intercellular junctions. This schematic representation of a polarized epithelial cell indicates the positioning of various junctions. The tight junctions and adherens junctions are linked to the actin cytoskeleton, while the desmosomes and hemidesmosomes are linked to the intermediate filaments. Desmosomes are only present in epithelial, not endothelial, cell layers. Hemidesmosomes anchor the cell to its matrix. (image from: Matter & Balda. 2003. Signalling to and from tight junctions. Nat. Rev. Mol. Cell Biol. 4:226)

like structures by lateral adhesion along the cell border (Matter and Balda, 2003; Bazzoni and Dejana, 2004). The organization of endothelial junctions may vary slightly from that in the epithelium, as the AJ and TJ are less well defined. Intracellular partners of transmembrane adhesive proteins vary during junction maturation and stabilization. Even after contacts have been stably established, adhesion proteins are still in a dynamic equilibrium and recycle continuously between the plasma membrane and intracellular compartments (Bazzoni and Dejana, 2004).

Junctions have been implicated in a number of different functions including the mediation of intracellular signals. These signals have been shown to affect both growth and apoptosis. It is suspected that information from the junction

dictates cell positioning, mediates contact-dependent growth inhibition and establishes cell polarity (Bazzoni and Dejana, 2004). Perhaps the most important aspect of junctional formation in the corneal endothelium is the establishment of barrier function and impermeability (see section 1.3.2).

1.3.5.1 Adherens junctions

The main component of the adherens junction (AJ) is the cadherin-catenin complex. The cadherin family of proteins, which mediate homophilic adhesion between cells, are transmembrane protein components. E- and N-cadherin have been shown to be expressed in the corneal endothelium (Beebe and Coats, 2000; Ickes et al., 2002). Studies in vascular endothelium suggests that N-cadherin may play a role in cell adhesion and also cell-cell communication with other cell types expressing N-cadherin (Gilbertson-Beadling and Fischer, 1993). Additionally, it has been suggested that N-cadherin may offer protection from apoptosis and may be able to induce growth, through activation of fibroblast growth factor receptors (Williams et al., 2001). The cytoplasmic tail of the classic cadherins are homologous and bind β-catenin and plakoglobin (γ-catenin), both of which bind α-catenin and anchor the complex to actin. α-Catenin also binds α-actinin and vinculin, which further anchors the AJ to the cytoskeleton (Weiss et al., 1998; Bazzoni and Dejana, 2004).

While ZO-1 is commonly considered an intracellular component of TJ, it can also be found at the AJ in the early stages of junctional organization. ZO-1 binding to α-catenin is responsible for its localization at the AJ, but this is transient, as the junction matures, ZO-1 moves away and concentrates at the TJ (Itoh et al., 1997).

While the classic cadherins tend to bind essentially the same molecules at their cytoplasmic domain, they may exert different biological activities (Bazzoni and Dejana, 2004). A prominent feature of β-catenin and plakoglobin are their ability to translocate to the nucleus to modulate gene expression with other transcription factors. These roles are thought to be more critical during development than later in life. Mutations in this machinery, especially β-catenin,

have been implicated in increased cell proliferation and decreased sensitivity to apoptosis (Ben-Ze'ev and Geiger, 1998). These findings support a role in tumorigenic transformation, as many tumor cells have altered junction formation. Similarly, expression and clustering of some cadherins (E-cadherin) at the junctions has been shown to activate small GTPases such as Rac, while reducing RhoA activation, which in turn help to stabilize the monolayer (Nakagawa et al., 2001). Other cadherins (N-cadherin), however, have been found to be associated with migratory phenotypes, inducing Rho activation and inhibiting Rac (Charrasse et al., 2002). In addition to GTPases, AJ have been noted to interact with several phosphatases and intracellular signalling molecules, including PI3 kinase and MAPK (Bazzoni and Dejana, 2004).

The AJ is key to the maintenance of a number of cell-specific properties and its molecular organization is complex. It is likely that further investigations will uncover more molecules that interact with or make up AJ (Bazzoni and Dejana, 2004).

1.3.5.2 Tight junctions

TJ were first described by electron microscopy as a specialization of the plasma membrane, named *zonula occludens*, in which it appeared as though the membranes of two cells were fused at one point on the apical side of the cell. However, closer investigation revealed that the membranes of the two cells were in fact separate but in tight contact with each other (Bazzoni and Dejana, 2004). The major function of TJ is to regulate paracellular permeability and maintain cell polarity by restricting both diffusion of solutes across the intercellular space (barrier function) and movement of molecules between the apical and basolateral faces of the plasma membrane (fence function).

Most research into TJ has been performed in epithelial cell lines, and while many of the details about epithelial TJ can be extrapolated to fit endothelial TJ, there are a few caveats to keep in mind. First, the precise location of the TJ and its definition from other junctions is less distinct in most endothelial cells as compared to epithelial cells. Second, even though the components of the

junction may be the same, their assembly and regulation may be different in epithelial and endothelial cells. Third, there is more variability across endothelial barriers with regard to development of TJ and permeability across monolayers (Bazzoni and Dejana, 2004).

The TJ plaque is composed of both transmembrane and intracellular molecules. There are 3 classes of transmembrane proteins that form TJ; occludin, claudins and adhesion proteins of the immunoglobulin superfamily, such as junctional adhesion molecules (JAMs). Occludin was the first transmembrane TJ protein to be discovered. It is composed of two extracellular loops and four transmembrane regions with both ends of the protein terminating in the cytoplasm, and exists as at least two different splice variants. Interestingly, the levels of occludin expressed have been found to correlate to the permeability of different monolayers. Endothelial cells of non-neural tissues tend to express occludin at a lower levels and have a greater permeability (Hirase et al., 1997). It was first thought that occludin contributed to intercellular adhesion, but surface expression and adhesion are not intrinsic properties of occludin. Organization of occludin at the membrane first requires that endogenous ZO-1 be organized at the membrane, possibly at AJ (Medina et al., 2000). The cytoplasmic domain of occludin binds directly to the ZO proteins in a reaction that is saturable (Furuse et al., 1994; Schmidt et al., 2001). Additionally, occludin-deficient mice are born with no gross phenotype, suggesting that occludin is dispensable for tight junction formation (Saitou et al., 1998). Further analysis determined that mice lacking occludin had postnatal growth retardation in a number of tissues, suggesting that occludins' role may not be related to its positioning at the tight junction, and that its positioning may merely be a regulatory mechanism (Saitou et al., 2000).

There are over 20 proteins which make up the family of claudins. Like occludin, these have four transmembrane domains, two extracellular loops and two cytoplasmic termini, however, the proteins are much smaller and bear no sequence similarity to occludin. The types of claudin expressed by cells are thought to determine the leakiness of the TJ barrier (Furuse et al., 1998).

Claudin-5 has been found to have an expression pattern restricted to endothelial cells (Morita et al., 1999). Interestingly, investigations into claudin expression in corneal endothelial cells revealed that these cells do not express claudin-5. Only claudin-1, -6 and -8 were found to be expressed in corneal endothelial cells (Kuang et al., 2003). It is clear that claudin-1 is vital for survival as genetic ablation of claudin-1 induces neonatal death and wrinkling of the skin due to increased permeability of water (Furuse et al., 2002). The claudins and occludin are thought to assemble into heteropolymers that form intramembrane strands. These strands have been proposed to contain fluctuating channels to allow selective diffusion of ions and small hydrophilic molecules (Matter and Balda, 2003; Bazzoni and Dejana, 2004). The ion size and selectivity of the paracellular diffusion pathway is dependent on the types and concentrations of claudins and occludin (Matter and Balda, 2003).

The most recently discovered transmembrane TJ proteins are junctional adhesion molecule-A (JAM-A) and related molecules. JAM-A is a glycoprotein with a single extracellular domain, with two Ig-like domains, one transmembrane segment and a short cytoplasmic tail. It is thought to play a role in transendothelial migration of leukocytes (Bazzoni and Dejana, 2004). Related molecules JAM-B, JAM-C, endothelial cell-selective adhesion molecule (ESAM) and Coxsackie- and adeno-virus receptor (CAR) are also thought to play roles in TJ assembly and regulation of paracellular permeability. Like the other transmembrane TJ proteins, JAM-A binds intracellular TJ protein ZO-1, possibly anchoring this protein to F-actin or other transmembrane TJ proteins (Bazzoni and Dejana, 2004). This feature may be instrumental in the stabilizing of the TJ strands.

In addition to the transmembrane components of TJ, there are a number of intracellular components of TJ. Cytoplasmic plaques are formed by a number of different proteins that include adaptor proteins and other proteins containing PDZ (*p*ostsynaptic density protein/*d*isc large-A/*Z*O-1) domains, regulatory components and signalling components. Adaptor proteins, including the zonula occludins (ZO), are thought to bind to transmembrane proteins and recruit other cytosolic

components to the tight junction. Protein kinases, GTPases and transcription factors, are among the cytosolic components recruited to TJ. The most extensively studied of the intracellular components is zonula occludens-1 (ZO-1). This was also the first protein component of the tight junction to be discovered (Stevenson et al., 1986). ZO-1 and its related proteins, ZO-2 and ZO-3, belong to the family of membrane-associated guanylate kinases (MAGUKs), which mediate a number of cellular functions, including anchoring to actin, establishment of cell polarity, membrane trafficking, cell signalling and control of gene expression (Bazzoni and Dejana, 2004). The distribution of ZO-1 is variable among cells, and only those cells forming distinct junctional complexes show restricted expression of ZO-1 at TJ. Cells with incomplete junctional development display ZO-1 localization at both TJ and AJ. The PDZ domains of ZO-1 are thought to be responsible for its binding to various other TJ proteins, including the transmembrane TJ proteins and other ZO proteins. ZO-1 is known to contain three PDZ domains, a Src homology 3 (SH3) domain, a guanylate kinase domain and an acidic and a proline-rich region (Bazzoni and Dejana, 2004). In addition to other TJ proteins, ZO-1 is also known to engage in interactions with a number of additional intracellular molecules. Interactions with F-actin are thought to be responsible for anchoring the TJ to the cytoskeleton and may play a role in the control of permeability (Cordenonsi et al., 1999). ZO-1 has also been shown to interact with a number of intracellular signalling molecules and transcription factors. Among these is the Y-box transcription factor ZONAB, which inhibits expression of the ErbB2 gene product (Balda and Matter, 2000). This interaction suggests a role for TJ and ZO-1 in the regulation of cell growth and proliferation. Interactions with members of the Ras family and Ras effectors also suggest that these proteins may play a role in the regulation of cell growth (Bazzoni and Dejana, 2004).

In human corneal endothelium, immature tight junctions begin to develop at the eighth week of gestation (Bron et al., 2001). Coinciding with the formation of aqueous humor, in the middle of the fourth month of gestation, the tight

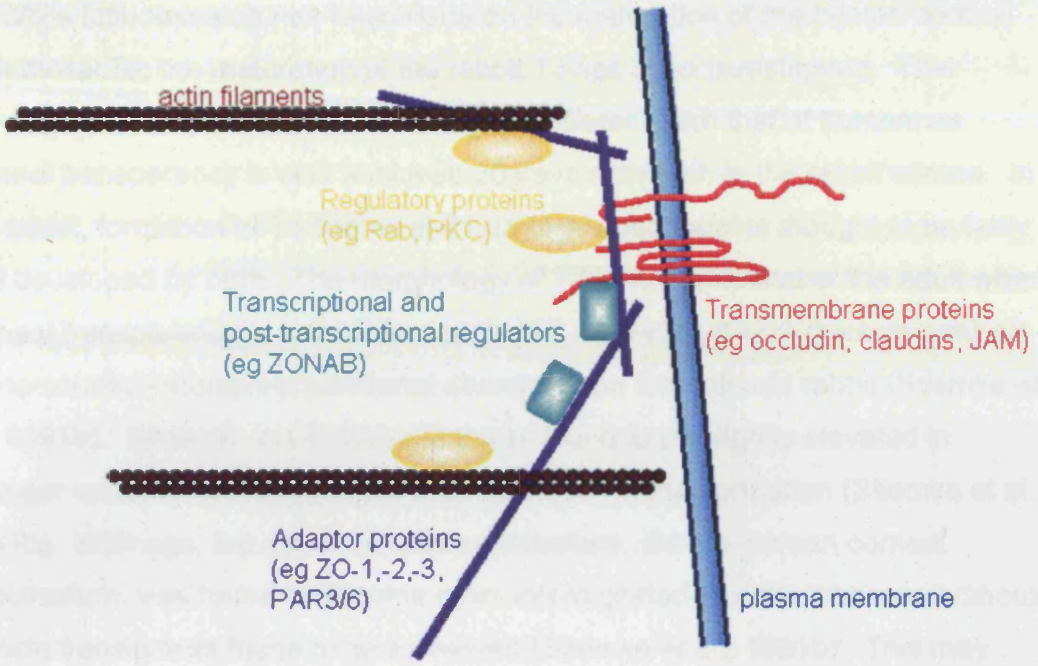

Figure 1.4: Composition of the tight junction. The tight junction plaque is made up of transmembrane proteins, which form heteropolymers that form the intramembrane strands. These transmembrane proteins bind to adaptor proteins, which help recruit other proteins to the tight junction. These include transcriptional and post-transcriptional regulators and regulatory proteins. Some examples of proteins involved in the formation of the tight junction are named above but this is by no means a comprehensive list. (image adapted from: Matter & Balda. 2003. Signalling to and from tight junctions. Nat. Rev. Mol. Cell Biol. 4:227)

junctions begin to mature. By the fifth month of gestation, the tight junctions are similar to those at birth (Bron et al., 2001). Further maturation and definition of TJ continues to take place after birth and may continue through the entire life of the individual. Immunofluorescence staining of human and cat corneal endothelium has revealed the junctional organization in these two species to be similar. Both show apical ZO-1 and cortical F-actin organization (Petroll et al., 1999). While cadherin and catenin form a tight band around the cells, ZO-1 staining appears to be discontinuous, with the largest gaps at the Y-junctions of adjacent cells (Petroll et al., 1999). These differences in staining suggest that ZO-1 localizes to the TJ and not the AJ, however, no transmembrane tight junction proteins have yet been visualized in the corneal endothelium.

While little research has been done on the maturation of the human corneal endothelial TJ, the maturation of the rabbit TJ has been investigated. The development of the rabbit cornea is slightly different from that of human, as corneal transparency is only achieved 20 days after birth in the rabbit cornea. In the rabbit, formation of TJ begins at 21 days gestation and is thought to be fairly well developed by birth. The morphology of TJ is similar to that of the adult when corneal transparency is established at day 20, however, freeze-fracture analysis demonstrated incomplete junctional strands in the 3 month old rabbit (Stiemke et al., 1991b). Similarly, paracellular flux was found to be slightly elevated in younger endothelium, suggesting incomplete junctional formation (Stiemke et al., 1991b). With age, the rabbit corneal endothelium, like the human corneal endothelium, was found to become more interdigitated and the intramembranous particle density was found to be increased (Stiemke et al., 1991b). This may represent a continually maturing junction with a continual recruitment of more junctional proteins. Some of these proteins may be endothelial cell pumps, responsible for maintenance of corneal clarity, as concentrations of the Na/K ATPase were found to increase with age, and newer models of the pump-leak hypothesis suggest that junctions are the sites for endothelial cell pumps (Stiemke et al., 1991a; Fischbarg and Maurice, 2004).

While it is clear that endothelial TJs play a major role in corneal hydration control, the development of these barriers in the human endothelium remains unclear.

1.4 Corneal endothelial cell survival

Unlike endothelial cells in most other tissues, corneal endothelial cells are almost incapable of proliferation, meaning that cell death has a significant impact on corneal endothelial cell densities. Human corneal endothelial cell densities are highest around birth and decrease slowly with age. Their incredibly long life span makes it is difficult to investigate factors that affect corneal endothelial cell survival. At present, the best model for studying decreasing corneal endothelial

cell densities are corneas which have been stored for transplantation. It has been documented that both cold storage (4°C) as well as organ culture methods (34°C) of corneal storage lead to an increase in cell death of the corneal endothelial cell monolayer, limiting the useful lifespan of corneas in storage (Albon et al., 2000; Crewe and Armitage, 2001; Thuret et al., 2003a). The cell death mechanisms which underlie these decreasing densities remain unknown and while most studies suggest that apoptosis is the main source of cell death in the corneal endothelial cell monolayer, necrosis is also thought to occur (Komuro et al., 1999; Albon et al., 2000).

1.4.1 Apoptosis

Apoptosis, or programmed cell death, is a distinctive mechanism of active cellular death characterized by a set of physiologically and chemically defined processes culminating in distinct cellular biochemical events (Wyllie et al., 1980). These cellular events include loss of membrane phospholipid asymmetry, loss of mitochondrial permeability and function, chromatin condensation, fragmentation of genomic DNA, compartmentalization of cellular cytosol and DNA and discrete packaging and blebbing of cellular components (Reed, 2000). By contrast, the less controlled process of cell death, necrosis, can be characterised by progressive swelling of the cell and random DNA and organelle degradation resulting in the eventual rupture of the cell and the spilling of cytosolic components. Due to the release of cellular components with necrotic cell death, it is also associated with an inflammatory response. This response is not, however, associated with apoptotic cell death, as the cell contents remain contained as they are degraded.

While there are many molecules involved in apoptotic signalling, most apoptotic pathways lead to the activation of a cascade of key proteases. This family of proteins is referred to as *c*ysteine *a*spartyl-*sp*ecific prote*ases,* or caspases, and these are responsible for many of the morphologic changes noted during apoptosis (Reed, 2000). These changes are induced by interactions of caspases with specific target proteins including structural proteins (cytoskeletal

proteins), regulatory proteins (PKC, PARP) and other pro-apoptotic proteins. Caspases reside in the cell as inactive zymogens, which can be triggered into the active state with proteolytic processing. Cleavage of the pro-protein at conserved asparagine residues generates two subunits of the active protein; a large and small subunit (Donepudi and Grutter, 2002). Similarly, caspases cleave their substrates at asparagine residues, which activate their proteolytic activity, suggesting that these proteins act in a proteolytic cascade. These cascades may include more than one caspase with one caspase activating another. Upstream caspases are typically referred to as initiator caspases, while the downstream caspases are termed effector caspases (Donepudi and Grutter, 2002).

There are two apoptosis pathways which can result in the activation of caspases; the intrinsic and extrinsic pathways. The intrinsic pathway involves the release of caspase-activating proteins from the mitochondria to the cytosol. Specifically, cytochrome c released from the mitochondria binds to caspase-activating protein Apaf-1. The binding of cytochrome c initiates a change in the conformation of Apaf-1 such that the protein aggregates and binds pro-caspase-9. The activation of caspase-9 is thought to be mediated by the induced proximity model, which suggests that the zymogen forms of caspases are not inactive but possess a very weak protease activity, such that when the proteins are brought into close proximity, the zymogens trans-process each other, resulting in fully active proteases (Martinou et al., 2000). Even after activation of caspase-9, the protease remains bound to Apaf-1 for full activity (Reed, 2000). The extrinsic pathway is mediated by ligand binding to death receptors, of these, the best studied is the TNF death receptor family. The cytosolic domains of the death receptors interact with adaptor proteins, which recruit pro-caspase-8. These complexes of caspases and adaptor proteins stimulate the activation of downstream caspases by the induced proximity mechanism. Upon activation, the N-terminus of the pro-protease is cleaved off to release the caspase into the cytosol to initiate apoptosis (Ashkenazi and Dixit, 1998). While these pathways

are commonly regarded as separate, there is often cross talk between the two at a number of different levels (Reed, 2000).

Proteins that control and participate in caspase activation pathways exist as families that can be recognized based on amino acid sequence or structural similarities. Interactions of these proteins are typically mediated by domains, which are associated with the regulation of apoptosis (Reed, 2000). These include caspase-associated recruitment domains (CARDs), death domains (DDs), death effector domains (DEDs), Bcl-2 homology (BH) domains, baculovirus inhibitor of apoptosis protein(IAP), repeat (BIR) domains of IAP proteins and NB-ARC domains, which represent nucleotide binding oligomerization domains (Reed, 2000).

Little research has been done on the cellular pathways activated in the apoptotic response of corneal endothelial cells, however, there are a number of studies concerning the expression of anti-apoptotic protein Bcl-2 (Li et al., 1998; Joo et al., 1999; Gain et al., 2001; Yamamoto et al., 2001). The mitochondrial-dependent apoptotic pathway is governed by the Bcl-2 family of proteins. Many of these proteins are constitutively located on mitochondrial membranes, while others are induced to target organelles, including the ER and nuclear envelope, in response to stimulation (Martinou et al., 2000). Others are normally found in the cytosol but can be induced to target the mitochondria, where they have a role in the release of cytochrome c, initiating the activation of cytosolic caspases (Martinou et al., 2000). There are both pro- and anti-apoptotic proteins within the Bcl-2 family, with many of the proteins binding to each other to form a network of homo- or heterodimers (Chao and Korsmeyer, 1998). Relative ratios of pro- and anti-apoptotic proteins present dictate the sensitivity of the cells to various apoptotic stimuli (Gross et al., 1999). At present, 20 members of the Bcl-2 family have been described comprising 6 anti-apoptotic and 14 pro-apoptotic proteins. Some of these are the products of alternative mRNA splicing, and may have opposing effects on apoptosis (eg anti-apoptotic Bcl-X_L and pro-apoptotic Bcl-X_S). Other proteins display differing activities in different cellular backgrounds (eg Boo/Diva, Bcl-2 and Bax). The Bcl-2 family can also be divided

into two groups according to protein structure. One sub-set is thought to form an α-helical pore or channel, similar to the pore-forming domains of bacterial toxins. Most of these proteins have conserved stretches of amino acid sequence homology, including Bcl-2 homology (BH) domains BH1, BH2, BH3 and occasionally BH4 (Gross et al., 1999). The other sub-set of proteins only contains the BH3 domain and all of these proteins are pro-apoptotic in function. Their cell death activity is dependent upon their ability to dimerize with anti-apoptotic Bcl-2 family proteins. These observations demonstrate that the dimerization of Bcl-2 family members is dependent upon the BH3 domain of the proteins (Gross et al., 1999).

1.4.2 Age-related effects on the corneal endothelium

It is well known that, with age, there is a general trend towards a decrease in endothelial cell densities and a corresponding increase in polymegathism and pleomorphism. This decrease reflects small accumulated cell loss over time from cell death from age or injury and negligible amounts of cell proliferation. Between the ages of 20 and 80 years, there is an annual reduction in cell density average of approximately 0.6%. These decreasing densities are illustrated in Figure 1.5. As the mean age of the population sample increases, however, there is an increased spread in the range of endothelial cell counts, suggesting environmental influences as well as age effects play a role in decreasing endothelial cell densities (Faragher et al., 1997). In the event of excessive cell loss, the barrier function of the endothelium can be compromised. Endothelial cells compensate for decreasing cell numbers by increasing the density of pumps on each cell (Crawford et al., 1995). There is, however, a cut off point at which the increased number of pumps on the remaining endothelial cells can no longer compensate for the increased leakage, due to loss of barrier function at decreased cell densities. At this point the function of the monolayer is compromised resulting in corneal hydration and opacity.

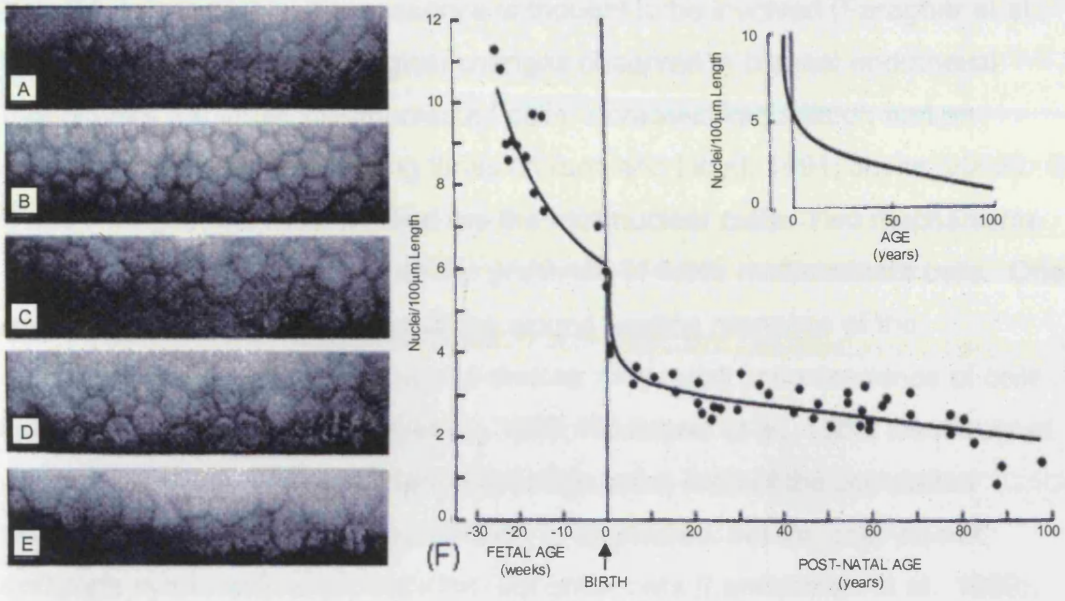

Figure 1.5 Corneal endothelial cell densities decrease with age. Clinical specular micrographs of the corneal endothelium of normal subjects; (A) 20 year old, (B) 44 year old, (C) 59 year old, (D) 69 year old and (E) 83 year old. Quantitation of the age-related decrease in corneal endothelial cell density suggests that this phenomenon occurs on a logarithmic scale, with the majority of cell death occurring in the first few years of life (F). (images from: Laing et al. 1976. Changes in the corneal endothelium as a function of age. Exp. Eye Res. 22:590; graph from: Murphy et al. 1984. Prenatal and postnatal cellularity of the human corneal endothelium. A quantitative histologic study. Invest.Ophthalmol.Vis.Sci. 25:316)

In addition to gradual cell loss with time, senescent phenotypes develop in some cells of the endothelium. Cellular senescence is the process that imposes a limit on the replicative lifespan of a cell, aiding in tumor suppression and lengthening the reproductive lifespan of an individual, however, the emergence of senescent cells contributes to the aging process (Faragher et al., 1997). There are two main routes by which cells become senescent. Constitutive cell senescence reflects the chance of senescence with each cell division and is typically explained in terms of shortened telomere lengths. Reactive cell senescence is similar to constitutive cell senescence but occurs more rapidly and is induced by mutation or mitogenic overload. It requires little, if any cell division (Faragher et al., 1997). As the corneal endothelium is not made up of actively proliferating cells, but senescent phenotypes occasionally develop in the

monolayer, reactive cell senescence is thought to be involved (Faragher et al., 1997). Among the morphological changes observed in corneal endothelial monolayers are large, multinucleated cells, increased vacuolation and an increase in population doubling times (Wilson and Lloyd, 1991; Joyce, 2003). Of these changes, the most studied are the multinuclear cells. Two mechanisms have been suggested to explain the presence of these multinucleate cells. One explanation arose from studies of the wound healing response of the endothelium suggesting that wound closure may result in coalescence of cells rather than cell division (Liang et al., 1983; Neubauer et al., 1983; Neubauer et al., 1984). An alternative explanation is that some cells of the population undergo amitotic division, in which DNA is duplicated, but the cells do not complete cytokinesis to produce two daughter cells (Landshman et al., 1989; Tuberville et al., 1989). These observations were noted in both the wound healing response of the endothelium and in the normal human corneal endothelium, which displayed an age-related increase in the number of polyploid cells (Ikebe et al., 1988). There also appeared to be a correlation between DNA content of the cell and the surface area of the cell, with multinucleate cells having a larger mean and maximum size and a more irregular shape than normal diploid cells (Ikebe et al., 1988). Similar results were noted for human corneal endothelial cell cultures, with those remaining longer in culture displaying senescent phenotypes (Wilson and Lloyd, 1991).

In addition to the development of a senescent phenotype, significant age-related differences were detected in the kinetics of cell cycle progression. Cells from older donors were found to enter the cell cycle more slowly than those from younger donors. In addition, fewer cells from older donors entered the cell cycle (Senoo and Joyce, 2000). Interestingly, sensitivity to mitogenic factors may also be decreased in older cells, as these cell require longer, stronger mitogenic stimulation in order to proliferate (Senoo and Joyce, 2000).

Assays of telomerase activity also reflect notable age-related differences in the human corneal endothelium. No measurable telomerase activity was found to be present in central corneal endothelial cells, but low levels of telomerase

activity was detected in the peripheral region (Egan et al., 1998). This low level of peripheral telomerase activity was higher in younger populations (Egan et al., 1998; Whikehart et al., 2002; Joyce, 2003). Higher cell densities and greater variations in cell shape at the periphery have also been noted (Schimmelpfennig, 1984; Holley et al., 2000). These observations have led some to suggest that these peripheral cells may represent a progenitor cell population for the corneal endothelium (Joyce, 2003).

1.4.3 Factors affecting corneal endothelial survival

Advanced glycation end products (AGEs) have been proposed as mediators for the pathogenesis of age-related diseases (Kaji et al., 2001). AGEs are produced by nonenzymatic reduction, oxidation and condensation of reducing sugars and proteins, collectively known as glycoxidation (Kaji et al., 2003). These modified proteins accumulate in tissue and cartilage with age, resulting in a deterioration or elimination of protein function. In addition, AGEs impair cellular function by increasing cellular oxidative stress by binding to specific cell surface receptors, including the receptor for AGE (RAGE) and galectin-3, to induce the deleterious effects commonly associated with the ageing process (Kaji et al., 2003). The presence of AGEs in the human cornea has been described, with levels of AGEs in Descemet's membrane found to increase with time (Kaji et al., 2000). The presence of AGEs in basement membranes has been reported to affect attachment and cell spreading in a number of cell types. Studies investigating glycation of fibronectin and laminin in corneal endothelial matrix showed a decreased number and surface area of attached corneal endothelial cells (Kaji et al., 2001). The expression of RAGE and galectin-3 was also noted in corneal endothelial cells (Kaji et al., 2003). The accumulation of AGEs in corneal endothelial cells was shown to result in increased generation of reactive oxygen species by the cells and consequently, increased apoptosis. It has been proposed that AGEs induce apoptosis partly by increasing amounts of reactive oxygen species (Kaji et al., 2003). Reactive oxygen species have been noted to induce both apoptosis and necrosis in cultured corneal endothelial cells (Cho et

al., 1999). Similarly, hydrogen peroxide, which is produced by the cornea and neighbouring tissues, has been shown to induce apoptosis in corneal endothelial cells (Hull et al., 1984; Hudde et al., 2002). The effects of oxidative stress have been found to be alleviated with catalase (Hull et al., 1984; Hudde et al., 2002). Extracellular superoxide dismutase (SOD) may also to have a cytoprotective role in protection of the corneal endothelium from oxidative stress. SOD null mice have been shown to have an increased concentration of extracellular superoxide radicals, enhancement of spontaneous age-related corneal endothelial cell loss and increased susceptibility to acute inflammation (Behndig et al., 2001). Cytoprotective effects were also noted in proteins found in the aqueous humor. One such protein is vasoactive intestinal peptide (VIP), which has been shown to increase corneal endothelial cell survival from oxidative insults (Koh and Waschek, 2000). Additionally, expression of anti-apoptotic proteins by corneal endothelial cells, themselves, may offer protection from cell death. Studies have noted expression of heat shock proteins (Hsp) 27, 60, 70 and 90, Bcl-2, Bax, Bcl-X_L, interleukin-1β converting enzyme, Fas and Fas-ligand by corneal endothelial cells (Wilson et al., 1996; Gain et al., 2001). The best studied of these is the anti-apoptotic protein Bcl-2, which was found in the nuclei and nuclear envelope of corneal endothelial cells (Yamamoto et al., 2001). Bcl-2 was found to be a negative regulator of caspase-dependent apoptosis in corneal endothelial cell cultures (Joo et al., 1999). External controls of corneal endothelial cell survival have been suggested from studies demonstrating protein(s) produced by the iris/ciliary body and present in the aqueous humor, which increase Bcl-2 gene transcription (Li et al., 1998). Also, because corneal endothelial cells express both Fas and Fas-ligand, additional controls by endothelial cells themselves are thought to help maintain their survival (Mohan et al., 1997).

1.4.4 Eye bank storage technique as a factor of endothelial cell survival

Various methods have been devised to prolong the viability of corneas destined for transplantation. Storage techniques preferred by eye banks in the United States differ from those in Europe. Organ preservation in Optisol-GS at

4°C is the preferred method of corneal storage in the United States and at Moorfields Eye Hospital, UK. Other UK Eye Banks and European Eye Banks tend to favour organ culture techniques in Chen's media at 31-34°C. Both storage techniques are designed to provide essential nutrients, stabilize metabolism and preserve cellular integrity of the cornea. Cell death in the endothelial cell layer is most important, as corneas with endothelium of insufficient quality for transplantation are discarded. Falling endothelial cell densities during storage accounts for approximately 30% of corneas being discarded from eye banks (Armitage and Easty, 1997). However, the integrity of the tight junction and actin cytoskeleton were found to be maintained in the corneal endothelium of organ cultured corneas for up to 3 weeks of storage (Crewe and Armitage, 2001). Cold storage (4°C) of corneas was found to increase the size of gaps in ZO-1 at the Y-junctions, however, this phenomenon was reversible with 24 hour incubation at 37°C (Hsu et al., 1999).

Despite attempts to maintain corneal tissue, cell viability has been found inversely correlate with storage time (Komuro et al., 1999). The gradual death of corneal cells during preservation may occur by two pathways: necrosis or apoptosis. Studies have suggested that apoptotic cell death occurs more often in the corneal endothelial cell monolayer than necrotic death (Komuro et al., 1999; Albon et al., 2000). The main distribution of apoptotic cells was found at the corneal folds, suggesting mechanic damage may affect corneal endothelial cell viability (Albon et al., 2000).

Corneal endothelial cell death in stored tissue may be the result of a number of factors. Bacterial contamination is a common problem in organ cultured corneas (Albon et al., 2001). Both bacterial LPS and endotoxins were detected in corneal culture media, which were found to enhance release of interleukin-6 (IL-6) and IL-8. Both of these cytokines increased degenerative phenotypes and death in the corneal endothelium (Sobottka Ventura et al., 1997). The addition of pentoxifylline to organ culture media was found to suppress the release of IL-6 and IL-8 and therefore increase corneal endothelial cell survival (Sobottka Ventura and Böhnke, 2001). Studies of corneal culture in serum-free media

show that corneal endothelial cell survival is comparable to that in Chen's media but with a lower risk of bacterial effects due to the lack of serum (Hempel et al., 2001; Moller-Pedersen et al., 2001).

Finally, effects of cryopreservation of corneal tissue have been examined and preliminary reports suggest that it may be sufficiently tolerated by endothelium. If further research validates this storage practice, it would have significant appeal in eye banking (Brunette et al., 2001; Armitage et al., 2002).

1.4.5 Mechanisms of corneal endothelial cell death

The intracellular mechanisms which underlie corneal endothelial apoptosis are largely unknown, though a number of studies implicate caspase-3 in the signalling cascade to cell death (Thuret et al., 2003a; Thuret et al., 2003b; Bourges et al., 2004). Cleavage of PARP, a molecule typically responsible for DNA repair, was also shown to play a role in staurosporine-induced apoptosis (Thuret et al., 2003b). Apoptosis induced by reactive oxygen species, however, was found to involve translocation of transcription factor NF-κB to the nucleus (Cho et al., 1999). Similarly, apoptosis by inflammatory cytokines was demonstrated to involve sustained activation of NF-κB, p38 and STAT-1 and de novo generation of nitric oxide (NO) by the inducible nitric oxide synthase (iNOS) (Sagoo et al., 2004).

In contrast to these results, Bourges et al. (2004) demonstrated corneal endothelial cell apoptosis, during acute graft rejection, to be caspase-3 independent and TUNEL negative, suggesting there may be additional mechanisms for activating apoptosis in the corneal endothelium. The cellular pathways which underlie the apoptotic response are still largely unclear and it may be that apoptosis resulting from different insults involve different cellular mechanisms, which terminate in the same response.

1.5 Diseases of the corneal endothelium

Classification of primary corneal endotheliopathies indicates four diseases within this category. These are Fuchs' dystrophy, posterior polymorphous dystrophy (PPD), congenital hereditary endothelial dystrophy (CHED), iridocorneal endothelial (ICE) syndrome and their intermediate forms. Examination of patients with primary corneal endotheliopathies also reveals a number of individuals with features of more than one of these categories, or a few characteristics of a number of these primary diseases. These have been classed as intermediate types. It may, in the future, be possible to diagnose these patients through genetic testing as genetic studies have indicated shared mutations leading to both Fuchs' and PPD, while other investigators have linked CHED to ICE syndrome (Biswas et al., 2001). Each of the four primary corneal endotheliopathies is discussed in further detail below.

1.5.1 Fuchs' dystrophy

Fuchs' dystrophy is an autosomal dominant trait which results in bilateral, but asymmetrical, disease whereby the endothelial cells gradually malfunction. It is by far the most common primary corneal endothelial disease but shows variable expressivity. Fuchs' dystrophy generally affects women more severely, and exhibits racial variation (Waring, III et al., 1982; Bourne, 2003). Typically, the disease becomes apparent in the later stages of life with the first changes appearing at middle age or later. There are three phases which characterize the clinical course of the disease, all of which begin at the centre of the cornea and progress toward the periphery over a period of 10 to 20 years (Waring, III et al., 1982). The first phase of the disease is asymptomatic as the posterior cornea develops small guttate excrescences. Some pigment is phagocytosed by the endothelium, and Descemet's membrane thickens to adopt a grey, uneven appearance. During the second stage, the patient experiences hazy visual acuity and glare as oedema develops. Increasing oedema results in water clefs within the stroma and within and beneath the epithelium. This oedema in turn leads to

an increased corneal thickness, which may even reach 1mm, a doubling from normal thickness. The third phase is the most severe as vascular subepithelial connective tissue invades the central region, rendering it completely opaque (Bergmanson et al., 1999). It is the presence of increased numbers of corneal guttae accompanied by corneal oedema which constitute Fuchs' dystrophy, with the corneal guttate forming the clinical hallmark of the disease (Waring, III et al., 1982). These discrete excrescences laid down by the endothelium are also the most striking histopathologic features of Fuchs' dystrophy. There are four patterns of excessive, abnormal matrix deposition; simple excrescences which protrude into the anterior chamber; multilaminar excrescences; excrescences buried in the multilaminar tissue and; multilaminar tissue without excrescences (Waring, III et al., 1982; Bergmanson et al., 1999). The excrescences, or warts, are most disruptive to the endothelial barrier as they interrupt the endothelial mosaic by pushing the endothelial nuclei into dumbbell or sickle shapes and thinning the overlying endothelial cells. The number of endothelial cells remaining is thought to be inversely proportional to the number of guttate excrescences (Waring, III et al., 1982; Borderie et al., 2000). The endothelial cells enlarge to fill the spaces left by cell death and can enlarge up to 1000μm^2, two and a half times greater than normal 400μm^2 cells (Waring, III et al., 1982; Bergmanson et al., 1999). This enlargement causes the cells to lose their characteristic hexagonal shape, but they maintain their covering. Remaining endothelial cells are often large and thin, with a shift in the uniform population of endothelium to a population containing cells with a dilated endoplasmic reticulum, in which can be found finely granulated material, phagocytosed pigment granules and increased cytolasmic filaments. This new cell population has been interpreted as endothelial cells which have differentiated to a fibroblastic phenotype and which may be responsible for the excretion of the posterior collagenous layer (Waring, III et al., 1982).

Recent genetic analyses have suggested a potential role for the extracellular matrix molecule type VIII collagen in Fuchs' dystrophy, with a mutation in the $\alpha 1$

chain of type VIII collagen linked to the disease (Biswas et al., 2001). Presently, the only effective treatment for Fuchs' dystrophy is corneal transplantation.

1.5.2 Posterior polymorphous dystrophy (PPD)

Posterior polymorphous dystrophy (PPD) covers a spectrum of inherited bilateral disorders (Bourne, 2003). While normally inherited as an autosomal dominant trait with extremely variable expressivity, in some families these traits have been found to be inherited as autosomal recessive (Waring, III et al., 1982). Possible genetic loci affecting the inheritance PPD have been identified (Biswas et al., 2001; Shimizu et al., 2004). Similarly, while PPD is typically bilateral, it has also been found to be asymmetrical or unilateral, such that one cornea demonstrates advanced polymorphic changes while the other has only a small area of grouped vesicles (Waring, III et al., 1982; Anderson et al., 2001). Ultrastructural studies have shown a normal anterior banded fetal Descemet's membrane but little or no posterior homogeneous Descemet's membrane, suggesting abnormal endothelial function begins at or around the time of birth (Waring, III et al., 1982). Despite its suspected early onset, many patients remain asymptomatic and are only identified during routine ophthalmologic exams or during family studies. Rarely is there a large compromise in visual acuity, as stromal opacities and epithelial oedema are uncommon. Only occasionally does the disorder progress to a state of stromal oedema requiring corneal transplantation (Waring, III et al., 1982; Cockerham et al., 2002).

Changes associated with PPD are at the level of Descemet's membrane with clusters of discrete vesicular lesions, with faint grey halos, larger blister-like lesions with denser halos, broad bands of matrix with ridges and sheets of irregular grey material that appear as beaten metal (Waring, III et al., 1982). The lesions are scattered randomly and vary from single discrete vesicles to total corneal opacity. The lesions are also regarded as distinct from the corneal guttata noted in Fuchs' dystrophy (Waring, III et al., 1982; Cockerham et al., 2002). Close examination of the posterior collagenous layers reveals a variety of morphologies. These layers constitute the lesions in Descemet's membrane.

Though termed vesicles, electron microscopy reveals these areas as depressions or pits (Waring, III et al., 1982).

Another of the distinguishing features of PPD is the presence of two distinct populations of cells. One population of cells resembles normal endothelial cells, albeit more pleomorphic and larger than average. The second cell population is found as clusters of epithelial like cells. Under specular microscopy, these abnormal cells show extreme pleomorphism, indistinct cell boundaries and in the area of the vesicular lesions, have the appearance of a bomb crater (Waring, III et al., 1982). Electron microscopy reveals microvilli, multilaminar stratification, desmosome junctions, minimal interdigitation of cell borders and sparse organelles. These cells also stain positively for human epidermal keratin, they may appear in isolated areas, across the entire endothelium or an intermediate between the two (Bourne, 2003). Extensive proliferation of the epithelial-like cells can, in severe cases, result in diffuse corneal oedema, peripheral anterior synechiae, glaucoma and a glassy membrane on the surface of the iris. Proliferation of this epithelial-like cell makes PPD similar to ICE syndrome, but can be distinguished by identification of discrete polymophic lesions in the posterior collagenous layer, observing the disease bilaterally and the identification of PPD in family members (Anderson et al., 2001).

1.5.3 Congenital hereditary endothelial dystrophy (CHED)

CHED is a corneal dystrophy characterised by diffuse bilateral corneal clouding resulting in impaired vision (Callaghan et al., 1999; Bourne, 2003). The cause of corneal oedema, resulting in corneal clouding, is severe endothelial dysfunction that begins relatively late in embryologic development. CHED is thought to arise as a result of mesenchymal dysgenesis (Waring, III et al., 1982). An autosomal recessive (AR) form is present at birth and is relatively stationary. AR CHED has been shown to be clinically and genetically distinct from the autosomal dominant (AD) variety, which develops in the first years and may progress to severe oedema (Callaghan et al., 1999). Stromal changes consistent with long-standing oedema are present in CHED with some cases showing

greatly enlarged collagen fibrils in the stroma. Descemet's membrane ranges in thickness from a complete absence to more than 40μm in width. Cases with thin or absent Descemet's membrane suggest that complete endothelial dysfunction occurred in utero, such that only the fetal banded portion of Descemet's membrane was secreted, whereas those with a thickened Descemet's membrane suggest a persistent dystrophic endothelium that has secreted a posterior collagenous layer (Waring, III et al., 1982; Cockerham et al., 2002).

1.5.4 Iridocorneal endothelial (ICE) syndrome

There are three syndromes (essential iris atrophy, Chandler's syndrome and Cogan-Reese iris nevus syndrome) that are now recognized to be varied manifestations of the same disorder known as iridocorneal endothelial (ICE) syndrome (Waring, III et al., 1982; Bourne, 2003). Typically unilateral, although occasionally bilateral, ICE syndrome appears to be acquired between the ages of 30 and 50 years and tends to be more prevalent among women (Waring, III et al., 1982; Bourne, 2003). The appearance of the endothelial monolayer is greatly varied with cells showing a beaten metal appearance and many epithelial cell characteristics, including microvilli, expression of cytokeratin markers and decreased permeability to fluorescein (Levy et al., 1995; Levy et al., 1996; Bourne, 2003). These epithelial-like cells also have opposite reflective properties to normal endothelium, with cell junctions appearing light and cell bodies dark. Corneal epithelial cells have these same reflective properties (Bourne, 2003; Grupcheva et al., 2004).

In most cases, the abnormal cells occupy only a portion of the cornea so that there is only partial coverage of the endothelial monolayer. Demarcation between the abnormal and normal cells is evident and it has been suggested that the abnormal cells are forcing the normal endothelium into smaller spaces, because the normal cells are smaller and at a higher density in the ICE cornea than in the normal cornea (Bourne, 2003; Grupcheva et al., 2004). The epithelial-like cells spread peripherally from the cornea to the iris to form a membrane across the anterior chamber angle, which can sometimes lead to a

small bridging synechiae between the iris and the cornea (Waring, III et al., 1982; Bourne, 2003). These complications typically only occur in the more severe forms of the disease.

1.5.5 Secondary corneal endotheliopathies

There are a number of factors which can disrupt the corneal endothelium but are not classically disease. These include endothelial effects of contact lens wear and surgical procedures. Hypoxia resulting from contact lens wear is thought to be responsible for the resulting polymegathism and pleomorphism of the endothelial layer. However, studies have failed to detect reliable effects on mean endothelial cell size and barrier or pump function with long-term contact lens wear. The effects of two surgical procedures have also been well studied and shown to elicit changes in corneal endothelial cell densities. These are cataract extractions and penetrating keratoplasty (corneal transplantation).

Variable decreases in endothelial cell density are noted 1-5 days after cataract extraction, depending on trauma incurred during surgery. After initial cell loss, endothelial cell density continues to decrease at an accelerated rate up to four times greater than that in unoperated eyes, for at least 10 years (Ing et al., 1998). The causes of accelerated density decrease are unknown but may relate to decreased nutrients from the aqueous humor, decreased innervation, increased subclinical inflammation and exposure to vitreous humor (Bourne, 2003).

During corneal transplantation, the central recipient cornea is replaced with that of an allogenic donor cornea. Immediately following transplantation, endothelial cell densities decrease by amounts that depend on method and duration of corneal storage and surgical trauma. This immediate cell loss is fairly rapid but gradually decreases over several years. 53% of the preoperative endothelial cell density was found to be lost by 3 years postop. Over this time, the endothelial cells spread from recipient to donor and vice versa to cover the cornea. As the transplanted corneas age and endothelial densities decrease, the donor cornea thickens.

1.6 Corneal endothelial cell proliferation

Human corneal endothelial cells are remarkably resistant to proliferative stimuli, even when freed from the constraints of contact inhibition. The ability to drive human corneal endothelial cells into the cell cycle would raise the possibility of restoring corneal endothelial cell densities in patients in situ, and therefore have significant therapeutic potential.

1.6.1 Cell cycle

The cell cycle is composed of four phases: S-phase for DNA synthesis, M-phase for mitosis and two gap or growth phases G1 (prior to DNA synthesis) and G2 (before mitosis). In addition to these four phases, there is a resting phase termed G0, from which the cells can re-enter the cell cycle.

The cycle is regulated by a family of proteins known as cyclin-dependent kinases (CDKs), which are in turn regulated by a family of proteins known as cyclins. Different cyclin/CDK complexes are formed throughout the cell cycle as illustrated in Figure 1.6. In mammalian cells, mitogenic stimulation induces the synthesis of D-type cyclins, which are absent in G0 cells. The first cyclin/CDK complex formed in the cell cycle is pairing of a D-type cyclin with CDK4 or CDK6 (Hulleman and Boonstra, 2001; Zieske et al., 2004). As the cells progress through G1, cyclin E is synthesized and becomes associated with CDK2. This association is necessary for the transition from G1 to S-phase. As the cells progress to S-phase, cyclin E is degraded and CDK2 associates with cyclin A, the synthesis of which is initiated late in G1. Active cyclin A/CDK2 complex is required for the passage through S-phase, as it is responsible for the phosphorylation of a number of transcription factors and other proteins necessary for DNA synthesis (Hulleman and Boonstra, 2001; Zieske et al., 2004). Finally, cyclin A and cyclin B complex with CDK1. Both of these complexes appear to be necessary for the cell to complete mitosis. Cyclin A/CDK2 activity peaks in G2 and is rapidly degraded in M phase, while cyclin B/CDK2 is required for S-phase

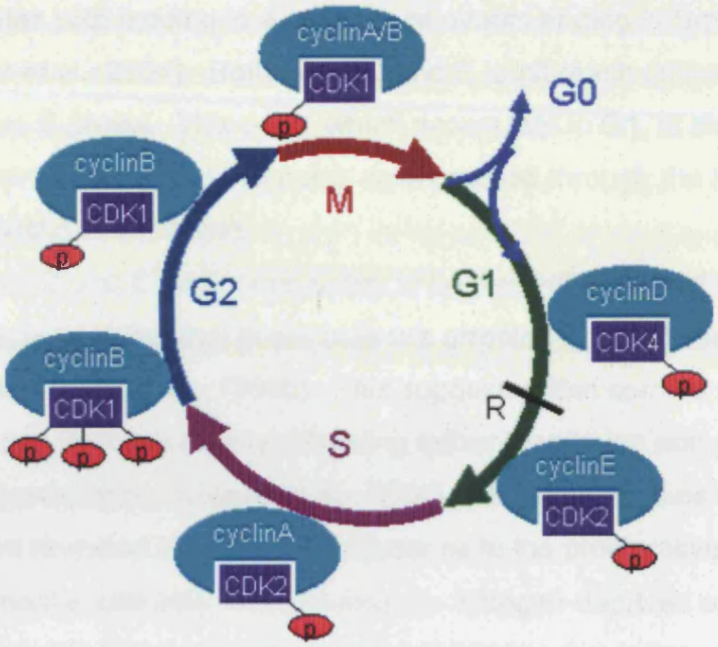

Figure 1.6: Representation of the cell cycle. The four phases of the cell cycle are the first growth phase (G1), DNA synthesis (S), second growth phase (G2) and mitosis (M). The G1 phase is contains the restriction point (R), beyond which the cell is committed to completing the cell cycle. Cyclin and cyclin dependent kinases (CDKs) associated with each of the stages of the cell cycle are illustrated at their approximate time of appearance. Additionally, some cells remain in a resting phase (G0). (adapted from: Zieske et al. 2004. Cell cycle regulators at the ocular surface. Exp. Eye Res. 78:449)

entry and exiting mitosis. There are also a number of additional cyclins and CDKs which play a lesser role in the regulation of the cell cycle (Hulleman and Boonstra, 2001; Zieske et al., 2004).

The decision to proliferate is made during the G1 phase of the cell cycle and is regulated by the cyclin D/CDK4(6) and cyclin E/CDK2 complexes. Mitogenic signals, including growth factors, trigger intracellular pathways to induce gene expression necessary for proliferation, including genes for cyclin D. Once expressed, cyclin D binds and activates CDK4(6), which phosphorylates target protein pRb. Resting cells contain a hypophosphorylated form of pRb that binds and inactivates transcription factor E2F (Joyce, 2003; Zieske et al., 2004). Phosphorylation of pRb, by the cyclin D/CDK4(6) complex, releases E2F, which stimulates a number of additional genes for DNA synthesis. One of these gene products is cyclin E, which binds to CDK2. The cyclin E/CDK2 complex also

phosphorylates pRb leading to a cascade of events ending in S-phase (Joyce, 2003; Zieske et al., 2004). Both cyclin D and E must reach critical mass before the cell enters S-phase. This point, which occurs late in G1, is also known as the restriction point and beyond this point, cells proceed through the remainder of the cell cycle (Zieske et al., 2004).

Both cyclin D and E have been noted to be present in normal corneal endothelium, suggesting that these cells are arrested in G1-phase rather than in the G0-phase (Joyce et al., 1996b). This suggested that corneal endothelial cells may be actively inhibited from proliferating rather than being non-proliferative due to a passive mechanism (Zieske et al., 2004). Additional studies of cell cycle proteins have revealed a number of insights as to the proliferative tendencies of different corneal endothelial cell populations. Mitogen-deprived or TGF-β treated cells were noted to have decreased levels of CDK4 compared to normal (Kim et al., 2001b). Conversely, SV40 transformed corneal endothelial cell lines showed elevated levels of CDK4 compared to normal (Schonthal et al., 1999). Inhibition of some protein kinase C isoforms was found to result in a decrease in levels of cyclin E, which corresponded with inhibition of corneal endothelial cell proliferation (Graham et al., 2000). Different localizations of cyclin E within the cell may also be responsible for differences in proliferative potential of rabbit and human corneal endothelium (Joyce et al., 1996b; Joyce, 2003).

In addition to positive regulatory factors, there are a number of CDK inhibitory proteins (CKI), which negatively regulate the cell cycle. There are two major families of CKI; INK4 and CIP/KIP. The INK4 family are selective inhibitors of CDK4 and CDK6, which act by binding the CDK subunit and prevent its association with cyclins (Zieske et al., 2004). Two of the INK4 family of inhibitors, p16INK4a and p15INK4b, have been localized to the corneal endothelium (Joyce et al., 1998) but were not found to have a direct role in the inhibition of proliferation in this tissue (Joyce et al., 2002). The CIP/KIP family of CKIs bind and inhibit the cyclin/CDK complexes involved in G1 and S-phase of the cell cycle. Of the three proteins making up this family, both p21cip1 and p27kip1 have been localized to the corneal endothelium. In many cell types,

p27kip1 helps to maintain cell cycle arrest in response to cell-cell contact and TGF-β (Polyak et al., 1994). p27kip1 inhibits both the cyclin D/CDK4(6) and cyclin E/CDK2 complexes and is phosphorylated and consequently degraded by the end of G1, such that the cells may progress in the cell cycle (Pagano et al., 1995; Morisaki et al., 1997). A number of recent studies have implicated p27kip1 in maintaining the corneal endothelium in a non-proliferative state. Levels of p27kip1 were found to be lower than normal in SV40 transformed cells (Schonthal et al., 1999) and also in cells stimulated with FGF-2 (Lee and Kay, 2003b). Conversely, p27kip1 was found to be upregulated when cells became contact inhibited and non-proliferative (Joyce et al., 2002).

1.6.2 Proliferative capacity of the corneal endothelium

Cell proliferation and migration of the neural crest-derived mesenchymal cells are responsible for the formation of the corneal endothelium. Proliferation of the presumptive endothelial cells ceases upon formation of cell contacts. Morphometric analyses of cell density provides evidence that, following monolayer formation, the human corneal endothelium does not replicate at a rate sufficient to replace dead or injured cells. Proliferation does not contribute significantly to cell density beyond the second trimester of gestation and it plays only a minor role in repair to the mature endothelial monolayer thereafter (Murphy et al., 1984). Instead, the corneal endothelium uses cell enlargement and migration as the major means of maintaining the monolayer. With injuries to small numbers of cells, healing involves enlargement of cells immediately adjacent to the wound site. Enlargement is initiated by membrane ruffling of the cells surrounding the wound area until they make contact with neighbouring cells. This mode of wound healing leads to a gradual flattening of the cells and the polymegathism and pleomorphism noted in aged and diseased endothelial monolayers (Sherrard, 1976). Repair of larger wounds occurs in a similar manner with a coordinated enlargement of cells adjacent to the wound, and also those cells a few rows behind the wound edge. These cells enlarge and migrate to cover the wound area without losing contact with neighbouring cells (Honda et

al., 1982; Schilling-Schon et al., 2000). This form of repair has been designated monolayer spreading (Joyce et al., 1990).

Due to the minor role played by proliferation in the wound healing response, it was suggested that corneal endothelial cells may lack proliferative capacity. Transformation with viral oncogenes to induce proliferation provides evidence that these cells do have proliferative capacity. Both the SV40 large-T antigen and E6/E7, from human papilloma virus, have been transformed into human corneal endothelial cultures to produce immortalized cells. With large numbers of population doublings, these cells retain normal morphologic characteristics and do not develop a senescent phenotype like untransfected cells (Feldman et al., 1993; Wilson et al., 1995; Bednarz et al., 2000). Further study of these cell lines revealed that populations of endothelial cells transformed with the E6/E7 proto-oncogene showed decreased telomere lengths but increased proliferation, with respect to normal cell populations (Egan et al., 1998). Telomere lengths of endothelial cells were also, on average, longer than those in corneal epithelial cells, which are known to be highly proliferative (Egan et al., 1998). Shortened telomere lengths can therefore not explain the lack of proliferation in corneal endothelial cells. The telomerase activity in corneal endothelial cells, however, may be insightful, since it is negligible in the corneal endothelium, with only low levels noted in peripheral cells (Egan et al., 1998).

The extent to which the corneal endothelium is likely to proliferate also appears to vary between species. In vivo, cell densities appear to decrease similarly with age; however, bovine, rabbit and rat endothelium have been found to proliferate readily in culture, whereas cat, monkey and human do not (Faragher et al., 1997; Joyce, 2003). Joyce et al. (1996) investigated the localization of various cell cycle proteins in both the highly proliferative rabbit corneal endothelium as well as the non-proliferative human corneal endothelium. It was found that the localization of all cyclins and cyclin dependent kinases (CDK) were the same with the exception of cyclin E, which was found in the nucleus of human corneal endothelial cells, but in the cytoplasm of rabbit corneal endothelial cells (Joyce et al., 1996a; Joyce et al., 1996b). Levels of CDK

inhibitors (CKI), p21cip1 and p27kip1, were also found to be lower in rabbit endothelium than in human endothelium (Schonthal et al., 1999). These results suggest that the mechanisms that regulate cell proliferation are controlled in different ways between species.

1.6.3 Age-related differences in proliferative capacity

Preliminary attempts to culture corneal endothelial cells revealed that cells derived from older donor tissue were more difficult to culture. Samples et al. (1991) noted human corneal endothelial cells from donors 20 years of age or younger showed a greater propensity to grow than those from older donors. Tritiated thymidine incorporation studies, used to quantify the proliferative response to wounding in young and old corneas, indicated that the younger specimens showed more proliferation (Simonsen et al., 1981). Proliferative capacity, however, was shown to be retained regardless of age with a modest degree of proliferation also occurring in an 89 year old donor (Simonsen et al., 1981). Further studies indicated that some of these differences may be related to the kinetics of cell cycle progression. Cells from older donors were found to enter the cell cycle more slowly than those from younger donors. It has also been suggested that a stronger mitogenic stimulus is required to induce cell proliferation in older donors (Senoo and Joyce, 2000).

1.6.4 Signals affecting proliferation in the corneal endothelium

There are a number of positive and negative regulatory factors which influence corneal endothelial cell proliferation, including the presence or absence of growth factors, cell contact and extracellular matrix. The combination of factors present at any time may determine the likelihood of the cell to proliferate. By understanding these mechanisms, it is hoped that we may be able to overcome the non-proliferative nature of the corneal endothelium.

1.6.4.1 Growth factors induce corneal endothelial cell proliferation

In vivo, the corneal endothelium is known to be bathed in aqueous humor containing a number of growth factors. These include fibroblast growth factor (FGF), epidermal growth factor (EGF), transforming growth factor β (TGF-β), insulin-like growth factor-I and –II (IGF-I and –II) and hepatocyte growth factor (HGF) (Joyce, 2003). In addition to those growth factors found in the aqueous humor, mRNAs for a number of growth factors and their receptors are expressed in corneal endothelial cells (Wilson and Lloyd, 1991). Expression of these mRNAs was found to be decreased in cultures with large numbers of cells with senescent morphology, as compared to proliferative populations (Wilson and Lloyd, 1991). It is thought that these growth factors may act in an autocrine or paracrine fashion to induce proliferation. The most extensively studied of these is basic FGF (FGF-2), which has been reported to be synthesized by the endothelium and deposited into Descemet's membrane through binding the heparan sulphate proteoglycan (Rieck et al., 1995). While some isoforms of FGF-2 remain unsecreted, the bioactive 18kDa FGF-2 isoform was found to be deposited in Descemet's membrane (Gu and Kay, 1998).

The FGFs belong to a family of multifunctional growth modulating peptides consisting of at least nine members. FGF-2 is one of the prototypic members of this family and is 10 to 100 fold more potent than FGF-1 in the eye (Gospodarowicz et al., 1977; Mason, 1994). One of the main features of FGFs is their high affinity for heparin. FGF also has a high affinity for its cell surface receptor, which is a single chain transmembrane glycoprotein containing a phosphotyrosine kinase (PTK) domain. Binding of FGF to its receptor has been found to trigger cell shape changes, mitosis and chemotaxis in the corneal endothelium of a number of species (Gospodarowicz et al., 1977; Landshman et al., 1987; Dabin and Courtois, 1991; Rieck et al., 1992; Grant et al., 1992; Woost et al., 1992; Hoppenreijs et al., 1994a; Rieck et al., 1995; Gualandris et al., 1996; Gu and Kay, 1998; Schilling-Schon et al., 2000; Imanishi et al., 2000).

Similar to FGF-2, the proliferative response of the endothelium to EGF has also been extensively studied. EGF is known to have a number of biological

activities, both mitogenic and non-mitogenic in nature. Its biological activities are regulated by binding to the EGF receptor, which belongs to PTK subclass I. Expression of EGF receptor mRNA was found in both proliferative and senescent cultures; however, the level of mRNA coding for EGF was decreased in senescent cells, suggesting an autocrine down-regulation (Wilson and Lloyd, 1991). Studies in numerous species have shown that while EGF is capable of inducing corneal endothelial cell proliferation in a variety of settings, the proliferative response to EGF is minimal (Gospodarowicz et al., 1977; Raymond et al., 1986; Couch et al., 1987; Brogdon et al., 1989; Lee et al., 1991; Samples et al., 1991; Grant et al., 1992; Hoppenreijs et al., 1992; Schultz et al., 1992; Woost et al., 1992; Raphael et al., 1993; Joyce et al., 1995; Imanishi et al., 2000; Mitsumoto et al., 2001).

In addition to EGF and FGF-2, the effects of a number of additional growth factors have been investigated, albeit less extensively. These growth factors include insulin (Schultz et al., 1992; Woost et al., 1992), insulin-like growth factor-1 (IGF-1) (Woost et al., 1992; Choi et al., 1995; Imanishi et al., 2000), hepatocyte growth factor (HGF) (Hoppenreijs et al., 1996; Imanishi et al., 2000; Mitsumoto et al., 2001), platelet derived growth factor (PDGF) (Hoppenreijs et al., 1994b; Kamiyama et al., 1995; Imanishi et al., 2000) and transforming growth factor-β (TGF-β) (Grant et al., 1992; Gipson and Inatomi, 1995; Imanishi et al., 2000; Chen et al., 2002). The most interesting of these is TGF-β, which has been noted to inhibit the G1/S phase transition in some cell types (Polyak et al., 1994). In order for TGF-β to exert an effect, both TGF-β receptor types I and II must be expressed (Wrana et al., 1994). Binding of ligand to TGF-β receptor II recruits TGF-β receptor I to form a complex, which then stimulates phosphorylation and intracellular signalling. Another receptor subtype, TGF-β receptor III, is not thought to participate directly in signal transduction but cooperates with the other receptor subtypes for signalling by TGF-β2, which otherwise has a low affinity for TGF-β receptor II. TGF-β1 was reported to be expressed by human corneal endothelium and TGF-β2 is known to be present in relatively high concentrations in aqueous humor (Cousins et al., 1991). RT-PCR

also demonstrated that all three TGF-β receptor subtypes are expressed in human (Joyce and Zieske, 1997) and rabbit corneal endothelial cultures (Harris and Joyce, 1999). Proliferation studies using TGF-β1 and TGF-β2 showed that both isoforms suppress proliferation in serum and FGF-stimulated cells (Chen et al., 1999; Harris and Joyce, 1999). Aqueous humor, at a dilution 1/10, showed a similar inhibition of proliferation, which was obliterated by pre-treatment with anti-TGF-β2 antibodies (Chen et al., 1999). These data suggest that, under normal conditions, TGF-β1, acting in autocrine/paracrine manner, and TGF-β2, from the aqueous humor, may be partially responsible for maintaining the G1-phase arrest of corneal endothelial cells (Joyce, 2003). Part of these actions may be due to effects of TGF-β on a cell cycle inhibitor, p27kip1 (Kim et al., 2001a; Kim et al., 2001b).

1.6.4.2 Cell contact

Contact-dependent inhibition of proliferation is common in many cell types. High cell densities induce cell cycle arrest even in the presence of mitogenic factors (Kato et al., 1997). Compelling evidence from a number of studies have shown that stable cell-cell contacts modulate gene expression, cell proliferation and differentiation (Matter and Balda, 2003). While the details remain unclear, expression levels of tight junction proteins, like ZO-1 have been shown to increase in cells at high density (Balda et al., 2003). Similarly, overexpression of ZO-1 in subconfluent cultures inhibits proliferation (Matter and Balda, 2003). The transcription factors ZONAB and CDK4 become sequestered at TJ in confluent cultures, thereby inhibiting their actions (Balda and Matter, 2000).

As maintenance of cell contact is vital to the functions of the corneal endothelial monolayer, it seems likely that cell-cell contact within the monolayer may play a role in establishing cell cycle arrest. Evidence in support of this hypothesis was first discovered in wound healing models, which showed small numbers of proliferating cells at the edge of the wound, following growth factor treatment. Cells distal to the wound, however, did not proliferate with the same treatment (Landshman et al., 1989; Huang et al., 1989; Hoppenreijs et al., 1992;

Hoppenreijs et al., 1994a; Hoppenreijs et al., 1994b; Petroll et al., 1995; Imanishi et al., 2000). Since the exposure of both cell populations to mitogen was similar, it is hypothesized that the difference in proliferation between cells at the wound edge and those distal to the wound was due to the lack of cell contact of cells at the wound edge. Additionally, releasing cell contacts, with the use of calcium chelators, and treatment with growth factors, was found to induce cell proliferation in a proportion of endothelial cells on the cornea, while treatment with growth factor alone did not (Senoo et al., 2000). These results further support the idea that cell contact plays an important role in maintaining cell cycle arrest of the corneal endothelium.

1.6.4.3 Extracellular matrix

The extracellular matrix (ECM) produced by cells is their natural substrate upon which to migrate, proliferate and differentiate in vivo. The importance of the ECM for normal growth and development in vivo is well established. The components of the corneal endothelial cell matrix, Descemet's membrane, are extensive and include matrix proteins, glycosaminoside and growth factors. All or some of these may contribute to the inhibition of proliferation in the corneal endothelium. Cancer cell lines seeded onto matrix generated by bovine corneal endothelial cells generated contact-inhibited monolayers with a regular morphology and appearance, supporting the idea that ECM plays a role in the regulation of the corneal endothelial monolayer (Fridman et al., 1985). In addition, alterations in matrix expression during injury or wound healing suggest that matrix proteins play a role in migration or proliferation (Ohkoshi et al., 1989). Expression of fibronectin by corneal endothelial cells was found to decrease with injury (Kenney et al., 1986), whereas expression of type I collagen was induced by polymorphonuclear cells, present during inflammatory responses (Kay et al., 1985). In addition, both TGF-β1 and TGF-β2, known to regulate the cell cycle, were shown to induce up regulation of fibronectin and laminin (Usui et al., 1998). A number of studies have also examined the effects of matrix proteins on the proliferative response. Increased proliferation of human and rabbit corneal

endothelial cells cultured on bovine corneal endothelial cell matrix was observed (Gospodarowicz and III, 1980; Blake et al., 1997) and, in some cases, the addition of growth factors produced further proliferative effects. Thus, the proliferative response of rabbit corneal endothelial cells was unaffected by FGF-2 (Gospodarowicz and III, 1980), whereas that of human corneal endothelium was enhanced by keratinocyte growth factor (KGF) or endothelial cell growth supplement, but unaffected by EGF or HGF (Blake et al., 1997). The proliferation of bovine corneal endothelial cells cultured on various matrices demonstrated the greatest response on fibronectin > laminin > tissue culture plastic > type I collagen > type IV collagen. The overall surface area covered by cells on these matrices, however, was found to be greatest for cultures grown on type IV collagen > type I collagen >> fibronectin > laminin > tissue culture plastic, with type IV and type I collagen showing the largest number of giant cells (Mitsumoto et al., 2001). These results suggest that different matrices may aid in the maintenance of the monolayer by enhancing either cell proliferation or cell spreading. The primary wound healing response of cell spreading may be partially explained by the fact that Descemet's membrane is primarily composed of type IV collagen. The proliferation of cells cultured on type IV collagen, however, was shown to be greatly enhanced with growth factor stimulation. Both EGF and HGF enhanced the proliferative response of cells cultured on type IV collagen, while treatment with TGF-β1, greatly decreased proliferation (Mitsumoto et al., 2001).

Despite the species-specific differences in these observations, the picture that emerges is one in which a combination of growth factors, extracellular matrix and cell contact all contribute to the proliferative response of the corneal endothelium in situ.

1.6.5 Intracellular signalling

In order to understand the reasons why the corneal endothelium remains in its non-proliferative state, studies have attempted to dissect signalling pathways that might overcome the mitotic block and lead to corneal endothelial cell

proliferation. The proliferative response of rabbit corneal endothelium is the best studied of all species. Lee et al. (2004) suggest that FGF-2 is responsible for the endothelial mesenchymal transformation. This proposed transformation involves not only proliferation but also cell shape changes and altered collagen expression. Prolonged and continuous exposure to FGF-2, for a period of at least 16 hours, was shown to increase rabbit corneal endothelial cell proliferation by approximately 60% (Kay et al., 1993; Kay et al., 1994). Initial studies suggested phospholipase Cγ1 (PLCγ1) signalling to be important, with antisense oligonucleotides able to inhibit basal levels of proliferation by 25% (Gu et al., 1996). Further studies, however, indicated that the effects of PLCγ1 may be more related to changes in cell shape, than the proliferative response (Kay and Oh, 1988; Gu et al., 1996; Kay et al., 1998). Kay et al. (1998) showed that the SH2 domains of PLCγ1 bind the FGF receptor, while the SH3 domain of PLCγ1 targets the cytoskeletal protein vinculin, bringing the two together. Antisense oligonucleotides generated against PLCγ1, however, could not override the mitogenic actions of FGF-2, suggesting that this may not be a major intracellular pathway involved in the mitogenic actions of FGF-2 (Gu et al., 1996). More recent studies have shown the phosphotidylinositol 3- kinase (PI3 kinase) pathway to be vital for FGF-2 mediated proliferation and migration (Kay et al., 1998; Rieck et al., 2001; Lee and Kay, 2003b; Lee et al., 2004). The selective PI3 kinase inhibitor, LY294002, completely blocked the proliferative response of rabbit corneal endothelial cells to FGF-2. Additionally, FGF-2 was shown to activate the PI3 kinase pathway with induction of phosphatidylinositol-3-phosphate (PI3P) and phosphorylation of Akt, two major downstream targets of PI3 kinase (Lee and Kay, 2003b). Lee et al. (2003) also found that treatment with FGF-2 increased protein levels and nuclear translocation of CDK4, indicating entry into the cell cycle. Consistent with this, levels of p27Kip1 were decreased due to increased phosphorylation and degradation of the protein following treatment with FGF-2 (Lee and Kay, 2003b). Antisense oligonucleotides targeting p27Kip1 have been shown to induce rat corneal endothelial cell cultures to proliferate (Kikuchi et al., 2004). p27Kip1 is also

thought to play a role in mediation of cell cycle arrest during the maturation of the endothelial monolayer (Joyce et al., 1998). Further studies in rat corneal endothelium suggest that protein kinase C (PKC) plays a role in serum-induced proliferation, as PKC inhibitors, and antisense targeting PKCα, significantly reduced proliferation and levels of cyclin E (Graham et al., 2000).

Studies of bovine corneal endothelium indicate that Ras may also play an important role in the proliferative response (Sosnowski et al., 1993). Activation of GTPases such as Ras, by FGF-2, was found to lead to changes in the F-actin cytoskeleton. FGF-2 treatment induced a phenotype with abundant stress fibres (Lee and Kay, 2003a). Disruption of cytoskeletal organization may aid proliferation, as disruption of microfilaments has been shown to induce mitosis in corneal endothelial monolayers (Gordon, 2002). Serum-induced proliferation was also found to increase the expression of immediate early genes c-fos (Feldman et al., 1992) and c-jun (Nguyen et al., 1994).

1.7 Project aims

Human corneal tissue that cannot be used for transplantation makes up the tissue available for research. While the annual number of corneal grafts in the UK has remained fairly constant over the past decade, the number of corneas donated to UK Eye Banks has been in slow decline (Figure 1.7). The small number of corneas available for research has necessitated the development of animal models of the human corneal endothelium. Currently, the most commonly used models include rat, rabbit and bovine corneal endothelium, all of which are known to be highly proliferative. Among the primary goals of this project was the development of a more reliable model for the human corneal endothelium. The culture of primary mouse corneal endothelium has been previously explored and SV40 transformed cell lines have been established (Joo et al., 1994). The methodology described by Joo et al. (1994) for the culture of mouse corneal endothelium relies on difficult microdissection techniques and descriptions of primary mouse corneal endothelial cell cultures are almost non-existent.

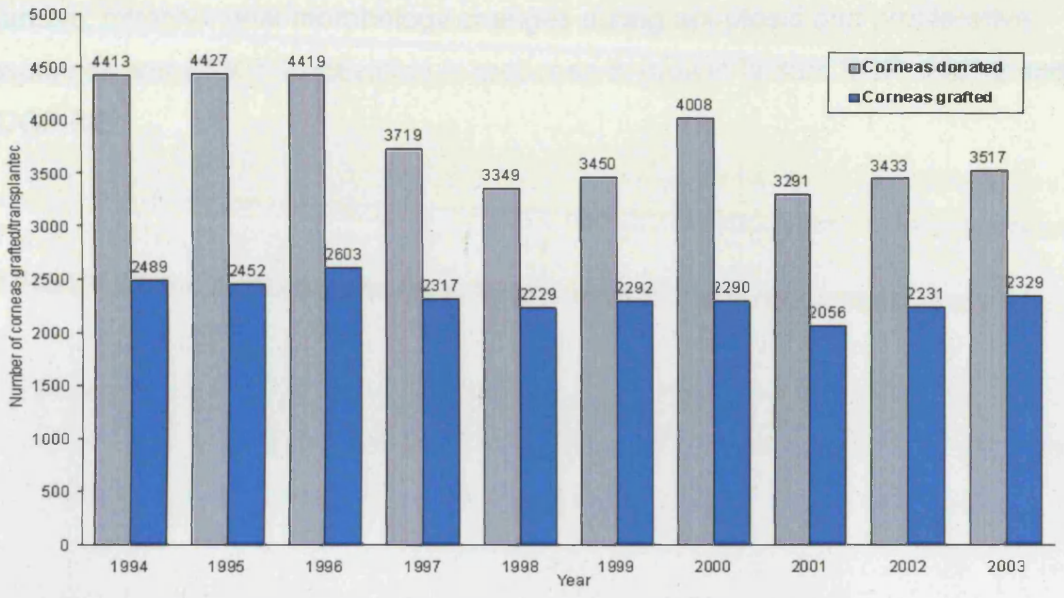

Figure 1.7 Numbers of corneas donated and corneas grafted in the UK from April 1993 – March 2003. While the numbers of corneas grafted each year has remained fairly constant, the numbers of corneas donated has been slowly decreasing. (from: Transplant activity in the UK 2002-2003, NHS UK Transplant)

One study revealed a similar propensity of both primary and SV40 transformed mouse corneal endothelial cells to adhere to Descemet's membrane and similar levels of EGF receptor and PDGF receptor expression (Joo et al., 1994). Primary mouse corneal endothelial cell cultures were also reported to stop proliferating by the third passage (Joo et al., 1994). Given these details, our goal was to establish a novel, simpler method of primary mouse corneal endothelial cell culture, which would yield reproducible and sufficiently pure cultures for research. Further characterisation of primary mouse cultures would then allow for meaningful comparisons between mouse and human corneal endothelium, and determine whether mouse cultures provide an appropriate model of the human endothelium. In addition, the culture of mouse corneal endothelial cells would open up the possibility of using the numerous transgenic and knockout strains of mice available to investigate corneal endothelial cell biology. Characterisation of the primary mouse corneal endothelial cell cultures would

involve localization of junctional proteins, expression of various apoptotic markers, mitochondrial morphology changes during apoptosis and proliferative responses and ERK 1/2 activation in response to growth factors EGF, FGF-2 and PDGF BB.

Chapter 2: Materials and Methods

2.1 Tissue Culture of Mouse Corneal Endothelial Cell Line

Immortalized mouse corneal endothelial cells were a gift from Dr. J. Wayne Streilein (Schepens Eye Research Institute, Boston). Cells were maintained in Minimum Essential Media with Earle's salts (Life Technologies) containing 10% fetal bovine serum (Life Technologies), 2mM L-glutamine (Life Technologies), 1% penicillin/streptomycin (Life Technologies), 1mM sodium pyruvate (Life Technologies) and 1% MEM vitamin solution (Life Technologies) at 37°C and 5% CO_2. Cells were split 1 in 5 at confluence, approximately every 3 to 5 days.

2.2 Primary Mouse Corneal Endothelial Cell Culture

The outer surfaces of mouse corneas were covered with 70% ethanol and the epithelial cell layers were scraped off using a razor blade. Eyes were enucleated from the mouse and washed for approximately 1 minute in povidone iodine, then dipped in 70% ethanol before dissecting the cornea from the eye in PBS. Corneas, free of epithelium, were placed endothelium side down onto tissue culture dishes. Approximately 5 drops of tissue culture media were carefully placed on top of each cornea. Corneas were incubated at 37°C and 5% CO_2 overnight to allow the endothelial cells to attach to the tissue culture dish. The following day, 1ml of culture media was slowly added to each cornea. Endothelial cell proliferation and migration from the cornea onto the tissue culture dish was monitored daily by microscopy (Figure 2.1A). Corneas were removed from the tissue culture dish after approximately 3 to 7 days in culture, dependent upon the rate of migration and proliferation of corneal endothelial cells onto tissue culture dishes. Growing cell populations were also monitored to ensure homogeneous cultures of corneal endothelial cells free of keratocytes. Following removal of corneas, endothelial cells were maintained at 37°C and 5% CO_2 for at least 2 weeks before use (Figure 2.1B). During this time, the tissue culture

media was changed approximately every 4 days. Culture media used for primary corneal endothelial cell culture was the same as that used for the SV40 transformed mouse corneal endothelial cell line.

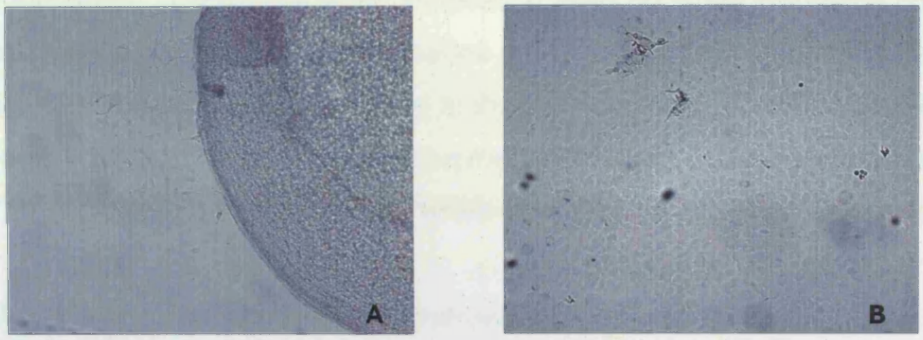

Figure 2.1: Primary mouse corneal endothelial cell culture. (A) Cornea placed endothelial side down to allow the endothelial cells to migrate out onto tissue culture plastic. (B) Once the cornea is removed, endothelial cells are allowed to proliferate to form a monolayer with classic hexagonal shape.

2.3 Primary Human Corneal Endothelial Cell Culture

Human corneal tissue was obtained from the eye banks in Moorfields Eye Hospital and CTS Eye Bank, Bristol. Tissue from Moorfields Eye Hospital had been maintained in Optisol-GS at 4°C for at most 2 weeks, while tissue from Bristol was organ cultured at 34°C in Chen's media according to EU regulations for at most 4 weeks. Irrespective of storage conditions, the corneas were transferred to Media 199 for at least an hour prior to dissection. For dissection, the cornea was placed on a 10 cm dish and Descemet's membrane was slowly peeled away from the corneal stroma. Pieces of Descemet's membrane, containing corneal endothelial cells, were placed in 1 ml of 0.02% EDTA solution and incubated for 1-2 hours at 37°C. Following incubation, the solution was triturated at least 50 times in a flame polished glass pipette. Cells were pelleted by centrifugation at 1000g for 5 minutes. Without disturbing the cell pellet, the EDTA solution was removed and cells were resuspended in 500 μl of growth media (Optimem-I media (Invitrogen) containing 10% FCS (Invitrogen), 200 μg/ml $CaCl_2$ (Sigma), 0.08% chondroitin sulfate (Sigma), 20 μg/ml ascorbic acid

(Sigma), 1/100 multiple vitamin solution (Invitrogen), 1/200 gentamicin (Invitrogen), 1/100 antibiotic/antimycotic solution (Invitrogen), 50 mg pituitary extract (Biogenesis), 5 ng/ml EGF (CN Bioscience) and 20 ng/ml NGF (Biogenesis)). Cells were again titurated at least 50 times in a flame polished glass pipette before plating onto dishes pre-coated with FNC coating (Athena ES). Cells were allowed to adhere to the culture dish and proliferate for approximately 1 week before the first media change. Cells were maintained at 37°C and 5% CO_2 and split 1 in 2 when confluent.

2.4 Reverse Transcriptase Polymerase Chain Reaction

2.4.1 Extraction of total RNA

Confluent 10 cm dishes of cells were used to extract RNA. Total RNA was extracted from corneal endothelial cells using the RNeasy kit according to the manufacturers instructions (Qiagen). Briefly, tissue culture media was discarded and dishes were placed on ice. 500μL of buffer RLT was added to each dish. Cell scrapers were used to remove all the cellular debris and the lysate was passed through a 21 gauge needle at least 5 times to shear the DNA. 1 volume (500 μl) of 70% ethanol was added to the homogenized lysate, and samples were mixed by pipetting up and down. 700 μl of lysate was added to an RNeasy mini spin column in a 2 ml collection tube. Tubes were pulse spun for approximately 30 seconds at 4°C, and flow-through was discarded. 700 μl of wash buffer RW1 was added to the RNeasy mini spin column. Following a pulse spin at 4°C, the collection tube and flow-through were discarded, and the RNeasy mini spin column was transferred to a new collection tube. 500 μl of buffer RPE was added to the spin column, and flow-through was discarded following a pulse spin at 4°C. A final wash of 500 μl of buffer RPE was added to the spin column, and the column was centrifuged at full speed for 2 minutes at 4°C to dry the membrane. Flow through was discarded and the empty spin column was cold centrifuged at full speed for 1 minute. The RNeasy mini spin column was then added to a 1.5 ml collection tube and 50 μl of RNase-free water

was added directly to the membrane. The column was cold centrifuged again at full speed for 1 minute to elute RNA. The concentration of RNA obtained was determined using an Eppendorf BioPhotometer.

2.4.2 Generation of cDNA

Generation of cDNA from total RNA was accomplished using the ProSTAR First-Strand RT-PCR kit (Stratagene). 10 μg of total RNA was used for each reaction. RNA was diluted to a final volume of 38 μl with DEPC-treated water. 3 μl of random primers (100 ng/ml) was added to each of the reactions. Reactions were mixed gently before incubation at 65°C for 5 minutes, followed by slow cooling to room temperature (approximately 10 minutes), to allow annealing of primers to RNA. For first strand synthesis, the following components were added to each reaction in order:

5 μl of 10x first strand buffer
1 μl of RNase Block Ribonuclease inhibitor (40 U/μl)
2 μl of 100 mM dNTPs (mix of all 4)
1 μl of StrataScript reverse transcriptase (50 U/μl)

Reactions were gently mixed and incubated at 42°C for 1 hour, followed by incubation at 90°C for 5 minutes. Completed first strand cDNA reactions were placed on ice for immediate use in PCR reaction or kept at -20°C for storage.

2.4.3 Polymerase Chain Reaction

Different annealing temperatures and elongation temperatures, as well as different primers, were used for different PCR reactions. Primers were designed for PCR amplification of α1 type VIII collagen in mouse and human corneal endothelial cell cultures. Primers targeting the β-actin sequence were used as a positive control. While these primers were designed to target the human β-actin

sequence, there was minimal mismatch of base pairs, such that the primers were also suitable for the mouse β-actin sequence.

Mouse type VIII collagen

COL8A1_forward 5' – cca gga cct cat gga ctt cc – 3'

COL8A1_reverse 5' – ctc ggc cca aga acc cca gg – 3'

Human type VIII collagen

COL8A1_forward 5' – gtt cca tca ggc tca ttc ag – 3'

COL8A1_reverse 5' – tcc ttt tgc ccc agg cat – 3'

β-actin

bact_forward 5' – **t**aa **g**ga gaa gct gtg cta **c**g – 3'

bact_reverse 5' – **g**gc agt **g**at ctc ctt ctg c – 3'

* highlighted, bold bases are those that differ between the human and mouse β-actin sequence

2.5 Immunofluorescence staining

2.5.1 Methanol fixation of cells

Cells were incubated on ice for 3 minutes. Cell culture medium was removed and cold methanol was added to fix the cells. Dishes of cells were incubated at -20°C for approximately 5 minutes. Cells were placed back on ice as the methanol was removed. Room temperature phosphate buffered saline (PBS) was added to rehydrate the cells. Cells were incubated in PBS at room temperature for approximately 5 minutes. Following rehydration, cells were incubated in a blocking solution containing 2% BSA in PBS, for approximately 30 minutes at room temperature.

2.5.2 Methanol fixation of whole corneal tissue

Corneas were fixed in cold methanol for 10 minutes at -20°C. Rehydration of the tissue using PBS was accomplished with 3 washes of 10 minutes each, at room temperature. Overnight treatment with 1% Triton-X100 solution in PBS was used to permeabilize the tissue, followed by an hour incubation in blocking solution, containing 4% BSA and 1% Triton-X100 in PBS.

2.5.3 Paraformaldehyde fixation of cells

Culture medium was removed and cells were treated with 3% paraformaldehyde solution for 15-30 minutes at room temperature. PBS was used to wash remaining paraformaldehyde from the cells prior to blocking with 2% BSA in PBS for approximately 30 minutes at room temperature.

2.5.3 Staining and Imaging

After blocking, primary antibody was used to target the proteins of interest. Dilutions of primary antibodies were routinely made in blocking solution. A list of antibodies used, the dilutions of antibody and sources of antibodies are listed in Table 2.1. Cells were treated with primary antibody for approximately 1-2 hours at room temperature. Following incubation with primary antibody, cells were washed 3 times with PBS before incubation with secondary antibody. For whole tissue staining, each wash was at least 10 minutes duration. Whole tissue staining also required another 10 minute treatment in block solution prior to secondary antibody. All secondary antibodies were used at a 1/500 dilution in PBS and incubated with the cells for at least an hour at room temperature. All secondary antibodies were coupled to Alexa fluorophores (Molecular Probes). In addition to secondary antibodies, occasionally a nuclear stain or actin stain would also be added to the cells during incubation with secondary antibody. Nuclear stains used included propidium iodide (Sigma, 5 mg/ml) used at 1/2000 dilution, To-Pro-3 (Molecular Probes, 1 mM) used at 1/500 dilution or DAPI (Sigma, 5 mg/ml) used at 1/100. Rhodamine phalloidin (Molecular Probes) was used at a dilution of 1/60 to stain actin.

Following treatment with secondary antibody, cells were washed 3 times with PBS and mounted with Vectashield (Vector Labs). Each wash for whole tissue samples was at least 10 minutes duration. Typically, staining of cells was imaged immediately using a confocal fluorescence microscope (Zeiss, Axiovert S100 TV) equipped with a Ne, He laser and software (Lasersharp 2000). Staining of whole tissue was imaged the following day using a confocal fluorescence microscope (Leica DMIRE2, sp2AOBS) with software (LCS version 2.v).

Table 2.1 List of primary antibodies used for immunofluorescence staining.

Antibody target	Species	Dilution	Source
Antibody 9.3E	Mouse	1/100	Dr. J. Bednarz
Claudin-1	rabbit	15 μg/ml	Zymed
Lamin B	goat	1/50	Santa Cruz
Occludin	mouse	1/200	Zymed
Pan-cadherin	rabbit	1/300	Sigma
PAR-3	rabbit	1/100	Zymed
Paxillin	rabbit	1/60	Santa Cruz
Phospho-ERK	mouse	1/1000	Sigma
ZO-1	mouse	20 μg/ml	Zymed
ZO-1	rabbit	1/400	Dr. Karl Matter
ZO-2	rabbit	1/500	Dr. Karl Matter

2.6 Live cell imaging using confocal microscopy

Live cell imaging was used to image mitochondrial morphology changes during staurosporine induced apoptosis. Cells were loaded with 300 nM Mitotracker Red (Molecular Probes) in growth media at 37°C for approximately 10 minutes. Once loaded, cells were washed twice in PBS and maintained in MEM with Earle's salts without phenol red (Life Technologies). Apoptosis was induced with 200 nM staurosporine in primary cells and 500 nM staurosporine in

the cell line. Images were captured approximately every 10 minutes to examine changes in mitochondrial morphology. Images were captured using a confocal fluorescence microscope (Zeiss, Axiovert S100 TV) equipped with a He laser and software (Lasersharp 2000).

2.7 Western blotting

Cultured cells were treated with growth factors, inhibitors or left untreated before lysing cells. Lysates were made using a 2x reducing sample buffer (125 mM Tris pH 8.0, 20% glycerol, 2% SDS and 350 mM DTT). Samples were forced through a 21G needle and heated to 95°C for at least 5 minutes before loading onto a 10% SDS-PAGE gel. Gels were run at 150V for approximately 90 minutes before transferring proteins to a P-Hybond membrane (Amersham). Membranes were treated with a blocking solution of 5% powdered milk in PBS for at least half an hour. Primary antibody solutions were prepared in blocking solution and membranes were incubated in primary antibody for at least an hour. A list of antibodies used and their dilutions can be found in Table 2.2. Following treatment with primary antibody, membranes were washed 3 times with PBST (PBS containing 0.2% Tween-20). Secondary antibody solutions were prepared in PBST and incubated with membranes for at least an hour. Following treatment with secondary antibody, membranes were treated to five 5 minute washes in PBST. Excess PBST was allowed to drip off the membranes and each blot was treated with 2 ml of ECL reagent (Amersham). Blots were imaged using the FujiFilm LAS-1000 system with Image Reader LAS-1000 software.

2.8 Proliferation assay

To examine the regulation of the corneal endothelial cell proliferative response, cells were treated with growth factors for 24 or 48 hours. Cells entering the cell cycle during this time were marked with 5-bromo-2-deoxyuridine (BrdU) (Sigma). Because BrdU is a thymidine analog, it is incorporated into DNA

Table 2.2 Primary and secondary antibodies used for western blotting

Primary antibodies	Dilutions	Source
α-tubulin	1/1000	Zymed
Apaf-1	1/250	Cell Signalling Technologies
Bad	1/500	Cell Signalling Technologies
Bax	1/250	Cell Signalling Technologies
Bcl-2	1/500	Cell Signalling Technologies
Bcl-X	1/500	Cell Signalling Technologies
BRUCE	1/250	Cell Signalling Technologies
CAS	1/1000	Cell Signalling Technologies
Caspase-2	1/1000	Cell Signalling Technologies
Caspase-3	1/1000	Cell Signalling Technologies
Caspase-7	1/1000	Cell Signalling Technologies
DFF45	1/500	Cell Signalling Technologies
FADD	1/250	Cell Signalling Technologies
Fas	1/5000	Cell Signalling Technologies
Fas-L	1/500	Cell Signalling Technologies
hILP	1/250	Cell Signalling Technologies
Mcl-1	1/1000	Cell Signalling Technologies
Nip-1	1/250	Cell Signalling Technologies
p53	1/500	Cell Signalling Technologies
PARP	1/500	Cell Signalling Technologies
RIP	1/1000	Cell Signalling Technologies
TRADD	1/250	Cell Signalling Technologies
Phospho-ERK	1/200	Santa Cruz
Secondary antibodies	**Dilutions**	**Source**
Anti-mouse	1/2000	Dako
Anti-mouse	1/5000	Santa Cruz
Anti-rabbit	1/2000	Dako
Anti-rabbit	1/5000	Santa Cruz

during S-phase and can therefore be used as a reporter of cell proliferation. Untreated cells served as a negative control, while cells treated with normal growth media, containing 10% serum, were used as a positive control.

In order to determine the intracellular pathways involved in these proliferative responses, cells were treated concomitantly with both growth factor and inhibitiors of various intracellular pathways. Again, cells entering the cell cycle were marked with BrdU.

2.8.1 Treatment of cells

All cells were maintained in media containing 100 μM BrdU for the duration of the experiment, either 24 or 48 hours. As previously mentioned, cells in base media, containing no serum or growth factors, were used as a negative control, while cells in base media, containing 10% serum, were used as a positive control. Concentrations of growth factors and inhibitors used are listed in Table 2.3.

Table 2.3 Growth factors and inhibitors used in proliferation assays

Treatment	Concentration used	Source
Epidermal growth factor (EGF)	100 ng/ml	CN Bioscience
Basic Fibroblast growth factor (FGF-2)	25 ng/ml	R & D
Platelet-derived growth factor BB (PDGF BB)	50 ng/ml	R & D
LY294002	20 μM	Calbiochem
PD980059	50 μM	Calbiochem
Genistein	100 μM	Calbiochem

2.8.2 Fixation and staining of cells

Treatment media containing growth factors were removed and cells were fixed in cold methanol for 10 minutes at -20°C. Remaining methanol was washed away with PBS and cells were treated with 1.5 M HCl for 30 minutes at room temperature, to denature DNA. Four washes of PBS, 10 minutes each, were used to wash away the remaining HCl before incubation in blocking solution

(1% BSA in PBS) for at least 30 minutes. A monoclonal anti-BrdU antibody (Amersham) was used to visualize cells which had entered the cell cycle during the experiment. Cells were incubated with anti-BrdU antibody for at least an hour at room temperature. Three washes with PBS were used to remove remaining primary antibody. Alexa Fluor 488 chicken anti-mouse IgG (Molecular Probes) was used at a dilution of 1/500 to detect BrdU positive nuclei. Cells were also treated with propidium iodide (1/2000) for at least an hour. Three washes with PBS were used to wash away remaining secondary antibody and propidium iodide.

2.8.3 Imaging, cell counting and statistical analysis

Nuclei were imaged on a Leica DM1L microscope with epifluorescence. Images were captured using Leica DC Viewer software. Captured images represented the entire field of cells. Images were transferred to software program Metamorph-4 and the proportion of BrdU positive nuclei as a percentage of the total population was determined. Information was combined in an Excel spreadsheet and significance was determined using unpaired Student's T-test.

Chapter 3: Characterisation of primary mouse corneal endothelial cell cultures

Due to the scarcity of human corneal tissue available for research, there is a need to investigate and establish alternative models for human corneal endothelium. The majority of studies of corneal endothelium have been conducted using bovine, rabbit and rat corneal endothelium. These species have advantages for experimentation as they provide relatively large, accessible amounts of tissue. None of these species, however, has proved to have an endothelium representative of human corneal endothelium. Bovine corneal endothelium is valuable as the corneas are large and it is therefore possible to obtain large numbers of corneal endothelial cells. However, it is increasingly difficult to obtain neurally derived bovine tissue, such as eye tissue, for research due to safety concerns relating to Bovine Spongiform Encephalopathy (BSE). Rabbit corneal endothelium is useful because of its propensity to proliferate though this markedly differentiates it from human corneal endothelium (Joyce et al., 1996). Rat corneal endothelium is similar to rabbit corneal endothelium in being highly proliferative. Rat corneal endothelial cultures also deviate from human corneal endothelium in that the cells become elongated and take on an increasingly fibroblastic appearance, even within the monolayer (Joyce et al., 1998). Because none of these models reliably represent the human corneal endothelium, there is a need to identify alternative models that may be useful for future research. Mouse corneal endothelium has been proposed as a potential model for human corneal endothelium, since this would have the benefit for further investigations using genetically modified animals. The major impediment of using mouse corneas is their extreme small size and consequent difficulties of microdissection and isolation. This also results in limited cell numbers for culture. Only one study has described a culture technique for mouse corneal endothelial cells, but the methodology requires extremely complicated microdissection techniques (Joo et al., 1994). A relatively simple experimental strategy for the derivation of mouse corneal endothelial cells that would yield

reproducible and sufficiently pure cultures would therefore be valuable. These primary cultures could then be compared to an SV40 transformed mouse corneal endothelial cell line, which is currently the only widely used mouse model. Because relatively little is known about primary mouse corneal endothelial cultures, it remains to be seen whether the SV40 transformed cell line is in fact a suitable, representative cell line for corneal endothelial cell research.

3.1 Mouse corneal endothelial cell morphology

The first goal was to devise a rapid and technically straight forward technique for the generation of primary mouse corneal endothelial cell cultures. Explant cultures of mouse corneal endothelium were established by placing the cornea, denuded of epithelium, onto tissue culture plastic. Endothelial cells, in contact with plastic, migrated away from the corneal button, and limited cell proliferation resulted in a small, ring-shaped, monolayer of cells (Figure 3.1A). Cells required 2 to 7 days to migrate off the cornea onto the tissue culture dish, with most migration occurring after 3 to 5 days. At this point the corneas were removed from the tissue culture dish and the cells cultured for at least a further two weeks before beginning experiments. The morphology of the cells migrating off the cornea differed from the morphology of cells composing the intact monolayer (Figure 3.1A-C). Migrating primary mouse corneal endothelial cells tended to have an elongated phenotype, frequently with three projections, giving the cells a triangular shape. Two of these projections were typically short and located close to the cell nucleus, while the final projection tended to be elongated, extending away from the cell body. Subconfluent cultures of SV40 transformed mouse corneal endothelial cells showed a similar phenotype to migrating primary cells but displayed a more variable number of cytoplasmic projections from the cell body (Figure 3.1D). As the cells became more densely packed, the cell phenotype shifted to a more typical endothelial appearance, resembling a cobblestone-like monolayer. However, cells in culture were not as regular and hexagonal in shape as cells on an intact, healthy cornea (Figure 3.1B,C,E).

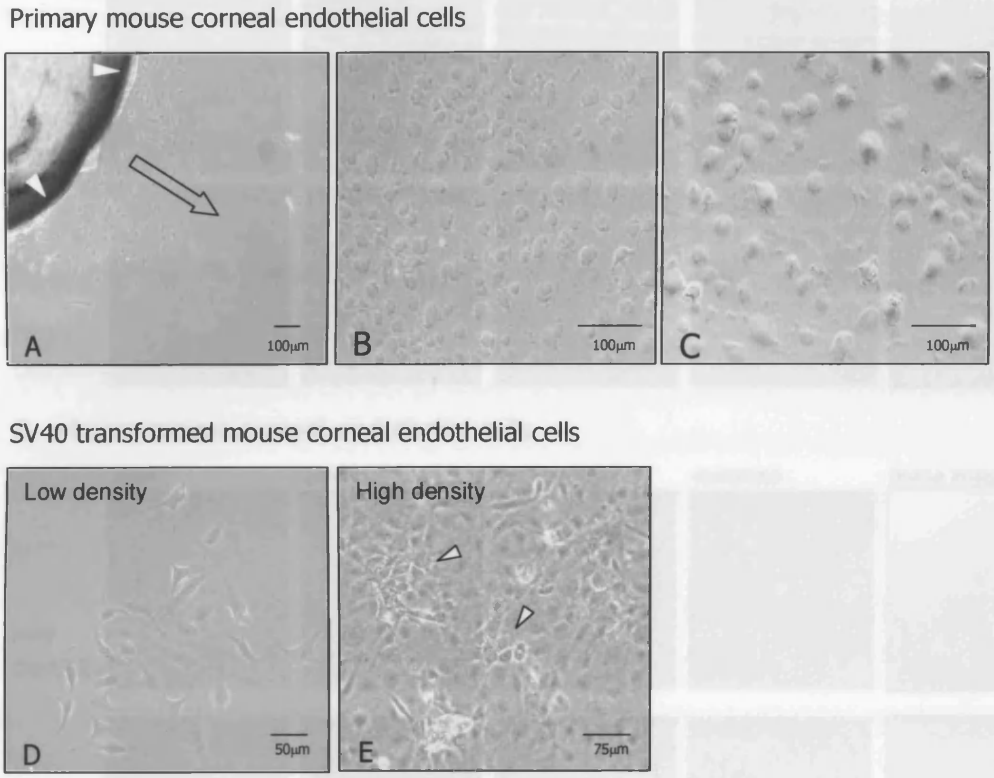

Figure 3.1 Phase images of mouse corneal endothelial cells in culture. Primary mouse corneal endothelial cells proliferate and migrate off corneas onto plastic tissue culture dishes (A). Arrowheads indicate the edge of the cornea and the arrow illustrates the direction of migration of cells from the cornea. Once a sufficient number of cells have migrated away from the cornea, it is removed and the cells are allowed to proliferate and fill the tissue culture dish (B,C). As the cells proliferate, they enlarge and spread. Cells at the edge of the monolayer (C) are far more heterogeneous in size and shape than those nearer the centre of the monolayer (B). The morphology of migrating cells is dramatically different to that of cells within the monolayer for both primary and SV40 transformed mouse corneal endothelial cells. Transformed cells continue to divide even after formation of the monolayer and progressively grow on top of each other (E). Cells growing on top of the monolayer are indicated by arrowheads (E).

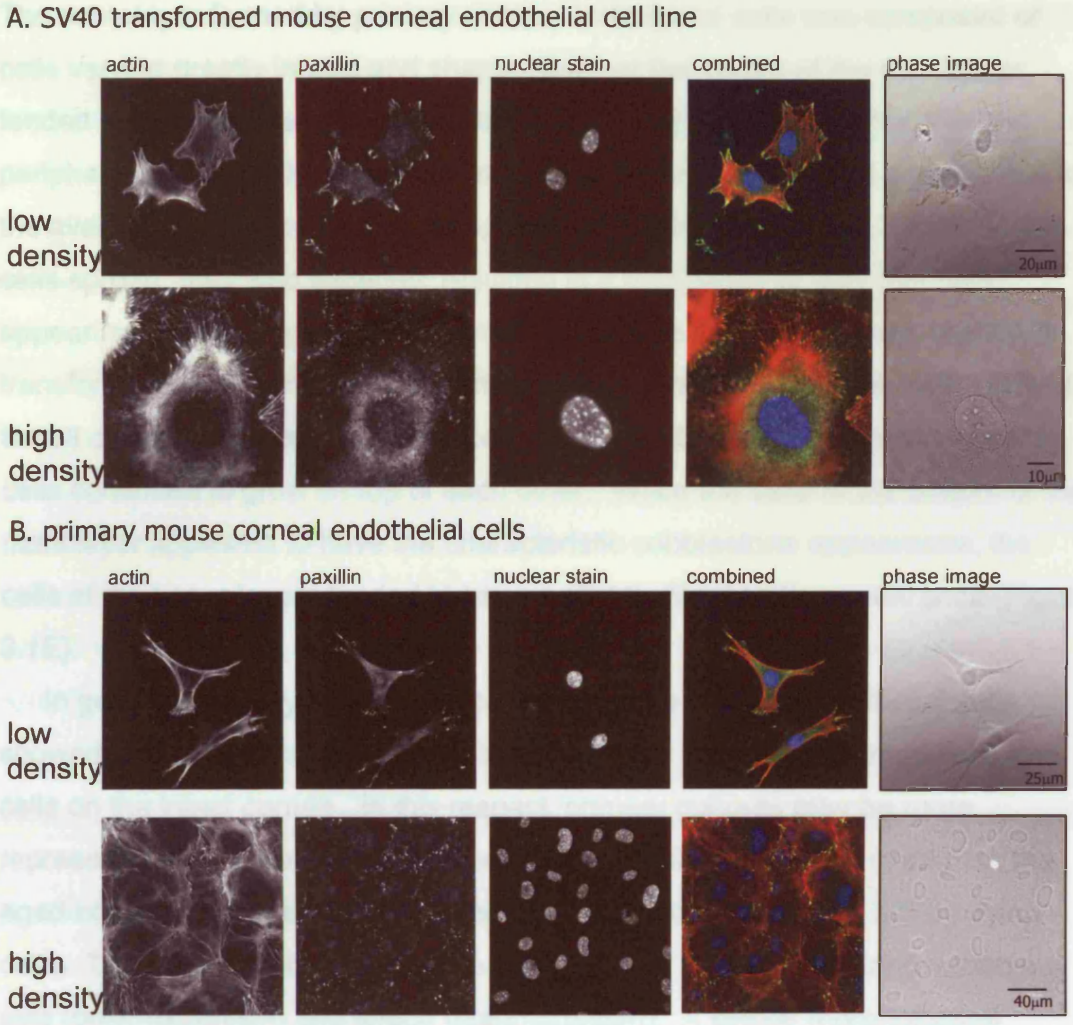

Figure 3.2 Morphology of mouse corneal endothelial cells at high and low density. Corneal endothelial cells cultured on tissue culture plastic were fixed with 4% paraformaldehyde and stained with antibody targeting paxillin. Staining of actin was obtained by treatment with rhodamine phalloidin and nuclei visualized with DAPI staining. Images were captured on a Leica AOBS microscope using software program LCS (v.2). At high density, the SV40 transformed mouse corneal endothelial cell line (A) and primary mouse corneal endothelial cultures (B) have a similar morphology, with thick bundles of cortical actin and focal adhesions dispersed around the edge of the cell and along the basal membrane. At low density, focal adhesions are concentrated at the ends of projections, which extend from the cell body. The migratory morphology of primary cells regularly showed three projections from the cell body, while that of the SV40 transformed cell line showed various numbers of projections.

The monolayer formed by primary corneal endothelial cells was composed of cells varying greatly in size and shape. Cells at the centre of the monolayer tended to be smaller and of a relatively even density, while cells towards the periphery were more heterogeneous with respect to cell size and density, due to the available space for the cells to spread and proliferate (Figure 3.1C). As the cells spread, they also flattened, resulting in a monolayer of very thin cells, appearing to have large protruding nuclei (Figure 3.1C). In contrast, the SV40 transformed cells formed a fairly homogeneous monolayer of cells, with respect to cell density and size. However, cell contact inhibition was impaired and the cells continued to grow on top of each other. While the cells of the bottom of the monolayer appeared to have the characteristic cobblestone appearance, the cells of the upper layers tended to have a slightly fibroblastic appearance (Figure 3.1E).

In general, primary cultures of confluent mouse corneal endothelial cells showed a more variable phenotype than confluent SV40 transformed cells and cells on the intact cornea. In this respect, primary cultures may be more representative of an aged human corneal endothelial monolayer in situ. In the aged cornea, endothelial cells spread and flatten to fill the space left by dying cells. The result is a heterogeneous monolayer of lower density and variable size (polymegathism) and shape (pleomorphism). A similar morphological arrangement is noted in primary cultures of mouse corneal endothelium. Cultured cells are larger and flatter than those in the cornea, as the space available in the tissue culture dish is much greater than that on the cornea. Cell spreading results in large variations in cell shape, with cultures containing occasional giant cells, leading eventually to a heterogeneous monolayer of endothelial cells.

In order to determine whether morphological differences could be attributed to differences in the F-actin phenotype, cultures of primary and SV40 transformed mouse corneal endothelial cultures were examined by confocal microscopy following fixation and staining for the focal adhesion protein paxillin. Immunofluorescence staining of both primary and SV40 transformed mouse

corneal endothelial cells revealed that focal adhesions were present at the ends of cytoplasmic projections in the migrating phenotype. These focal adhesions were connected to cortical actin strands, which extend around the circumference of the cell (Figure 3.2). Confluent cultures of both the primary and SV40 transformed cells showed a thick ring of cortical actin and a fairly even distribution of focal adhesions along the basal membrane of the cell and at the cell contacts (Figure 3.2). The similarity in F-actin phenotypes between these two experimental models indicates that the cytoskeletal organization of these cells is comparable.

Primary cultures of mouse corneal endothelial cells were maintained in culture for periods as long as 4 months to determine the lifespan of primary cultures. Although, prolonged culture of primary mouse corneal endothelial cells was possible, it resulted in a number of additional phenotypic changes, specifically to the morphology of the nucleus. Alterations in the appearance of the nuclei coincided with an increased incidence of binucleate cells (not shown). The nuclei appeared to shift from a round or oval shape to a kidney bean shape in the majority of primary mouse corneal endothelial cells cultured for periods longer than a month. As many as 10% of the cells in primary mouse cultures were also found to have two or more nuclei. Propidium iodide staining of these nuclei also revealed a difference in the arrangement of genetic material within the nucleus. While cells on whole cornea show bright, even staining with propidium iodide, cultured cells had an overall fainter staining of the nucleus with smaller punctate regions, possibly nucleoli, staining brightly (Figure 3.3B). This punctate staining of nucleoli was also apparent in SV40 transformed cells, as was the occurrence of kidney bean shaped nuclei, though both were less common than in primary cultures (Figure 3.3A). No binucleate cells were noted in SV40 transformed cultures.

Time spent in culture also appeared to affect the ability of cells to attach to the tissue culture dish. While two weeks in culture yielded relatively few cell numbers, passaging these cells proved to be uncomplicated. Beyond two weeks of culture, however, primary cells became increasingly difficult to remove from

A. SV40 transformed mouse corneal endothelial cell line

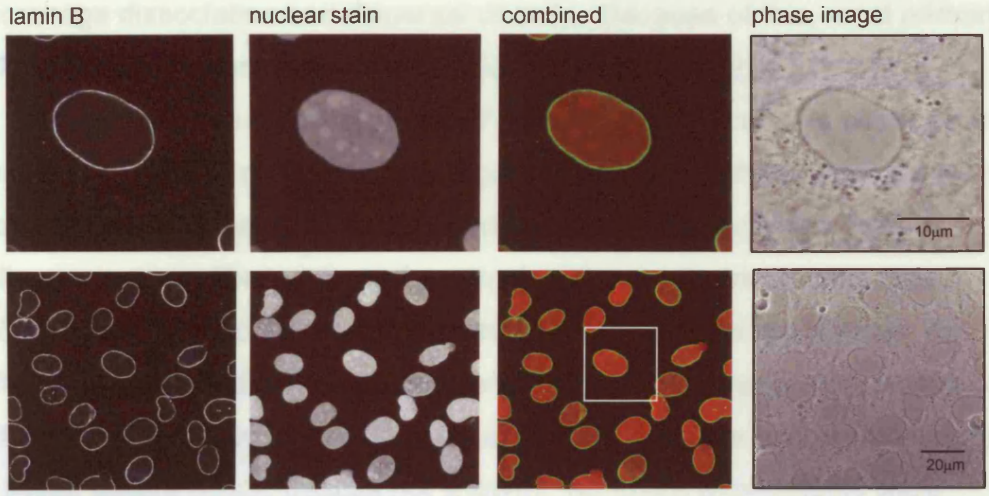

B. primary mouse corneal endothelial cells

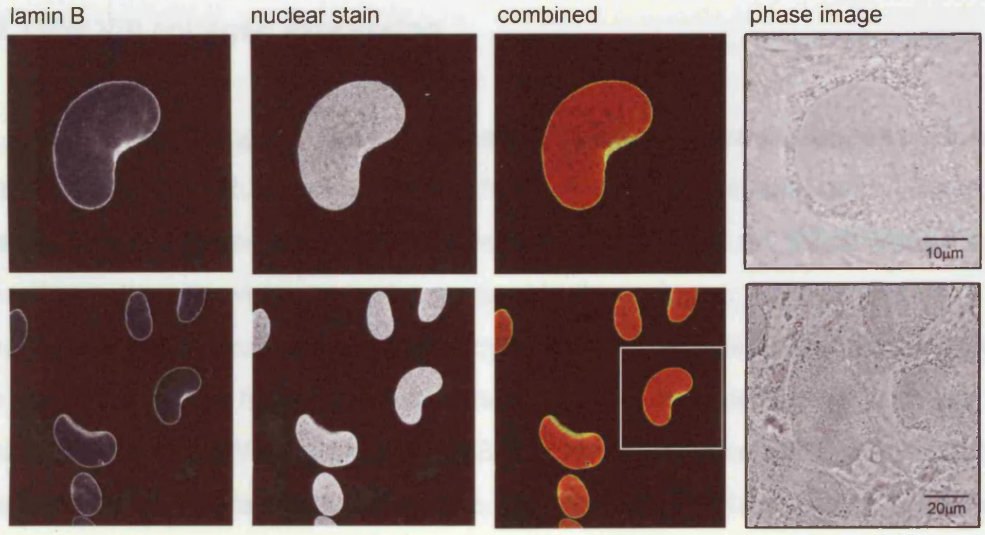

Figure 3.3 Nuclear morphology of mouse corneal endothelial cells. Corneal endothelial cells cultured on tissue culture plastic were fixed in cold methanol and stained with antibodies targeting the nuclear envelope protein lamin B. Nuclei were also stained with propidium iodide. Images were captured using a Leica AOBS microscope with LCS (v.2) software. Nuclei of SV40 transformed mouse corneal endothelial cells tend to be oval in shape and regular in size (A). Primary mouse corneal endothelial cells also have oval nuclei but with increasing time in culture, nuclei begin to form a bean shape (B). Changes in nuclear shape were illustrated by a component of the nuclear envelope, lamin B.

the tissue culture dish and longer, harsher treatments were required to encourage dissociation and dispersal of cells. Because of this, most primary cultures used in future experiments were not passaged prior to study.

Both primary mouse cultures and SV40 transformed cultures were grown on a number of different matrices to investigate the effects of these matrices on cell morphology. The matrices investigated included type I collagen, type IV collagen, laminin, fibronectin and matrigel. Of these matrices, only type IV collagen, laminin and fibronectin are found in Descemet's membrane. No difference was noted in the cellular morphology or the overall appearance of the established monolayer with culture on any of the matrices tested when compared to tissue culture plastic (results not shown). All future experiments were therefore carried out on tissue culture plastic.

3.2 Type VIII collagen expression

Despite displaying a typical endothelial phenotype, it was necessary to verify that the isolated cultured cells were indeed corneal endothelial cells. Because the cells were derived from a cornea denuded of epithelium, there were only two possible cell types which could be present in the cultures; keratocytes or endothelial cells. Both corneal keratocytes and endothelial cells are thought to be derived from the neural crest and thus express an overlapping profile of neuronal markers (Waring III et al., 1982). However, a major difference between the two cell types are the matrix molecules expressed. Keratocytes produce large amounts of type I collagen, to maintain the corneal stroma, while corneal endothelial cells produce type VIII collagen, a major component of Descemet's membrane. Reverse transcriptase polymerase chain reaction (RT-PCR) was therefore used to demonstrate type VIII collagen expression in corneal endothelial cell cultures. Similar reactions were performed on corneal keratocyte cultures as a negative control.

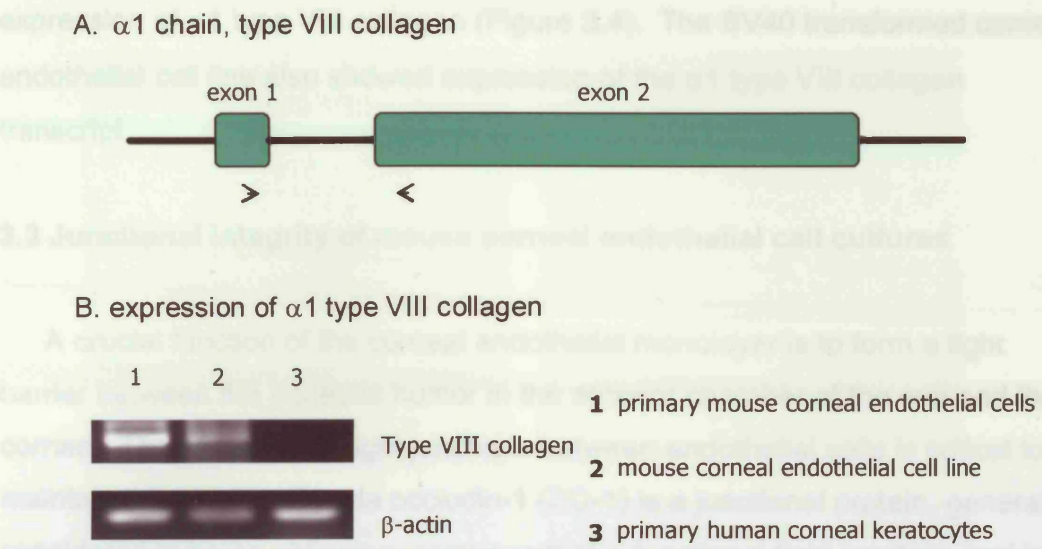

Figure 3.4 Tissue cultured mouse corneal endothelial cells express α1 type VIII collagen. The α1 type VIII collagen gene contains 2 exons. A forward primer was designed at the end of exon 1 and a reverse primer designed at the beginning of exon 2 such that an RT-PCR reaction would yield a product of 526bp (A). A PCR product using the same primers from contaminating genomic DNA would also contain an intron, generating a much larger product, allowing amplification from mRNA to be distinguished. Total mRNA was isolated from primary corneal endothelial and keratocyte cultures as well as cultures of the SV40 transformed mouse corneal endothelial cell line. RT-PCR reactions using total mRNA were used to determine expression of α1 type VIII collagen. Both primary mouse corneal endothelial cell cultures as well as those from the mouse corneal endothelial cell line show a 526bp RT-PCR product, corresponding to α1 type VIII collagen. Similar RT-PCR reactions for a transcript of β-actin was used to confirm the quality of the mRNA, particularly from the corneal keratocytes.

Primers for the PCR reaction were designed such that the forward primer-binding site lay in exon 1 of the α1 type VIII collagen gene, while the reverse primer-binding site was located in exon 2 of the same gene (Figure 3.4A). The total length of the expected PCR product amplified from mRNA was 526 base pairs. The length of a potential PCR product amplified from contaminating genomic DNA would have been much longer, as it would also contain the intron, thus ensuring that a PCR product of the correct predicted size could only be amplified from precursor mRNA. RT-PCR reactions from corneal keratocyte cultures and corneal endothelial cell cultures both showed mRNA expression of β-actin, demonstrating acceptable mRNA quality (Figure 3.4B). Only the corneal endothelial cell cultures yielded the predicted 526bp band indicating mRNA

expression of α1 type VIII collagen (Figure 3.4). The SV40 transformed corneal endothelial cell line also showed expression of the α1 type VIII collagen transcript.

3.3 Junctional integrity of mouse corneal endothelial cell cultures

A crucial function of the corneal endothelial monolayer is to form a tight barrier between the aqueous humor in the anterior chamber of the eye and the cornea. The formation of tight junctions between endothelial cells is critical to maintain this barrier. Zonula occludin-1 (ZO-1) is a junctional protein, generally considered to be an obligatory component of a functional tight junction, and is expressed in tight junctions in epithelial and vascular endothelial monolayers throughout the body. In immature junctions, or cell layers which do not form tight juctions, ZO-1 can also be found at the adherens junctions. The distribution of ZO-1 can, therefore, be used to determine the relative maturity of the junctions.

Mouse corneal endothelial monolayers in situ showed a relatively tight band of ZO-1 distributed around the cell borders (Figure 3.5B). This pattern of ZO-1 staining is consistent with mature tight junction formation, as would be expected in the cornea. While the SV40 transformed mouse corneal endothelial cell line appears to produce a proper monolayer, as judged by phase microscopy, the pattern of ZO-1 staining suggests that this is not the case. Immunofluorescence staining for ZO-1 shows that the cells are in contact only at small, regular, punctuate areas around the cell borders (Figure 3.5A). This discontinuous staining is likely to be representative of improper or early junction formation. The barrier function of such a monolayer is likely to be compromised.

The distribution of ZO-1 in primary cultures of mouse corneal endothelial cells was variable and differed from both the corneal endothelial cell line and endothelial monolayers of the cornea. The expression and localization of ZO-1 appeared to be affected by the length of time cells remained in culture. Primary

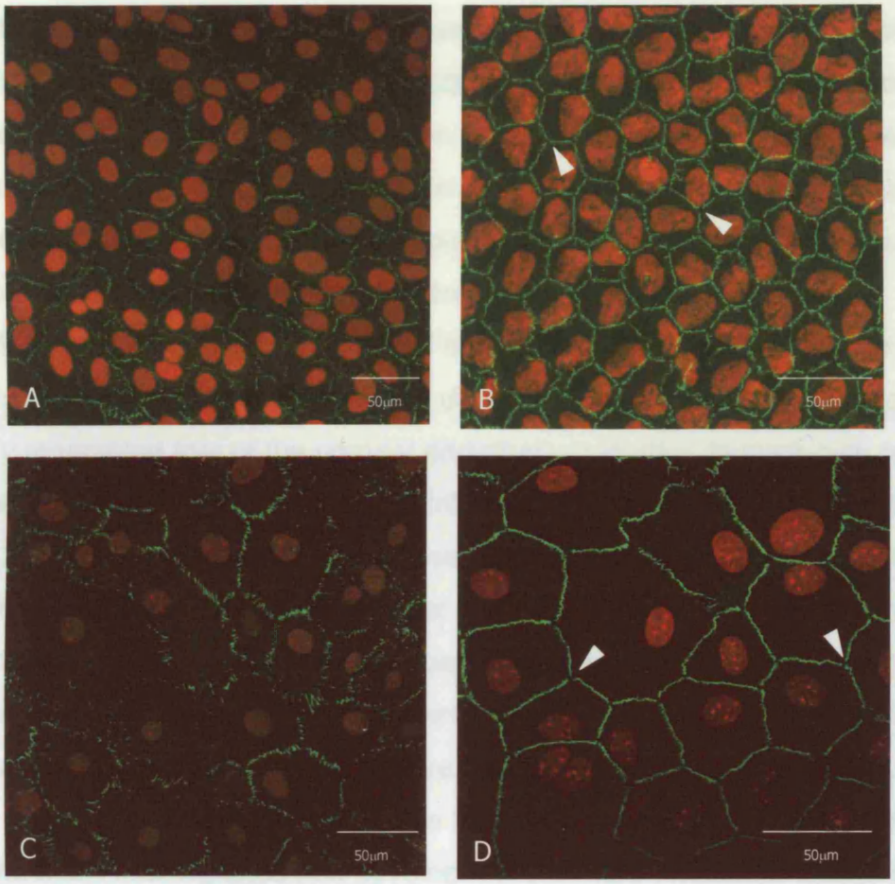

Figure 3.5 Distribution of ZO-1 in mouse corneal endothelial cells. Cultured corneal endothelial cells and whole corneal tissue was fixed in cold methanol and then stained using antibodies against tight junction protein ZO-1. Nuclei were stained with propidium iodide. Images were captured using the Zeiss axiovert microscope with Lasersharp 2000 software. The distribution of junctional protein ZO-1 is different in the mouse corneal endothelial cell line (A) compared to corneal endothelial cells in situ (B). Distribution of ZO-1 in the mouse corneal endothelial cell line is similar to that noted for immature junctions, while endothelial monolayers on the cornea form a tight band around the cell with gaps at the Y-junctions (arrowheads). The same discrepancy is noted between primary cultures that have been in culture for only a few weeks versus those in culture for a few months. Primary corneal endothelial cell monolayers, which have only spent a few weeks in culture (C) show a similar distribution of ZO-1 to the cell line while mature monolayers of primary corneal endothelial cells (D) have a similar pattern of ZO-1 staining to cells on the cornea. Primary cultured cells are also much larger than those of the cell line or those found on the cornea.

cultures, which had been passaged or which had been in culture for only short periods of time (2 weeks or less), showed a distribution of ZO-1 which was similar to that of the mouse corneal endothelial cell line. ZO-1 staining of these cultures also produced a discontinuous, punctate pattern of staining around the cell borders (Figure 3.5C). This pattern of staining highlights the fact that these primary cells form an incomplete monolayer with small intercellular gaps, which are sometimes even apparent under phase microscopy.

Primary mouse corneal endothelial cells which had been cultured for a few months, however, presented a slightly different distribution of ZO-1, which more closely resembled that of the corneal endothelium in situ. In such cultures, a regular band of ZO-1 was evident, distributed around the cell borders (Figure 3.5D). While these bands did not appear as tight or intense as those of the endothelium in situ, these data suggest that correct assembly of functional tight junctions may simply require an adequate period of time in culture. Also, these results are consistent with the appearance of the cells under phase microscopy. Cells which have spent longer in culture no longer have discernable cell borders under phase microscopy. It is possible that as the monolayer matures, the cells become more interdigitated and develop more mature junctions, similar to development of the endothelial monolayer of the cornea. This in turn may be reflected in the tighter pattern of ZO-1 staining. While the junctional maturity of primary cells with prolonged culture closely resembles that of endothelial monolayers in situ, primary corneal endothelial cells are much larger than those of endothelial monolayers in vivo, with most primary cells appearing two to three times the size of endothelial cells in the cornea. This apparent difference in cell size is likely the result of cell spreading, rather than a difference in cell volume.

In addition to ZO-1, the distribution of the transmembrane tight junction proteins claudin-1 and occludin was also investigated. Immunofluorescence staining showed a similar pattern of expression of claudin-1 to that of ZO-1 in situ (Figure 3.6 A,B). Claudin-1 was localized in a band at the cell borders of corneal endothelial cells (Figure 3.6B). However, it was not possible to determine the distribution of occludin, although it is likely that occludin is present in the mouse

corneal endothelial tight junctions. Similarly, it was not possible to establish the distribution of any transmembrane tight junction proteins in primary cultures or the SV40 transformed cell line. It is likely, therefore, that cultured cells, whether SV40 transformed or primary, are unable to fully recapitulate the molecular complexity and integrity of tight junctions observed in corneal endothelial cells in vivo.

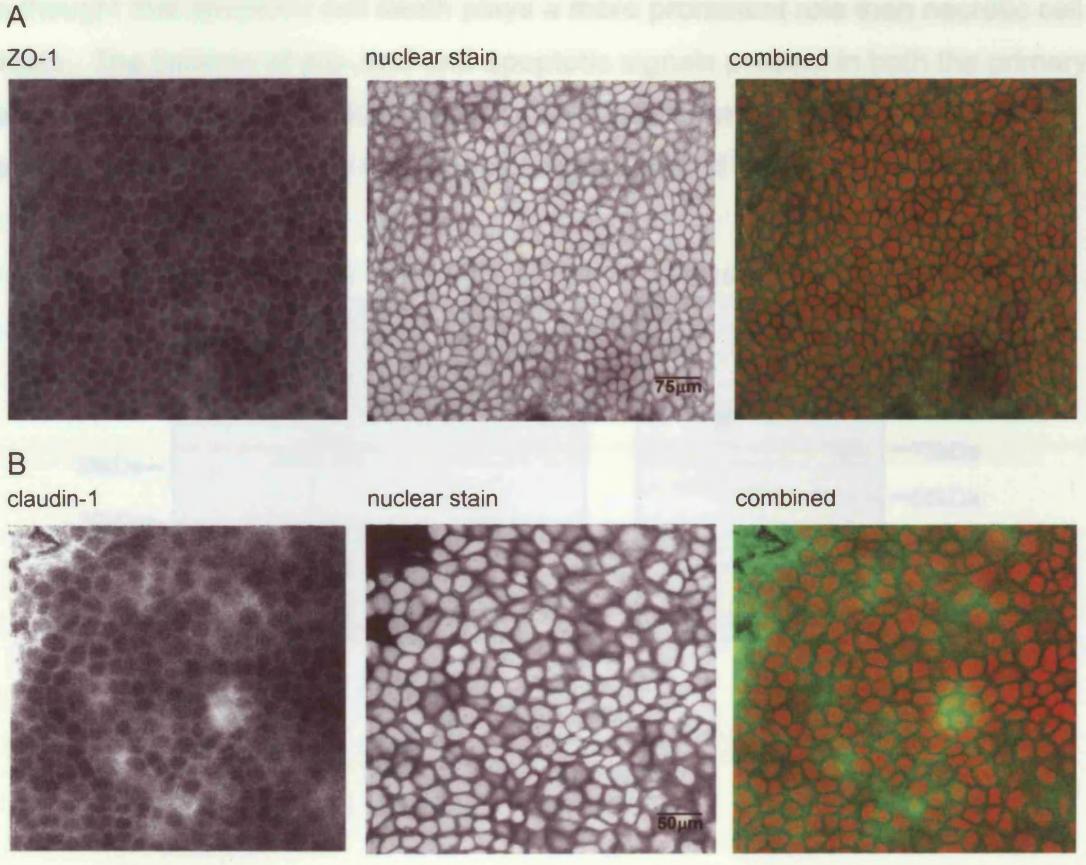

Figure 3.6 Distribution of tight junction proteins ZO-1 and claudin-1 in the endothelial monolayer of the mouse cornea. Whole mouse corneas were fixed in cold methanol and stained with antibodies to either ZO-1 or claudin-1. Nuclei were visualized with propidium iodide stain and images captured using a Zeiss axiovert microscope with Lasersharp 2000 software. Both ZO-1 (A) and claudin-1 (B) localize to the cell borders in corneal endothelial monolayers of the mouse cornea.

3.4 Apoptotic markers

Decreasing corneal endothelial densities are the consequence of two factors; negligible corneal endothelial cell proliferation and corneal endothelial cell death. Thus, in the absence of any proliferation, corneal endothelial cell survival is particularly important for the maintenance of cell densities in vivo. While the mechanisms of cell death in corneal endothelial cells are still largely unknown, it is thought that apoptotic cell death plays a more prominent role than necrotic cell death. The balance of pro- and anti-apoptotic signals present in both the primary corneal endothelial cell cultures and the SV40 transformed corneal endothelial cell line was determined by western blotting a panel of apoptotic markers.

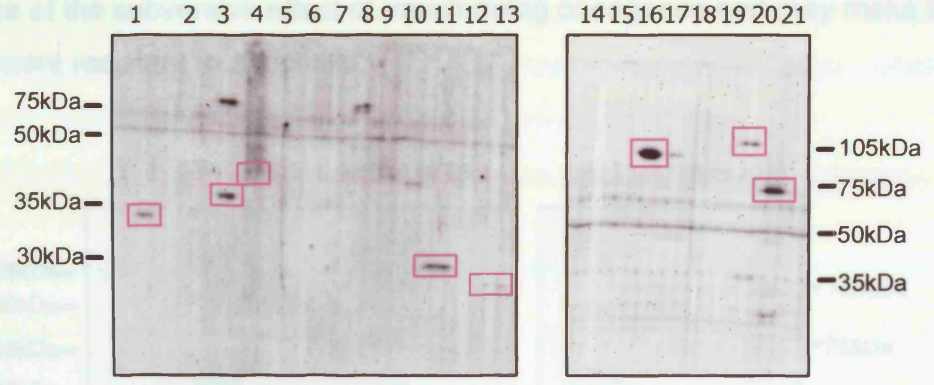

1 caspase-3	6 DFF 45	11 Bcl-2	16 CAS
2 TRADD	7 caspase-7	12 Bax	17 hILP
3 Fas-L	8 Nip-1	13 Bad	18 p53
4 Fas	9 Mcl-1	14 Apaf-1	19 caspase-2
5 FADD	10 Bcl-XL	15 BRUCE	20 PARP
			21 RIP

Figure 3.7 Apoptotic markers expressed in primary cultures of mouse corneal endothelial cells. Cell lysates of primary mouse corneal endothelial cells cultured on tissue culture plastic were used to determine the expression of a number of apoptotic markers, using the Transduction Labs Apoptosis Sampler Kits I and II. Primary mouse corneal endothelial cells showed expression of CAS, PARP, RIP, caspase-3, Fas-L, Fas, Bcl-2 and Bad (bands highlighted with pink boxes). A number of other non-specific bands also appeared on the blot but these did not correspond with the correct molecular weight for the expected product.

Cultures of primary mouse corneal endothelial cells and the SV40 transformed cell line were grown on tissue culture plastic and lysed directly into reducing sample buffer. A BioRad Mini-Protean II Multi Screen was used for western blot screening of Transduction Labs Apoptosis Sampler Kits I and II. The proteins expressed in the SV40 transformed cell line were slightly different to those expressed in primary mouse corneal endothelial cultures. Expression of pro-apoptotic proteins CAS, RIP, caspase-3, Fas, Fas-L and Bad and anti-apoptotic proteins PARP and Bcl-2 was noted in primary mouse cultures (Figure 3.7). However, the SV40 transformed cell line was found to express fewer pro-apoptotic proteins, Apaf-1, CAS, RIP, Fas and Bad, and more anti-apototic proteins, Bcl-2, Bcl-X_L and Bax (Figure 3.8). The expression of increased numbers of anti-apoptotic proteins in the SV40 transformed cell line is a typical feature of the subversive effect of transforming oncogenes and may make these cells more resistant to apoptosis.

Figure 3.8 Apoptotic markers expressed in an SV40 transformed mouse corneal endothelial cell line. Cell lysates of SV40 transformed mouse corneal endothelial cells cultured on tissue culture plastic were used to determine the expression of a number of apoptotic markers, using the Transduction Labs Apoptosis Sampler Kits I and II. SV40 transformed cells showed expression of Apaf-1, CAS, RIP, Fas, Bcl-2, Bcl-X_L, Bax and Bad (bands highlighted with pink boxes). A number of other non-specific bands also appeared on the blot but these did not correspond with correct molecular weight for the expected product.

3.5 Mitochondrial morphology changes during apoptosis

Because of the observed differences in apoptotic proteins between primary mouse corneal endothelial cells and SV40 transformed mouse corneal endothelial cells, it was of interest to examine whether or not this might reflect differences in the susceptibility of the cells to an apoptotic stimulus. Changes in mitochondrial morphology are known to accompany loss of functional integrity and mitochondrial pore transition and are an early indication of apoptosis. As metabolically active cells, the corneal endothelium contains an extensive mitochondrial network, so alterations in mitochondrial morphology can be measured to provide an early indicator of apoptosis. Mouse cultures were loaded with 100nM MitoTracker Red to monitor changes in mitochondrial morphology and mitochondrial membrane integrity during apoptosis. Differences in kinetics and strength of signal required to initiate apoptosis in both primary cultures and the SV40 transformed cell line were compared.

Induction of apoptosis with 200nM staurosporine resulted in dramatic changes to mitochondrial morphology in primary mouse corneal endothelial cells within 1 hour of treatment. Untreated cells displayed a mitochondrial reticulum throughout the cell, appearing in confocal cross section as numerous bright dots and lines (Figure 3.9A). 10 minutes after staurosporine treatment there was little change in mitochondrial morphology (Figure 3.9B) but after 50 minutes of treatment, the mitochondria appeared as large, bright clumps or vesicles within the cell (Figure 3.9C). These vesicles likely represented mitochondrial tubules which have coalesced. By 1 hour of treatment with staurosporine, the mitochondrial vesicles appeared to have migrated from being uniformly distributed around the cytoplasm, to clusters surrounding the nucleus (Figure 3.9D). As the mitotracker dye appears fainter than in previous images, Figure 3.9D also reports the loss of mitochondrial membrane potential that occurs at mitochondrial pore transition, allowing Mitotracker Red dye sequestered in the mitochondria to leak out. Coalescence of the mitochondria and breakdown of mitochondrial membranes are an early indicator of apoptosis. In primary corneal

endothelial cells, these features were visible in most cells within an hour of treatment with 200nM staurosporine.

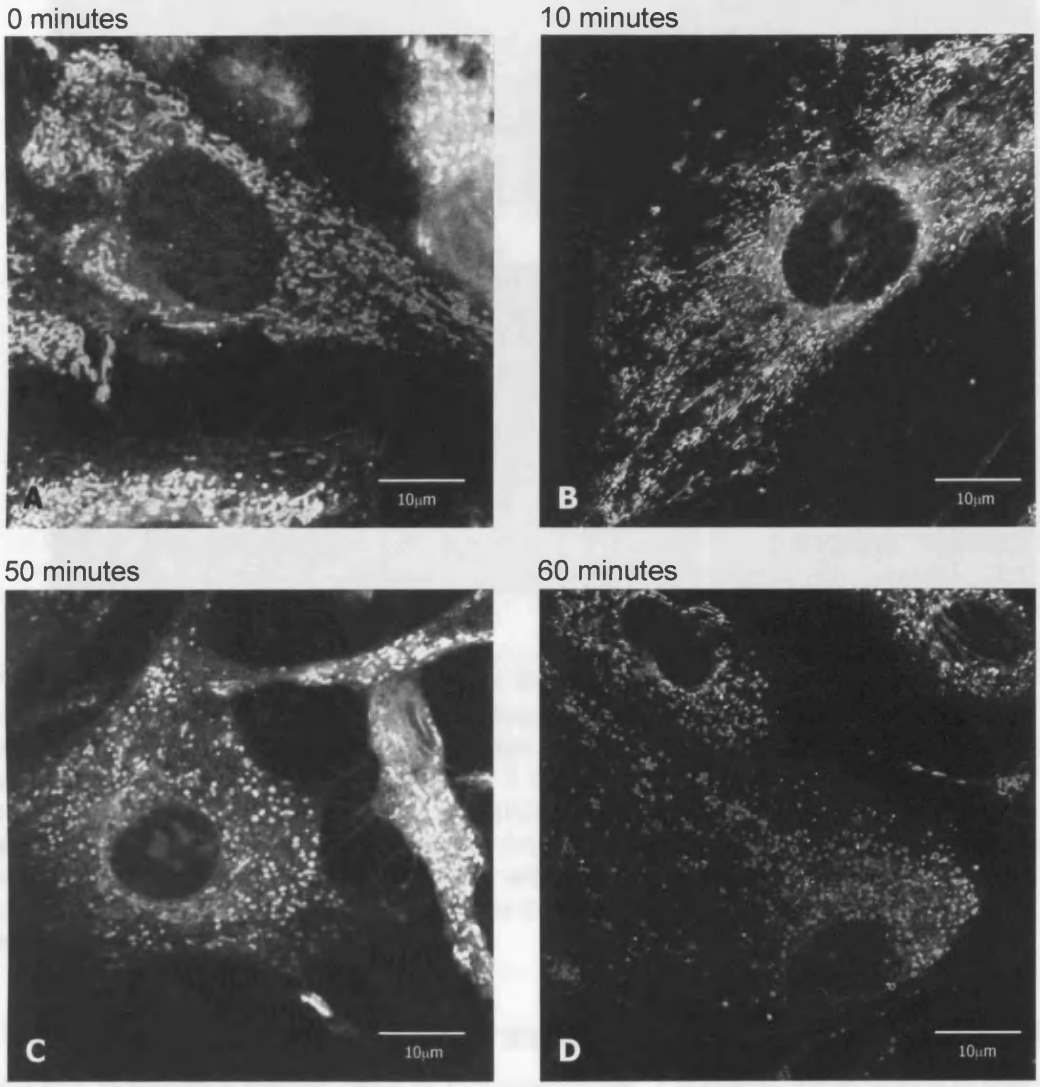

Figure 3.9 Mitochondrial morphology of primary mouse corneal endothelial cells is disrupted by staurosporine. Primary mouse corneal endothelial cells cultured on glass coverslips were loaded with 100nM Mitotracker Red and treated with 200nM staurosporine for 0 minutes (A), 10 minutes (B), 50 minutes (C) and 1 hour (D). Confocal images of mitochondrial morphology were captured on a Zeiss axiovert microscope with Lasersharp 2000 software. The morphology of the mitrochondria change dramatically after 50 minutes. After 1 hour of treatment with staurosporine, the mitochondria have coalesced and the weaker signal suggests that the mitochondrial membranes are breaking down.

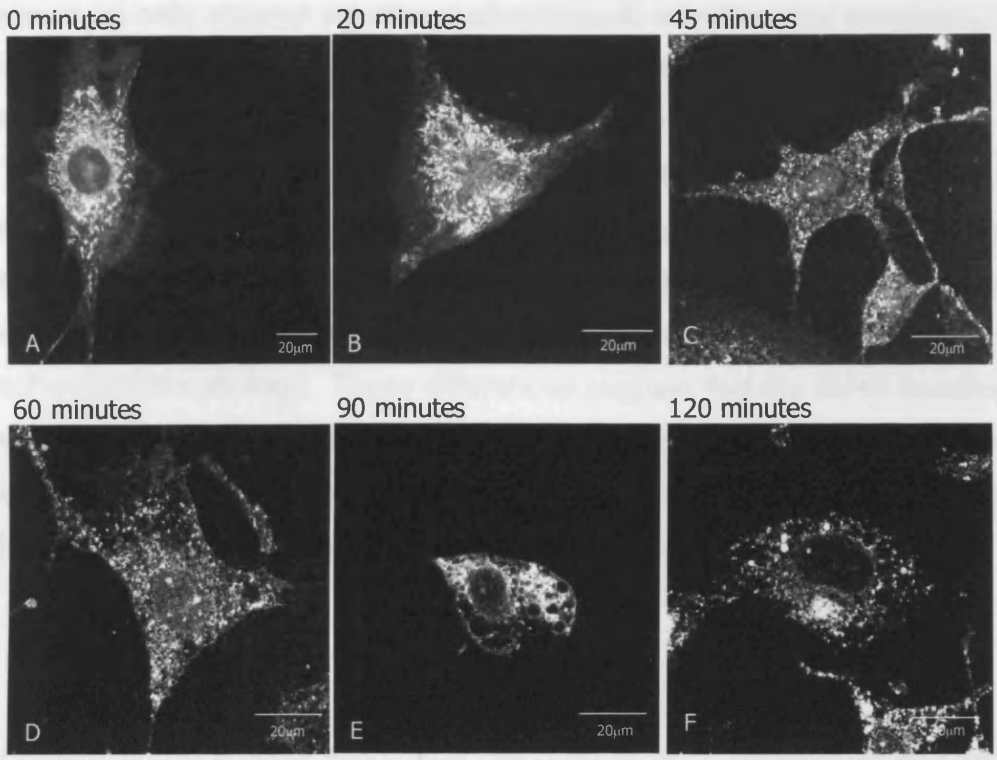

Figure 3.10 Effects of staurosporine on SV40 transformed mouse corneal endothelial cell mitochondrial morphology. SV40 transformed mouse corneal endothelial cells cultured on glass coverslips were loaded with 100 nM Mitotracker Red and treated with 500nM staurosporine for 2 hours. Confocal images of mitochondrial morphology were captured on a Leica AOBS microscope with LCS (v.2) software. Mitochondrial morphology begins to alter dramatically after 45 minutes of exposure to staurosporine. After 2 hours of treatment with staurosporine, the mitochondria have coalesced and the weaker signal suggests that the mitochondrial membranes are breaking down.

Induction of apoptosis in the SV40 transformed mouse corneal endothelial cell line required a higher dose of staurosporine. Changes were noted in the mitochondrial morphology of all cells after two hours of treatment with 500nM staurosporine. Untreated SV40 transformed cells had a similar mitochondrial morphology to that of primary cultures, with the mitochondrial reticulum appearing as numerous dots and lines in confocal cross section (Figure 3.10A). There was little change to mitochondrial morphology after 20 minutes of exposure to staurosporine (Figure 3.10B), but coalescence of mitochondria was evident after approximately 45 minutes (Figure 3.10C). After two hours of

exposure, all cells showed significant alterations to mitochondrial morphology including rounding up of mitochondria and breakdown of mitochondrial membranes (Figure 3.10F).

The SV40 transformed cell line and primary cells thus required different doses of staurosporine to induce apoptosis, and displayed different kinetics with regard to mitochondrial breakdown. Specifically, the SV40 transformed cell line required a higher dose and longer time period for all cells to show significant changes in mitochondrial morphology. These differences suggest that the SV40 transformed mouse corneal endothelial cells are more resistant to apoptosis than the primary mouse corneal endothelial cells, and are consistent with the identification of more anti-apoptotic proteins present in the SV40 transformed cell line.

3.6 Summary

Primary mouse corneal endothelial cell cultures were established with the development of an explant culture model. This model of mouse corneal endothelial cell culture generates a reproducible culture system that is relatively simple in comparison to that described by Joo et al. (1994). In addition, work in this chapter provides a more extensive characterisation of primary mouse corneal endothelial cells. In the explant model the cells migrate off the cornea onto tissue culture dishes to form a halo of growing endothelial cells. These migrating cells have a different morphology to cells found in the intact monolayer. Migrating cells take on a triangular shape, with three cytoplasmic projections extending away from the cell body, and focal adhesions concentrated at the ends of these projections. With time in culture, these cells cease to proliferate and form a monolayer. The densities of these monolayers are much lower than those of corneal endothelial monolayers in situ, but the cells still display a relatively cobblestoned appearance. The densities of these monolayers were highest close to where endothelial cell migration from the cornea was first initiated and densities were lowest at the edge of the monolayer. The shape of cells towards the edge of the monolayer was also more variable and this region contained a

large number of giant cells. These trends were unaffected by culture of the cells on various matrices.

Overall, the gross appearance of the SV40 transformed mouse corneal endothelial cell line was found to exhibit significant differences to that of the primary cultures. First, migrating cells typically had many more than three projections extending from the cell body. Second, cells were uniformly distributed throughout the entire tissue culture dish, and were fairly homogeneous in shape and size. Finally, and perhaps most importantly, SV40 transformed cells continued to proliferate after the monolayer had become established, resulting in cell overgrowth and multiple cell layers. This final difference suggests that cell contact inhibition, which normally feeds back to control proliferation, may be overridden in the SV40 transformed cell line. Cell contact inhibition of proliferation has been shown to play an important role in corneal endothelial cell proliferation in vivo (Senoo et al., 2000), and elimination of this control as a result of oncogenic transformation may explain its highly proliferative nature.

Since corneal endothelial cells are the only cell type within the cornea known to express type VIII collagen, expression of α1 type VIII collagen by RT-PCR in both primary and SV40 transformed mouse corneal endothelial cells was used to confirm that these cultures were indeed endothelial (Kapoor et al., 1988). Corneal endothelial cells are also known to form tight junctions, as a part of their barrier function (Waring, III et al., 1982) and several studies have used the tight junction associated protein ZO-1 as a marker of tight junction formation in corneal endothelial monolayers (Senoo et al., 2000, Petroll et al., 1999). Here, ZO-1 was used to compare the junctions in corneal endothelial monolayers in culture with those in situ. On whole corneal tissue, ZO-1 was found to be in a tight band around the cell borders with apparent discontinuities at the Y-junctions. This pattern of ZO-1 staining has been described previously in the corneal endothelium of a number of species, including rat (Gordon, 2002), cat {Petroll, 1999 426 /id} and human (Senoo et al., 2000){Petroll, 1999 426 /id}. A close approximation of this staining pattern was noted in primary mouse corneal

endothelial cells which had been in culture for a few months, with ZO-1 distributed in a fairly regular band around the cell with spaces at the Y-junctions. The establishment of more authentic junctions in these cells may contribute to cessation of proliferation and difficulties passaging cells after prolonged culture. In contrast, short term cultures of primary cells showed a discontinuous band of ZO-1 around the cell borders, similar to the distribution of ZO-1 in the SV40 transformed cell line. Such localization of ZO-1 is consistent with immature junction formation. As previously mentioned, the SV40 transformed cell line appears to be able to override cell contact inhibition of proliferation, and incomplete junction formation may contribute to this characteristic. Similarly, primary cells which have spent little time in culture may remain proliferative due to their incomplete junction formation.

Electron microscopy has revealed the presence of tight junctions in the corneal endothelium in situ, thus transmembrane tight junction proteins must be present in the corneal endothelial tight junction plaque (Waring, III et al., 1982). Consistent with this, the transmembrane tight junction protein claudin-1 was noted in corneal endothelial cell monolayers in situ. However, occludin was not observed in corneal endothelial monolayers. It is highly unlikely that occludin does not form a part of the corneal endothelial tight junction plaque, the absence of staining is instead likely due to steric hinderance by tight junction associated proteins, including ZO-1. However, this explanation cannot account for the clear absence of both claudin-1 and occludin in primary mouse corneal endothelial cells in culture. As ZO-1 distribution in primary cultures varies depending on time in culture, there may also be a time dependent effect on the distribution of transmembrane tight junction proteins. Tight junctions in endothelial cells of the developing cornea are known to mature over long periods of time. While corneal endothelial cell proliferation ceases by the third month of gestation, tight junction formation does not begin until the fourth month of gestation and junctions do not mature until the fifth month (Bron et al., 2001). The apparent organization of ZO-1 in primary cells that have been cultured for longer periods, suggests that in these cells junctions may be properly constructed. As proper organization of ZO-

1 is known to be required prior to the assembly of transmembrane tight junction proteins, it is possible that more prolonged culture of primary mouse corneal endothelial cells might eventually reveal the expression of transmembrane tight junction proteins (Bazzoni and Dejana, 2004).

Corneal endothelial densities decrease with time due to corneal endothelial cell G1 phase arrest and cell death. Apoptosis is thought to be the primary mode of cell death in the corneal endothelium (Albon et al., 2000; Komuro et al., 1999). An assessment of apoptotic markers in both primary mouse corneal endothelial cell cultures and the SV40 transformed mouse corneal endothelial cell line revealed that the cell line expressed more anti-apoptotic proteins and fewer pro-apoptotic proteins than the primary cultures. In general, expression of cell death receptors, such as Fas and RIP, were noted in both the cell line and primary cultures. Members of the Bcl family of proteins, Bcl-2 and Bad, were detected in both the cell line and the primary cells, and additional anti-apoptotic members of the Bcl family, Bcl-X_L and Bax, were also observed in the cell line. Homo or heterodimers of anti-apoptotic Bcl proteins, Bcl-2, Bcl-X_L and Bax, offer protection from cell death. Pro-apoptotic Bad, however, interrupts these dimers to induce apoptosis (Adams and Cory, 1998). A balance of pro- and anti-apoptotic proteins thus determines cell susceptibility to cell death. While the SV40 transformed cell line was found to express a wider range of anti-apoptotic Bcl proteins than primary cultures, further investigations of levels of expression of these proteins would be needed to determine whether these differences contribute significantly to cell survival.

The analysis of apoptotic protein expression also revealed some surprising results, particularly the identification of the **c**ellular **a**poptosis **s**usceptibility (CAS) protein. Typically, elevated levels of CAS are noted in rapidly dividing cells, with levels decreasing during growth arrest. Consistent with this, the SV40 transformed cell line is known to be highly proliferative and shows an expected expression of CAS. However, primary cultures exhibited reduced levels of proliferation and are largely thought to be G1 phase arrested, making expression of CAS unexpected in these cells. It would be of interest to know whether or not

corneal endothelial cells in situ express CAS. Also surprising was the expression of poly(ADP-ribose) polymerase (PARP) by primary cultures but not by the SV40 transformed cell line. As a molecular nick sensor, central to DNA repair, PARP is thought to be constitutively and ubiquitously expressed. It may be that levels of PARP in the SV40 transformed cell line were low and thus undetectable by western blotting. Similarly, pro-apoptotic Apaf-1, a component of the large apoptosome complex for caspase activation (Reed, 2000), was found to be expressed solely in the SV40 transformed cell line.

In addition to apoptotic markers expressed, mitochondrial morphology and mitochondrial membrane integrity were investigated during the apoptotic response of both the primary mouse corneal endothelial cell cultures and the SV40 transformed cell line. The protein kinase C inhibitor, staurosporine, was used to induce apoptosis. Sensitivity to staurosporine differed in the two experimental models, with the cell line requiring a dose of staurosporine two and a half times greater than that required for the primary cultures to induce apoptosis. Staurosporine (200nM) has been reported to induce corneal endothelial cell death in both bovine and human corneal endothelial cell cultures (Joo et al., 1999; Thuret et al., 2003). The same dose of staurosporine induced significant changes in mitochondrial morphology and compromised mitochondrial membrane integrity after 1 hour of treatment in primary mouse corneal endothelial cells. Mitochondria coalesced to form blebs within the cell, and failure of mitochondrial membrane potential was demonstrated by leakage of dye into the cytoplasm. A dose of 500nM staurosporine was required to induce a similar response in the SV40 transformed mouse corneal endothelial cell line. While mitochondria began to coalesce after 45 minutes of exposure to staurosporine in some cells, mitochondrial membranes appeared to remain intact at this time. Only after two hours did all the cells show fragmentation and rounding up of mitochondria and loss of mitochondrial membrane integrity. This is the first report of mitochondrial changes associated with apoptosis in corneal endothelial cells. Because the corneal endothelium is rich in mitochondria, and these changes take place over a relatively short time frame, mitochondrial

morphology changes provide an early indicator of apoptosis in the corneal endothelium. The increased dose of staurosporine required to induce apoptosis and the kinetics of the apoptotic response in SV40 transformed mouse corneal endothelial cells, suggests that these cells are more resistant to apoptosis. This cytoprotection may be limited to the expression of certain apoptotic proteins, particularly anti-apoptotic members of the Bcl family.

In conclusion, work presented in this chapter provides new insight into the isolation and characterisation of primary mouse corneal endothelial cells. While Joo et al. (1994) found no differences between primary mouse corneal endothelial cells and the SV40 transformed mouse corneal endothelial cell line, our results demonstrate that there are a number of significant differences between the two. First, the SV40 transformed cell line is not contact inhibited. Second, expression of various apoptotic markers differs between the cell line and primary cells, which may explain the different sensitivities to staurosporine-induced apoptosis. This analysis shows that care must be taken in the interpretation of results obtained using the SV40 immortalized cell line, since it does not fully replicate all the characteristics of either primary cultured mouse corneal endothelial cells, or endothelial cells in an intact monolayer.

Chapter 4: Proliferative response of primary mouse corneal endothelial cells

It is generally accepted that the normal adult human corneal endothelium has virtually no mitotic activity, with cells held in G1 phase arrest. Mitotic activity is essentially complete by birth. Injury to the corneal endothelium resulting in cellular attrition leads predominantly to enlargement and translocation of remaining endothelial cells, rather than replacement of lost cells by mitosis. During this atypical wound healing response, there is an increase in variation in cell shape (pleomorphism) and variation in cell size (polymegathism). These changes may compromise the barrier function of the monolayer. It would therefore be beneficial to have therapeutic strategies designed to restore endothelial cell density and regenerate damaged monolayers. As growth factors are multifunctional regulatory proteins that have the potential to drive cells from G1 arrest into the cell cycle, a set of experiments was undertaken to examine the full effects of growth factors on the proliferative response of newly established primary mouse corneal endothelial cell cultures (see Chapter 3). The growth factors investigated were epidermal growth factor (EGF), which in most contexts is not mitogenic, basic fibroblast growth factor (FGF-2) and platelet derived growth factor BB (PDGF BB), the latter both being mitogenic in other cell types. These factors were chosen as primary mouse corneal endothelial cell cultures and SV40 transformed mouse corneal endothelial cells have both been demonstrated to express EGF and PDGF BB receptors at similar levels, and FGF-2 is known to be synthesized by and act on corneal endothelial cell cultures (Joo et al., 1994; Choi et al., 2000).

However, relatively little is known about the intracellular events that mediate proliferation in corneal endothelial cells. Studies on rabbit corneal endothelium indicate that the PI3 kinase pathway is important for the proliferative response (Kay et al., 1998). Evidence from other cell types demonstrate that the *m*itogen-*a*ctivated *p*rotein *k*inase (MAPK) pathway is also typically activated in a proliferative response (Murphy et al., 2002). In order to determine whether the

MAPK pathway is involved in the corneal endothelial proliferative response, the kinetics of *e*xtracellular signal *r*egulated *k*inase (ERK) activation in response to growth factor stimulation were investigated by western blotting. In addition, specific inhibitors of various intracellular signalling pathways were used to further delineate the relative importance of these signalling pathways in the proliferative response.

Studies were conducted in parallel in both the SV-40 transformed mouse corneal endothelial cell line and in primary mouse corneal endothelial cell cultures. Comparisons between these two model systems determined whether intracellular signalling pathways underlying the proliferative response were the same in the primary cultures as the cell line. This would provide insight as to the utility of the transformed cell line as a model for primary cultures.

4.1 Proliferative response of mouse corneal endothelial cells

It has been suggested that rodent corneal endothelium is unrepresentative of the human corneal endothelium as it is highly proliferative. However, this view is based largely upon studies conducted in the corneal endothelium of the rat, and results presented in chapter 3 suggest that mouse corneal endothelial cells do not readily proliferate. Moreover, the appearance of rat and mouse corneal endothelial monolayers displays a major difference between these two species. Primary rat corneal endothelial monolayers tend to be composed of cells with an elongated or fibroblastic appearance, while primary mouse corneal endothelial monolayers generally adopt a cobblestone appearance, similar to that which is noted in situ. Since phenotypic differences exist between the two species, it is also possible that mouse corneal endothelial cells might differ from the rat endothelium in their proliferative potential and therefore more closely resemble the human corneal endothelium. To gain futher insight into these issues, the proliferative responses of primary mouse corneal endothelial cultures were assessed following exposure to a number of different growth factors, including EGF, FGF-2 and PDGF BB.

4.1.1 Proliferative response of a mouse corneal endothelial cell line

Growth factor-induced proliferation was first investigated in the SV40 transformed mouse corneal endothelial cell line in order to establish optimal doses of growth factor. Subconfluent cultures were serum starved for 24 hours prior to experimentation. Cultures were then concomitantly treated with 5-bromo-2-deoxyuridine (BrdU) and growth factors overnight. BrdU is a thymidine analog that is incorporated into DNA during S-phase of the cell cycle and can therefore be used as a reporter of cell proliferation. Immunofluorescence staining using an anti-BrdU antibody allowed visualisation of cells which had entered the cell cycle during the period of treatment. Propidium iodide staining of all cell nuclei allowed the proportion of BrdU positive cells to be identified as a percentage of the total cell population (Figure 4.1A-F). Representative fields of cells were counted. Due to the high basal levels of proliferation in the SV-40 transformed cell line, however, growth factor stimulation did not exert any additional or discernable effect on the proliferative response. Approximately 80-90% of cells underwent at least one round of cell division, even in the absence of mitotic factors (Figure 4.1G). Due to this high basal level of proliferation, it was therefore impossible to test the proliferative response to each growth factor. Doses of growth factor selected for use in experiments with primary cultures were chosen based on those published in the literature. EGF was used at 100ng/ml, a saturating dose typically used to stimulate most cultured cells. A dose of 25ng/ml FGF-2 has been reported to stimulate corneal endothelial cells (Hoppenreijs et al., 1994) and 50ng/ml PDGF BB is the dose used to stimulate corneal keratocytes/fibroblasts (Hoppenreijs et al., 1993).

4.1.2 Proliferative response of primary mouse corneal endothelial cell cultures to growth factor stimulation

Primary mouse corneal endothelial cell cultures were treated in a similar manner to the SV-40 transformed cell line. Cultures were serum starved for 24 hours prior to treatment for either 24 or 48 hours with growth factor and BrdU.

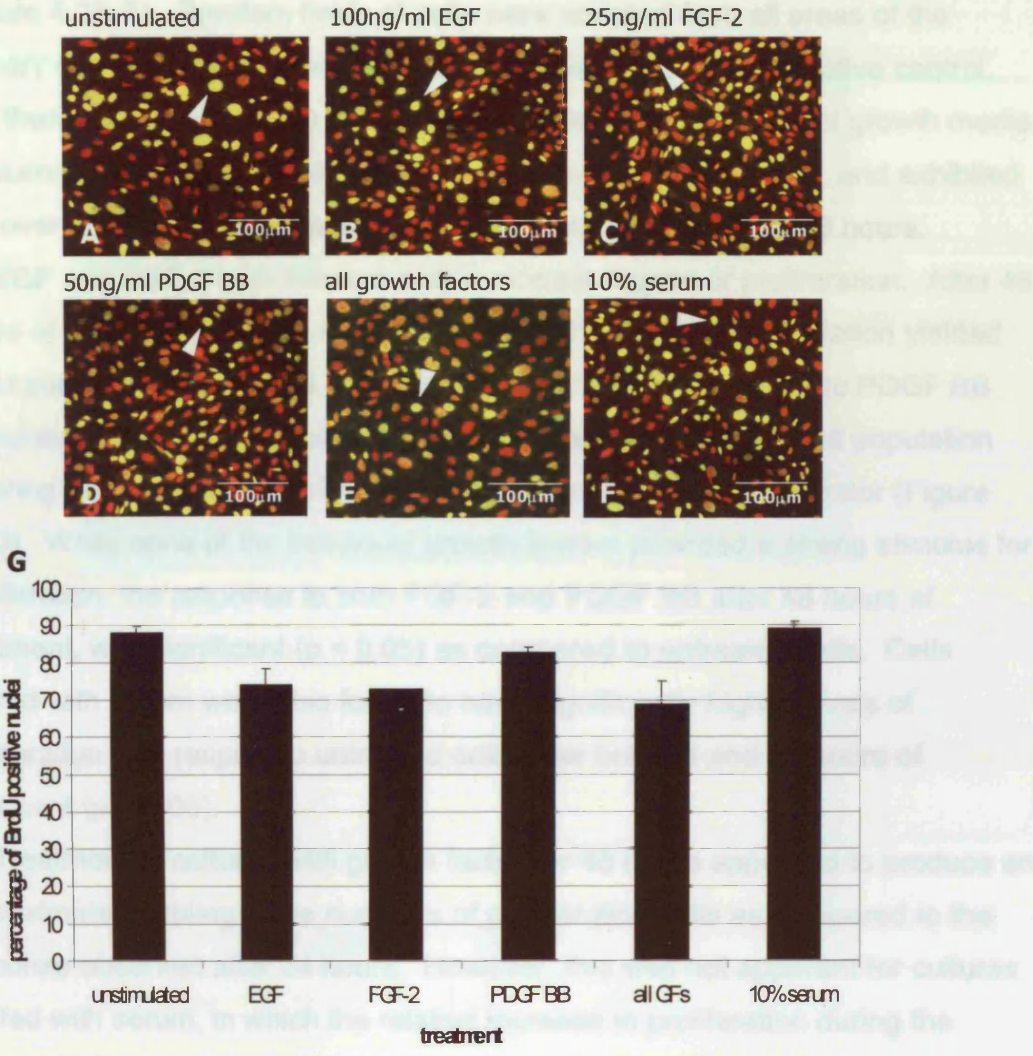

Figure 4.1. Proliferative response to growth factor stimulation in an SV40-transformed mouse corneal endothelial cell line. Sub-confluent mouse corneal endothelial cell cultures were used to investigate growth factor-induced proliferation. Cells were treated concomitantly with BrdU and growth factor. Propidium iodide was used to stain the total cell population, while antibody staining for BrdU was used to identify the proliferating cells. Yellow nuclei, indicated with arrowheads, represent proliferating cells, while red nuclei represent quiescent cells. The proportion of BrdU positive nuclei were counted as a proportion of the total cell population. At least 3000 cells were counted for each treatment. Basal levels of proliferation (A), however, were extremely high and it was impossible to distinguish the effects of growth factors (B,C,D,E) or serum treatment (F). Results for all growth factors are displayed in a graph, showing no difference between treatments (G). (n=3)

Proliferating cells were identified as a percentage of the total cell population (Figure 4.2A-F). Random fields of cells were counted from all areas of the primary cell monolayers. Untreated cultures were used as a negative control, and these elicited almost no proliferation. Cells cultured in normal growth media (containing 10% fetal calf serum) were used as a positive control, and exhibited just over 40% of the cell population entering into S-phase after 48 hours.

EGF and FGF-2 both induced only a modest degree of proliferation. After 48 hours of treatment with either growth factor, 10% of the cell population yielded BrdU positive nuclei (Figure 4.2B,C). The proliferative response to PDGF BB stimulation was slightly greater, with approximately 15% of the cell population entering into the cell cycle after 48 hours of exposure to growth factor (Figure 4.2D). While none of the individual growth factors provided a strong stimulus for proliferation, the response to both FGF-2 and PDGF BB after 48 hours of treatment, was significant ($p < 0.05$) as compared to untreated cells. Cells treated with serum were also found to have significantly higher levels of proliferation with respect to untreated cells after both 24 and 48 hours of treatment ($p < 0.05$).

Treatment of cultures with growth factor for 48 hours appeared to produce an approximate doubling in the numbers of proliferating cells as compared to the response observed after 24 hours. However, this was not apparent for cultures treated with serum, in which the relative increase in proliferation during the second 24 hour period was comparatively small. Interestingly, proliferation in all groups appeared to take place in patches rather than along the edge of the monolayer, as might have been expected.

4.1.3 Proliferative response of primary mouse corneal endothelial cell cultures to stimulation with multiple growth factors

Primary mouse corneal endothelial cell cultures were treated with combinations of two or more growth factors to investigate the possibility of synergistic actions of multiple mitogens on the proliferative response. Cultures were serum starved for 24 hours, prior to treatment with BrdU and growth factor

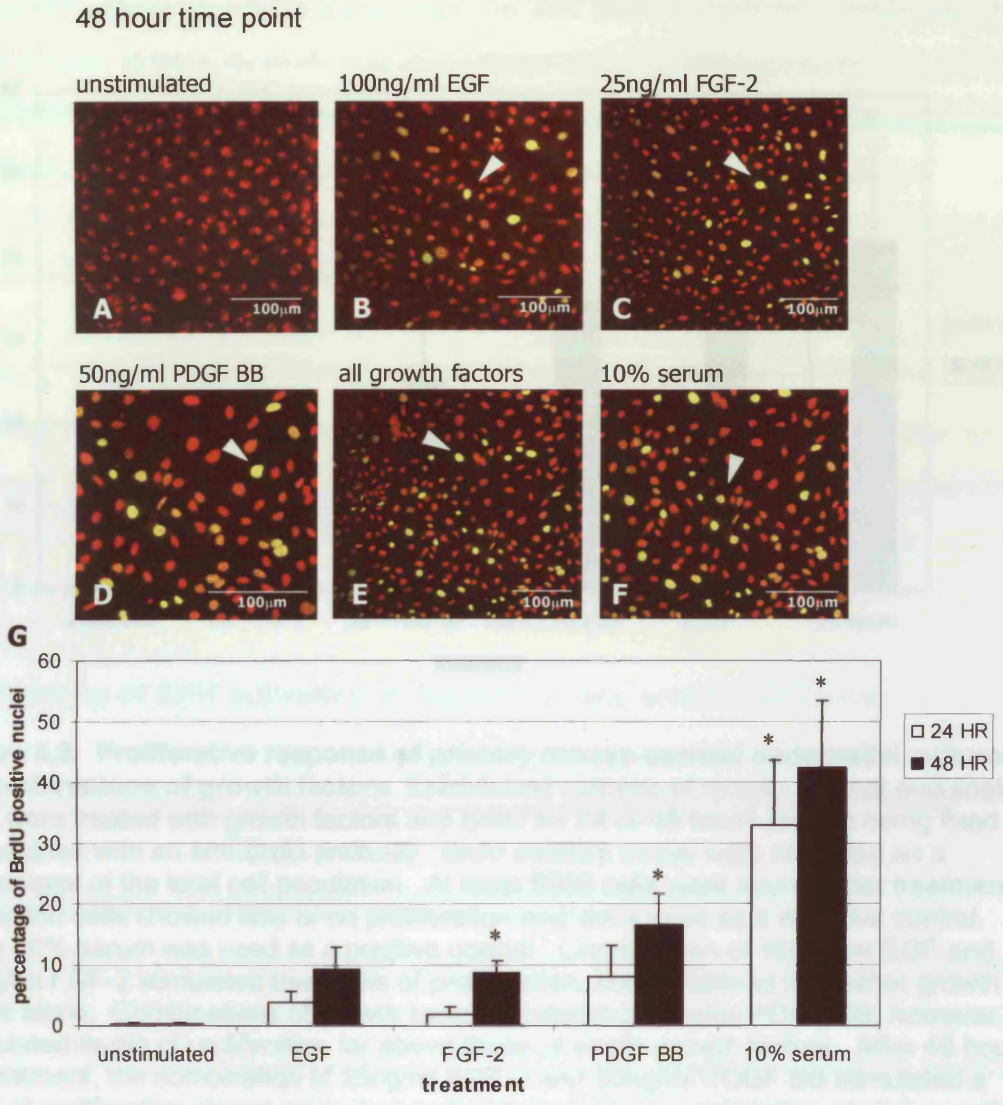

Figure 4.2. Proliferative response of primary mouse corneal endothelial cells to growth factor stimulation. Established cultures of primary mouse corneal endothelial cells were treated with both growth factors and BrdU for 24 or 48 hours. Nuclei were stained with propidium iodide and antibody staining for BrdU was used to identify proliferating cells. BrdU positive nuclei (yellow nuclei, indicated with arrowheads) were a measured as a percentage of the total cell population. At least 5000 cells were counted per treatment. Untreated cells showed little or no proliferation and were used as a negative control (A), while cells treated with 10% serum were used as a positive control (F). 100ng/ml EGF (B) appeared to stimulate proliferation but the response was not significant. 25ng/ml FGF-2 (C) and 50ng/ml PDGF BB (D) stimulated a significantly greater amount of proliferation than untreated cells. * represent cell populations with a significantly ($p<0.05$) higher proliferative response as compared to unstimulated cells. ($n>3$)

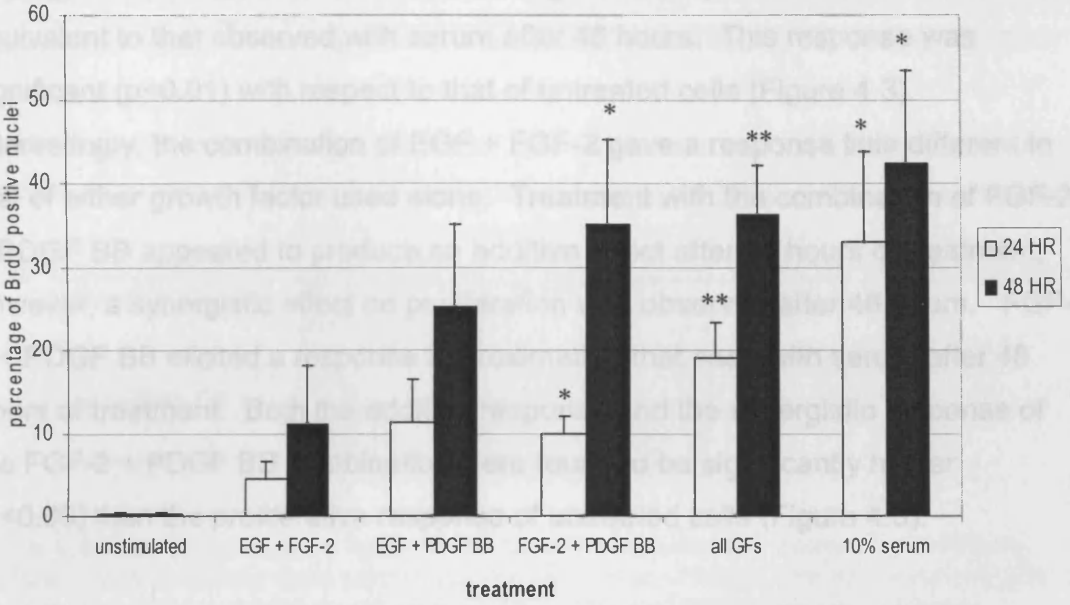

Figure 4.3. Proliferative response of primary mouse corneal endothelial cultures to combinations of growth factors. Established cultures of mouse corneal endothelial cells were treated with growth factors and BrdU for 24 or 48 hours prior to being fixed and stained with an anti-BrdU antibody. BrdU positive nuclei were identified as a percentage of the total cell population. At least 5000 cells were counted per treatment. Untreated cells showed little or no proliferation and were used as a negative control, while 10% serum was used as a positive control. Combination of 100ng/ml EGF and 25ng/ml FGF-2 stimulated low levels of proliferation, comparable to that either growth factor alone. Combinations of growth factors containing 50ng/ml PDGF BB, however, stimulated levels of proliferation far above those of single growth factors. After 48 hours of treatment, the combination of 25ng/ml FGF-2 and 50ng/ml PDGF BB stimulated a level of proliferation almost equivalent to that induced by a combination of all 3 growth factors (all GFs) or serum. Responses significantly above that of unstimulated cells are represented as follows: * $p<0.05$, ** <0.01 ($n > 3$)

for a further 24 or 48 hours. Untreated cells were again used as a negative control, while those treated with growth media containing 10% serum, were used as a positive control.

Most of the combinations of growth factors produced an additive rather than synergistic effect on proliferation. Combinations of EGF + PDGF BB, and EGF + FGF-2 + PDGF BB, elicited proliferative responses that appeared to represent the additive effects of the proliferative responses of each growth factor used

alone. The maximal proliferative response was noted in cultures treated with all three growth factors, in which the percentage of BrdU positive nuclei was almost equivalent to that observed with serum after 48 hours. This response was significant ($p<0.01$) with respect to that of untreated cells (Figure 4.3). Interestingly, the combination of EGF + FGF-2 gave a response little different to that of either growth factor used alone. Treatment with the combination of FGF-2 + PDGF BB appeared to produce an additive effect after 24 hours of treatment, however, a synergistic effect on proliferation was observed after 48 hours. FGF-2 + PDGF BB elicited a response approximating that seen with serum after 48 hours of treatment. Both the additive response and the synergistic response of the FGF-2 + PDGF BB combination were found to be significantly higher ($p<0.05$) than the proliferative response of untreated cells (Figure 4.3).

4.2 Kinetics of ERK activation in mouse corneal endothelial cells

Mitogen-activated protein kinase (MAPK) involvement in growth factor-induced proliferation has been well documented {Weber, 1997 431 /id}. The classical MAPKs in mammalian cells are the Extracellular signal Regulated Kinases (ERK) 1 and 2, and these are activated by phosphorylation downstream of the small GTPases Ras and Raf. In order to test whether the growth factors used to stimulate proliferation also activate the MAPK pathway, western blotting of phospho-ERK1/2 was performed on lysates of growth factor treated cell cultures.

4.2.1 ERK activation in a mouse corneal endothelial cell line

SV-40 transformed mouse corneal endothelial cells were serum starved for at least 2 hours prior to treatment with 100ng/ml EGF, 25ng/ml FGF-2 or 50ng/ml PDGF BB for 0, 5, 15, 30, 60, 90 or 120 minutes. Cell lysates were western blotted for the phosphorylated and unphosphorylated forms of ERK 1/2. All growth factors showed a similar pattern of ERK 1/2 phosphorylation, peaking after 5 minutes of exposure to growth factor (Figure 4.4). The same blots were

also probed for α-tubulin to ensure equal protein loading. Quantitative evaluation revealed little difference in the kinetics of ERK1/2 activation, irrespective of growth factor used. These results are reasonably consistent with the proliferation data (Figure 4.2).

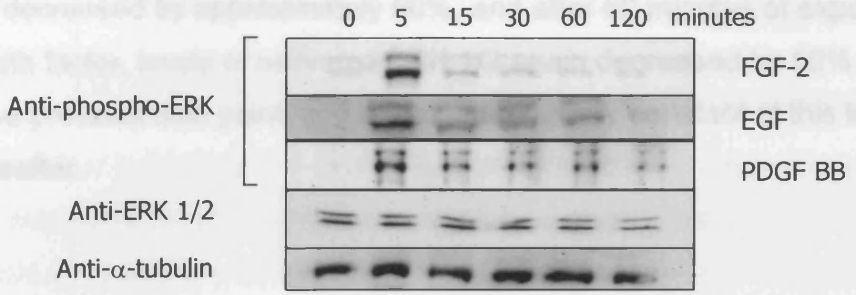

Figure 4.4 ERK 1/2 activation in an SV40 transformed mouse corneal endothelial cell line. Cells in culture were serum starved for at least 2 hours prior to treatment with growth factor. 25ng/ml FGF-2, 100ng/ml EGF or 50ng/ml PDGF BB was added to serum-free culture media at 0, 5, 15, 30, 60 and 120 minute intervals. Lysates were made directly in reducing sample buffer. Western blotting revealed that all 3 growth factors elicited a similar pattern of ERK activation following growth factor stimulation. ERK phosphorylation peaked after 5 minutes of treatment with growth factor and returned to basal levels after 2 hours. Levels of total protein per sample were assessed to be equal by blotting samples for α-tubulin and total levels of ERK 1/2. This also revealed that levels of ERK 1/2 remained unchanged.

4.2.2 ERK activation in primary mouse corneal endothelial cell cultures

Primary mouse corneal endothelial cultures showed a different pattern of ERK activation to that observed in the cell line. Cultures were serum starved overnight prior to treatment with growth factor for 0, 5, 15, 30, 60, 90 or 120 minutes. Growth factors were used at the same concentrations as in previous experiments to stimulate cell proliferation; namely 100ng/ml EGF, 25ng/ml FGF-2 or 50ng/ml PDGF BB. Whole cell lysates were western botted for phosphorylated and unphosphorylated ERK 1/2 and α-tubulin.

EGF stimulated cultures demonstrated a peak in ERK 1/2 activation after 5 minutes of stimulation, which was sustained after 15 minutes of EGF stimulation.

After 30 minutes of treatment with EGF, however, levels of phosphorylated ERK 1/2 had returned to approximately basal levels (Figure 4.5).

PDGF BB stimulated cultures produced a more sustained ERK 1/2 activation. ERK 1/2 becomes activated after only 5 minutes of stimulation PDGF BB, with a peak in activation after 15 minutes. By 30 minutes, levels of phospho-ERK 1/2 had decreased by approximately 50%, and after 60 minutes of exposure to growth factor, levels of activated ERK 1/2 again decreased by 50% with respect to the previous time point, and remained relatively constant at this level thereafter.

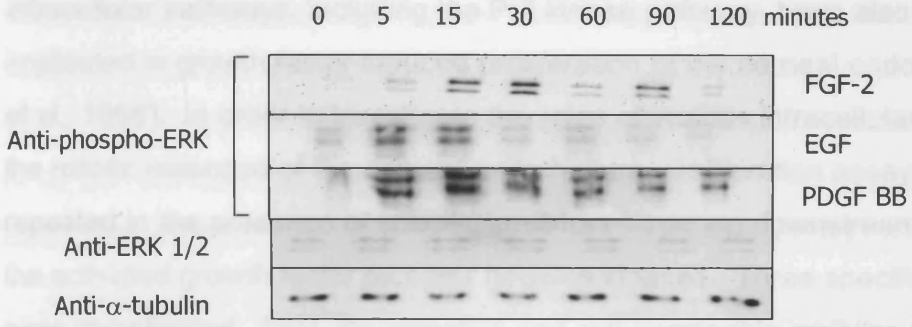

Figure 4.5 ERK 1/2 activation in primary mouse corneal endothelial cells treated with growth factors. Cells in culture were serum starved for at least 2 hours prior to treatment with growth factor. 25ng/ml FGF-2, 100ng/ml EGF or 50ng/ml PDGF BB was added to serum-free culture media at 0, 5, 15, 30, 60 and 120 minute intervals. Lysates were made directly in reducing sample buffer. Both EGF and PDGF BB showed a peak in ERK 1/2 activation after 15 minutes of treatment with growth factor. FGF-2 stimulated a biphasic activation of ERK 1/2, with the first peak in activation after 30 minutes of stimulation and the second after 90 minutes of stimulation. Levels of total protein per sample were assessed to be equal by blotting samples for α-tubulin and total levels of ERK 1/2. This also revealed that levels of ERK 1/2 remained unchanged.

Cells stimulated with FGF-2 showed the most distinctive pattern of ERK 1/2 activation, eliciting a biphasic profile of ERK 1/2 activation over a 2 hour time frame. This was a highly reproducible observation, which showed the first peak in activation occurs after 30 minutes of stimulation, and the second 90 minutes after stimulation. In this experiment activated ERK 1/2 began to accumulate in the cell after 5 minutes, and continued to increase in intensity resulting in a peak

after 30 minutes. By 60 minutes, levels of activated ERK 1/2 had fallen to almost basal levels, before peaking again after 90 minutes. At the end of 120 minutes of treatment, the levels of activated ERK 1/2 return to almost basal level. It is possible that further cycles of ERK 1/2 activation might occur in longer kinetic experiments.

4.3 Inhibition of the proliferative response

While it is clear from these experiments that the MAPK pathway is activated following growth factor stimulation of corneal endothelial cells, the question arises as to whether this pathway is vital to the proliferative response. Other intracellular pathways, including the PI3 kinase pathway, have also been implicated in growth factor-induced proliferation of the corneal endothelium (Kay et al., 1998). In order to investigate the roles of various intracellular pathways in the mitotic response of the corneal endothelium, proliferation assays were repeated in the presence of specific inhibitors targeting downstream effectors of the activated growth factor receptor tyrosine kinases. Three specific inhibitors were investigated. First, the selective and cell-permeable inhibitor of MAPK kinase (MEK), PD98059 (2'-amino-3'-methoxyflavone), was used to block the MAPK pathway. PD98059 inhibits the activation of MAPK and subsequent phosphorylation of MAPK substrates. Second, the potent, specific and cell-permeable inhibitor of PI3 kinase, LY294002 (2-(4-morpholinyl)-8-phenyl-4H-1-benzopyran-4-one), acts on the ATP-binding site of the kinase to block the PI3 kinase pathway. Third, the non-specific protein tyrosine kinase inhibitor, genistein (4',5,7-trihydroxyisoflavone), was used as a general inhibitor of tyrosine phosphorylation. The effects of each of these inhibitors were investigated with regard to the proliferative responses of primary mouse corneal endothelial cultures to serum and various growth factors.

4.3.1 Dose response curves of inhibitor concentrations in a mouse corneal endothelial cell line

In order to determine the appropriate concentrations of inhibitor to use for these studies, dose response curves were conducted for each inhibitor on the SV40 transformed mouse corneal endothelial cell line. Cells in culture media, containing 10% serum, were treated with BrdU and four different doses of inhibitor overnight. BrdU positive cells were counted as a percentage of the total cell population. Western blotting was used to reveal the effects on downstream signalling molecules of various concentrations of inhibitor.

Doses of PD98059 tested included 1, 10, 50 and 100μM, with a dose of 50μM producing a maximal, though modest, inhibitory effect on proliferation. Doses of 2, 10, 20 and 40μM of inhibitor LY294002 produced a typical dose response curve, with a dose of 20μM LY294002 halving the proliferative response. Doses of 10, 50, 100 and 250μM genistein also produced a typical dose response curve, with 100μM proving to be the optimal inhibiting dose (Figure 4.6).

Western blotting was used to confirm that the inhibitors were indeed targeting the anticipated intracellular pathways. The effects of PD98059 were tested by blotting for phosphorylated ERK 1/2, which was found to be decreased with 50μM PD98059. Phosphorylation of Akt (Protein Kinase B), a downstream effector of PI3 kinase, was appropriately decreased with treatment of 20μM LY294002, and a decrease in tyrosine phosphorylated polypeptides was also noted at a dose of 100μM genistein (Figure 4.6).

While each of these studies was completed over a 16 hour time course, the results were similar for cells treated for 24 hours. From the dose response curves, concentrations of inhibitors were selected for use in studies on primary cells. 50μM PD98059, 20μM LY294002 and 100μM genistein were used for all further inhibitor studies. Taken together, these results suggest that tyrosine phosphorylation, and activation of the PI3 kinase pathway, contribute more to the proliferative response than the MAPK pathway in the SV40 transformed mouse corneal endothelial cell line.

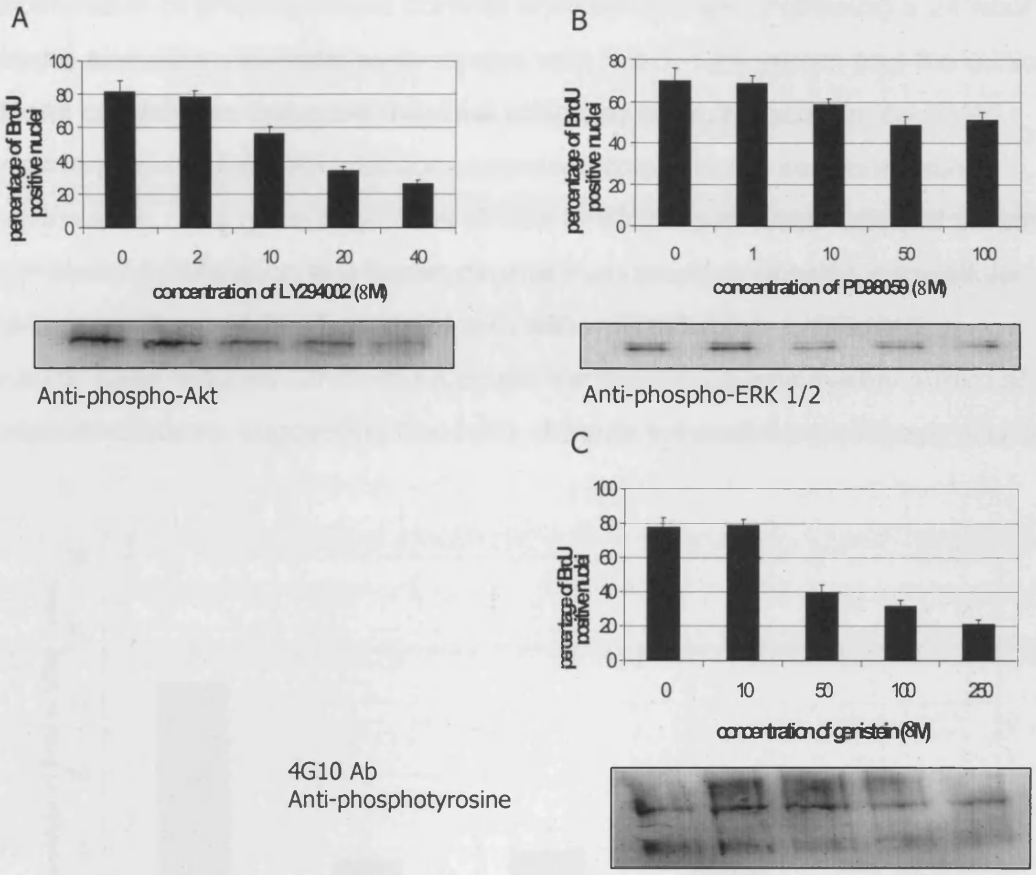

Figure 4.6 Inhibition of serum-induced proliferation in an SV40 transformed mouse corneal endothelial cell line. Cells were treated with serum and various inhibitors; PI3 kinase inhibitor, LY294002 (A), MAPK inhibitor, PD98059 (B) and tyrosine kinase inhibitor, genistein (C) for 16 hours. BrdU staining was used to visualise proliferating cells. 20μM LY294002 halved the proliferative response to serum and also reduced levels of phosphorylated Akt (A). 50μM PD98059 inhibited corneal endothelial cell proliferation and significantly decreased levels of phophorylated ERK1/2 (B). Treatment with 100μM genistein produced a significant decrease in tyrosine phosphorylation coinciding with a reduction in serum-induced proliferation (C).

4.3.2 Inhibition of serum-induced primary mouse corneal endothelial cell proliferation

Initially, the effects of these inhibitors were tested on serum-induced proliferation of primary mouse corneal endothelial cells. Following a 24 hour serum starvation, the cells were treated with BrdU, 10% serum and the minimal doses of inhibitors that gave maximal inhibition of proliferation in the SV40 transformed cell line. All inhibitors appeared to attenuate serum-induced proliferation. The general tyrosine kinase inhibitor, genistein, reduced serum stimulated proliferation to a lesser degree than blocking specific intracellular pathways (Figure 4.7). Treatment with either PD98059 or LY294002 substantially reduced serum-induced proliferation to approximately a third of the original response, suggesting that both of these intracellular pathways play a role

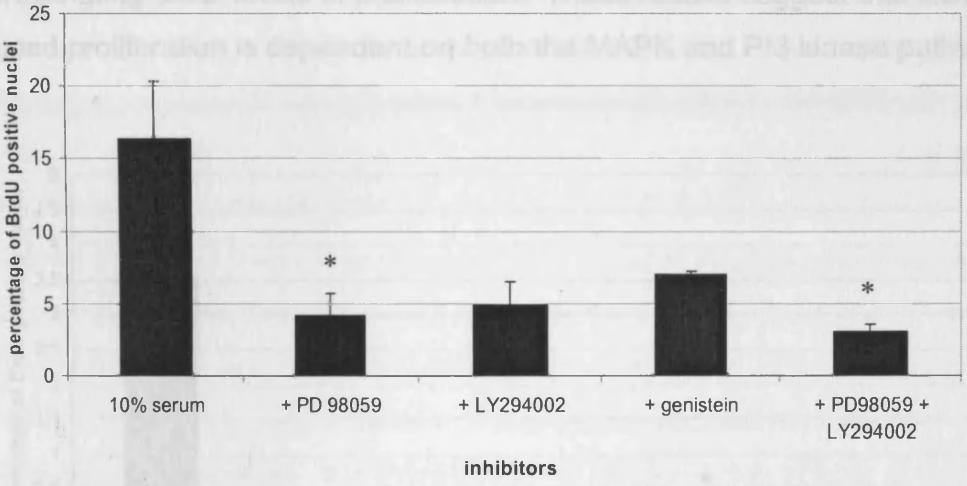

Figure 4.7 Effects of various inhibitors on serum-induced proliferation of primary mouse corneal endothelial cells. Mouse corneal endothelial cell cultures were treated with BrdU, 10% serum and inhibitor for 24 hours. BrdU positive nuclei were identified as a percentage of the total cell population. The strength of inhibition of the serum-induced proliferative response is as follows: MAPK inhibitor (PD98059) > PI3 kinase inhibitor (LY294002) > tyrosine kinase inhibitor (genistein). The combination of both PD98059 and LY294002 produced a greater inhibitory effect than either of the two inhibitors alone. Serum-induced proliferation was significantly reduced with PD98059 and a combination of PD98059 and LY294002 (*$p < 0.05$). None of the inhibitors or combinations of inhibitors completely abolished the proliferative response of mouse corneal endothelial cells to serum. (n=3)

in the serum-induced proliferative response, however, only PD98059 yielded a statistically significantly reduced serum stimulated proliferation ($p<0.05$). The combination of these two inhibitors produced a greater effect on serum-induced proliferation than either of the inhibitors alone. This result was also found to be significant ($p<0.05$).

4.3.3 Inhibition of EGF-induced primary mouse corneal endothelial cell proliferation

Primary mouse corneal endothelial cell cultures were serum starved for 24 hours prior to treatment with 100ng/ml EGF, BrdU and a panel of inhibitors for 48 hours. The proliferative response elicited by EGF treatment was modest with approximately 3.5% of the total cell population entering mitosis. Treatment with any of the inhibitors, however, reduced this proliferative response to levels approximating basal levels of proliferation. These results suggest that EGF-induced proliferation is dependent on both the MAPK and PI3 kinase pathways.

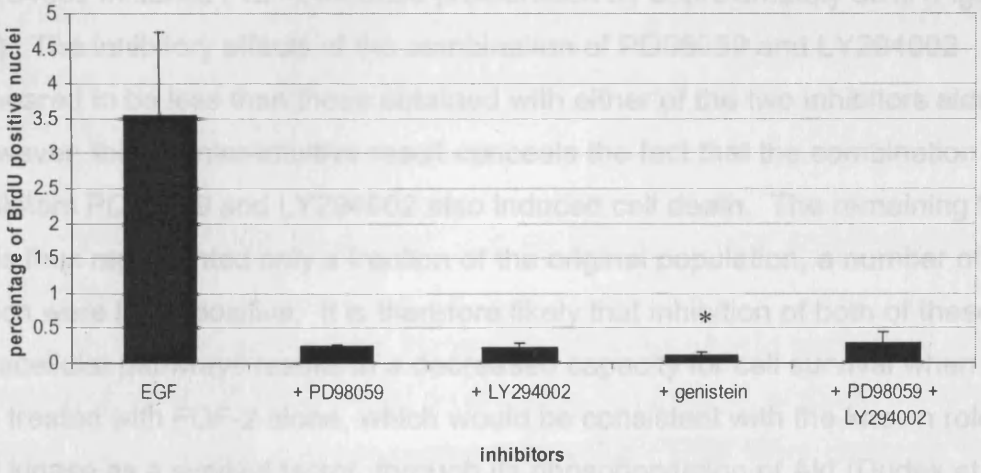

Figure 4.8 Effects of various inhibitors on EGF-induced proliferation on mouse corneal endothelial cells. Primary mouse corneal endothelial cell cultures were treated with BrdU, 100ng/ml EGF and inhibitor for 48 hours prior to fixation and staining for BrdU. BrdU positive nuclei were identified as a percentage of the total cell population Only the inhibitory effects of genistein was found to significantly reduce EGF-induced proliferation (* $p<0.05$). (n=3)

Additionally, tyrosine phosphorylation of various intracellular targets clearly plays a vital role in the proliferative response, as inhibition of tyrosine phosphorylation significantly reduced EGF stimulated proliferation (Figure 4.8).

As these studies revealed the proliferative response of primary mouse corneal endothelial cell cultures to EGF to be very low, the effects of inhibitors in this experiment are unavoidably limited, hence it is not possible to draw conclusions from these results.

4.3.4 Inhibition of FGF-2-induced primary mouse corneal endothelial cell proliferation

Primary cultures were serum starved for 24 hours prior to treatment with 25ng/ml FGF-2, BrdU and various inhibitors for 48 hours. Both PD98059 and LY294002 inhibited FGF-2-induced proliferation to a greater degree than genistein, though all three inhibitors significantly reduced FGF-2 stimulated proliferation ($p<0.05$). Treatment with genistein more than halved the proliferative response to FGF-2, while treatment with either PD98059 or LY294002 inhibited FGF-2 induced proliferation by approximately 65% (Figure 4.9). The inhibitory effects of the combination of PD98059 and LY294002 appeared to be less than those obtained with either of the two inhibitors alone. However, this counter-intuitive result conceals the fact that the combination of inhibitors PD98059 and LY294002 also induced cell death. The remaining living cells thus represented only a fraction of the original population, a number of which were BrdU positive. It is therefore likely that inhibition of both of these intracellular pathways results in a decreased capacity for cell survival when cells are treated with FGF-2 alone, which would be consistent with the known role of PI3 kinase as a survival factor, through its phosphorylation of Akt (Dudek et al., 1997).

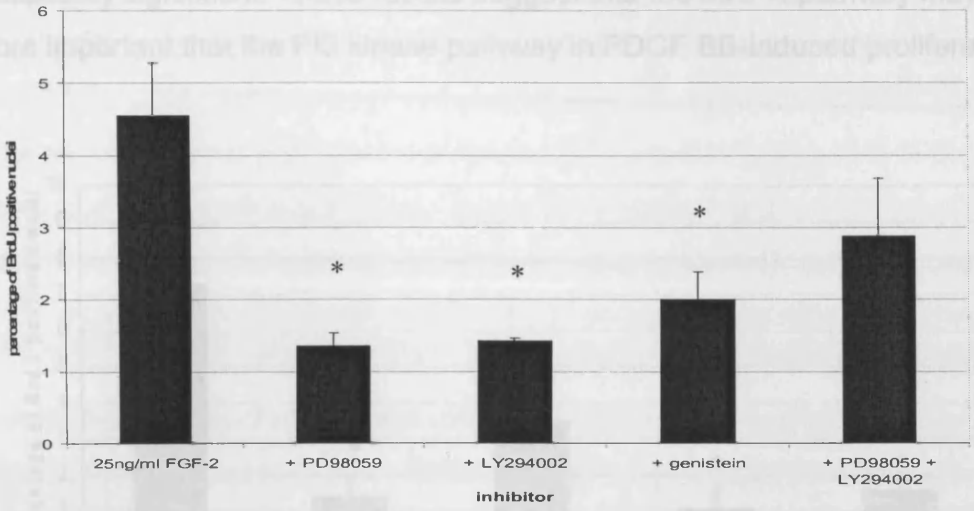

Figure 4.9 Effects of various inhibitors on FGF-2-induced proliferation on mouse corneal endothelial cells. Primary mouse corneal endothelial cell cultures were treated with BrdU, 25ng/ml FGF-2 and inhibitor for 48 hours. BrdU positive cells were identified by antibody staining, and identified as a percentage of the total cell population. Ether MAPK inhibitor, PD98059, and PI3 kinase inhibitor, LY294002, produced a greater inhibitory effect than tyrosine kinase inhibitor, genistein. However, each of these inhibitors significantly reduced FGF-2 stimulated proliferation ($p<0.05$). The combination of PD98059 and LY294002 produced far less of an inhibitory effect on the FGF-2-induced proliferative response than PD98059 or LY294002 alone. This result may be unrepresentative, as the combination of both inhibitors also promoted cell death. None of the inhibitors, or combinations of inhibitors, were able completely abolished the proliferative response of mouse corneal endothelial cells to FGF-2.

4.3.5 Inhibition of PDGF BB-induced primary mouse corneal endothelial cell proliferation

Primary cultures were serum starved for 24 hours prior to testing the effects of inhibitors on PDGF BB-induced proliferation. LY294002 inhibited PDGF BB-induced proliferation to a lesser degree than either PD98059 or genistein, both of which significantly reduced PDGF BB stimulated proliferation ($p<0.05$). LY294002 approximately halved the mitotic response to PDGF BB, while PD98059 and genistein were more potent in reducing the proliferative response to 15% of the control value (Figure 4.10). The combination of both PD98059 and LY294002 produced a similar effect to PD98059 alone, though this result was not

statistically significant. These results suggest that the MAPK pathway may be more important that the PI3 kinase pathway in PDGF BB-induced proliferation.

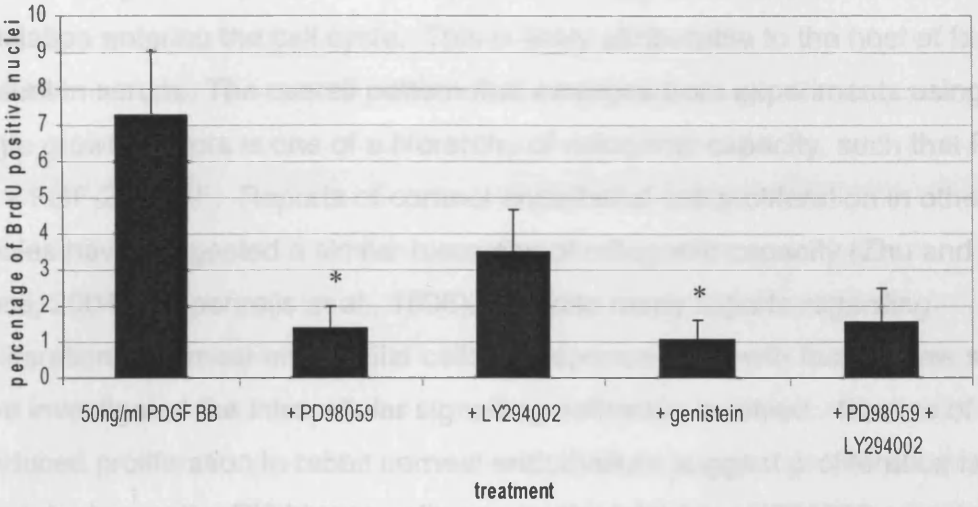

Figure 4.10 Effects of various inhibitors on PDGF BB-induced proliferation on mouse corneal endothelial cells. Primary mouse corneal endothelial cell cultures were treated with BrdU, 50ng/ml PDGF BB and inhibitor for 48 hours. BrdU positive nuclei were identified as a percentage of the total cell population. Treatment with MAPK inhibitor, PD98059, and tyrosine kinase inhibitor, genistein, both showed significant inhibition of PDGF BB-induced proliferation (*$p<0.05$). PI3 kinase inhibitor, LY294002, decreased PDGF BB-induced proliferation but to a lesser degree than that induced by the other inhibitors. Combination of both PD98059 and LY294002 did not inhibit proliferation more than PD98059 alone. None of the inhibitors or combinations of inhibitors completely abolished the proliferative response of mouse corneal endothelial cells to PDGF BB. (n=3)

4.4 Summary

Unstimulated, confluent primary mouse corneal endothelial cultures showed negligible levels of proliferation. However, even this very low level of proliferation was unexpected as corneal endothelial cells are generally considered to be G1-phase arrested. This low level of proliferation may be related to the lack of proper junction formation. Cell junctions have been demonstrated to play an important role in maintaining the non-proliferative status of the corneal

endothelium (Senoo et al., 2000) and, as primary cultures do not form junctions as effectively as endothelium in situ, the lack of cell contact inhibition may account for a modest degree of cell proliferation. Treatment with 10% serum induced the greatest proliferative response with approximately 40% of the cell population entering the cell cycle. This is likely attributable to the host of factors present in serum. The overall pattern that emerges from experiments using single growth factors is one of a hierarchy of mitogenic capacity, such that PDGF BB > FGF-2 > EGF. Reports of corneal endothelial cell proliferation in other species have suggested a similar hierarchy of mitogenic capacity (Zhu and Joyce, 2004; Hoppenreijs et al., 1996). Despite many reports regarding proliferation of corneal endothelial cells in response to growth factors, few studies have investigated the intracellular signalling pathways involved. Studies of FGF-2-induced proliferation in rabbit corneal endothelium suggest proliferation is dependent upon the PI3 kinase pathway, as the inhibitor LY294002 completely abolishes the mitotic response to FGF-2 (Lee and Kay, 2003b). Though LY294002 significantly reduced FGF-2 stimulated proliferation in mouse corneal endothelial cultures, it did not completely abolish the proliferative response. Additionally, the MAPK inhibitor, PD98059, and the tyrosine kinase inhibitor, genistein, also significantly reduced FGF-2 induced proliferation. The discrepancy between these results may be due to the difference in proliferative potential of the corneal endothelium of the species used in each study. Lee and Kay (2003b) used a model of rabbit corneal endothelium, which is known to be relatively proliferative even when unstimulated. In contrast, unstimulated mouse corneal endothelial cultures showed a negligible amount of proliferation, this was far below that noted in rabbit corneal endothelium. Furthermore, treatment of FGF-2 stimulated mouse corneal endothelial cultures with a combination of inhibitors LY294002 and PD98059 was found to induce cell death. Therefore, it seems likely that these pathways play a role not only in the proliferative response, but also in the maintenance of mouse corneal endothelial cell survival.

Intracellular signalling pathways initiated by EGF or PDGF BB stimulation have not been investigated in the corneal endothelium. While both the MAPK

inhibitor, PD98059, and the PI3 kinase inhibitor, LY294002, reduced EGF stimulated proliferation of mouse corneal endothelial cultures, only the tyrosine kinase inhibitor, genistein, provided a significant block to EGF-induced proliferation. It is, however, difficult to draw conclusions from these data, since EGF increased levels of proliferation only marginally above those observed in unstimulated cells. Conversely, PDGF BB elicited the greatest mitogenic response in mouse corneal endothelial cultures. Only PD98059 and genistein were able to significantly reduce the proliferative effects of PDGF BB. While LY294002 reduced PDGF BB stimulated proliferation, the reduction in proliferation was not significant. These results suggest that PDGF BB induced proliferation is more reliant on the MAPK pathway than the PI3 kinase pathway.

Similar studies were perfomed in parallel in the SV40 transformed cell line. No difference was noted between the proliferative response of unstimulated cells and those treated with growth factors or serum, due to the high intrinsic proliferative capacity of these cells, however, the effects of inhibitors on this proliferative response were easily discernable. LY294002 and genistein reduced proliferation more potently than PD98059 in the SV40 transformed cell line.

Differences between primary cells and the SV40 transformed cell line were also apparent in MAPK activation, in response to growth factor stimulation. Both the kinetics and the pattern of ERK signalling differed between the SV40 transformed mouse corneal endothelial cell line and primary mouse corneal endothelial cultures. The overall kinetics of activation appeared to be slower in the primary cells as compared to the cell line. Growth factor treatment initiated a peak in ERK 1/2 phosphorylation after 5 minutes in the cell line, while a peak in ERK 1/2 activation required at least 15 minutes of stimulation in primary cells. However, the most dramatic discrepancy between primary cells and the cell line was noted in FGF-2 treated cultures. The SV40 transformed cell line responded to FGF-2 treatment with a small peak in activation after 5 minutes, which then returned to basal levels after 15 minutes. Primary cells treated with FGF-2, however, showed a biphasic pattern of ERK1/2 activation. The first peak occurred after 30 minutes of FGF-2 stimulation and the second after 90 minutes.

The implications of this difference in ERK1/2 signalling are unclear but warrant attention as the MAPK pathway has been demonstrated to be an important mediator of growth factor-induced proliferation. Biphasic activation of MAPK has previously been reported (Meloche et al., 1992) and is suggested to be necessary for a full mitogenic response. Presumably, SV40 transformation overrides the mechanism that regulates this pathway.

Unsurprisingly, studies in this chapter show that the proliferative responses of the SV40 transformed mouse corneal endothelial cell line and primary mouse corneal endothelial cells are different. SV40 transformation clearly provides a driving force for proliferation that cannot be matched in primary cultures, even when these are subjected to optimal concentrations of serum and growth factors. Further study suggests that these differences in proliferation may be the consequence of changes to intracellular signalling pathways involved in the growth factor induced proliferative response.

Chapter 5: Primary human corneal endothelial cell culture

The techniques for primary culture of human corneal endothelial cells are well established (Baum et al., 1984; Engelmann et al., 1988; Engelmann and Friedl, 1989). Isolation of endothelial cells from the human cornea involves separation of Descemet's membrane and the associated monolayer of endothelial cells from the corneal stroma. Cells can then be detached from Descemet's membrane by treatment with EDTA. Culture medium for human corneal endothelial cells is routinely supplemented with growth factors to enhance proliferation and assist survival. At present, it remains unclear which growth factors are responsible for the proliferative response and which growth factors play a role in cell survival. To gain insight into these questions, studies in this chapter make use of three growth factors; EGF, FGF-2 and PDGF BB. Both EGF and FGF-2 are routinely used to supplement human corneal endothelial culture media and their proliferative effects have been investigated in both culture (Samples et al., 1991; Senoo and Joyce, 2000; Zhu and Joyce, 2004) and wound healing models (Hoppenreijs et al., 1992). Only one study has investigated the proliferative effects of PDGF BB on human corneal endothelial cells (Zhu and Joyce, 2004). The intracellular pathways which mediate the proliferative response of the human corneal endothelium have not been investigated. Because cell contact has been demonstrated to play a role in human corneal endothelial cell expansion (Senoo et al., 2000), analysis of cell junctions was also undertaken in conjunction with cell proliferation studies. Analysis of cell junctions and growth factor-induced proliferation enable comparisons to be made between human and mouse corneal endothelial cultures, and thus develop an informed view as to whether mouse corneal endothelial cultures present an appropriate model for human corneal endothelium.

5.1 Characterisation of primary human corneal endothelial cultures

5.1.1 Human corneal endothelial cell morphology

Following previously described methods for the isolation of human corneal endothelial cells, Descemet's membrane was separated from the cornea and endothelial cells were detached using trypsin and EDTA. Dissociation of corneal endothelial cells from Descemet's membrane typically resulted in patches of the endothelial monolayer separating from the matrix. Isolated corneal endothelial cells were plated into tissue culture dishes coated with a mixture of matrix proteins. Initial densities of human corneal endothelial cultures were low (Figure 5.1A), allowing the cells to spread and proliferate and adopt a variety of morphologies. Generally, the cells spread and flattened and come into close contact with neighbouring cells, resulting in enlarged surface areas and nuclei, which appeared as bulges in the membrane (Figure 5.1A). As the cells continued to proliferate, cultures reached a higher density and eventually covered the cell culture dish. Overall, densities of corneal endothelial cells varied over the surface of the tissue culture dish, with the greatest density of cells at the centre (Figure 5.1C) and the lowest densities at the perimeter of the culture dish (Figure 5.1D). The heterogeneous cell population at the edge of the culture dish included large flattened cells with nuclei forming a low bulge at the cell surface, similar to those noted in low density cultures (Figure 5.1D). The central region of the dish contained a relatively homogeneous population in which cells displayed a more regular morphology (Figure 5.1C). Phase images also appeared to suggest a decrease in cell surface area, which is likely the result of progression from thin, flattened cells to columnar shaped cells. As the cells became columnar in shape, they no longer displayed protruding nuclei (Figure 5.1C). The characteristics of human corneal endothelial cultures were distinctive from those of potentially contaminating corneal keratocytes/fibroblasts. Unlike corneal endothelial cells, corneal keratocyte cultures quickly proliferated to form layers of elongated cells in swirling patterns (Figure 5.1B).

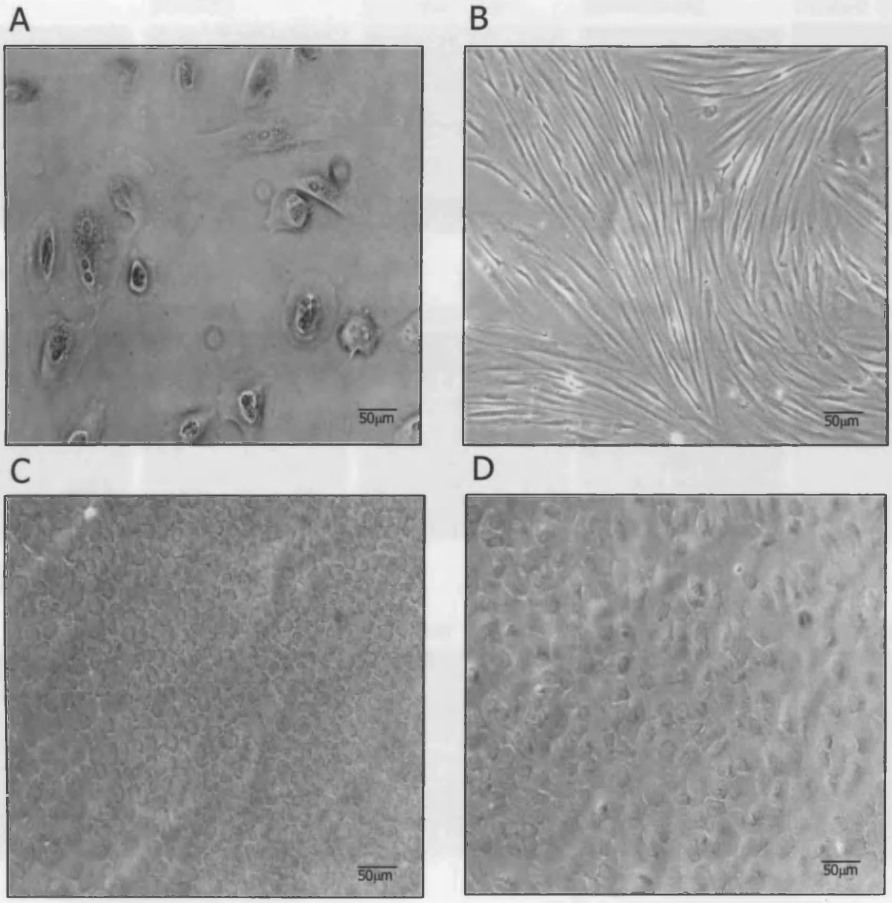

Figure 5.1 Phase images of human corneal endothelial and keratocyte cultures. Human corneal endothelial cell cultures were established by separating Descemet's membrane from organ cultured corneas and isolating the endothelial cell population from this membrane. At the beginning of culture, the cells are large, as they spread to fill the available space (A). After approximately 8-12 weeks in culture, cell populations become densely packed and begin to more closely resemble endothelial monolayers of the cornea. Towards the centre of the culture dish, the cells form a densely packed monolayer (C), however, at the edge of the culture dish, a less dense, heterogeneous cell population exists (D). While the phenotype of corneal endothelial cells varies depending on cell density, it consistently remains distinct from that of corneal keratocytes/fibroblasts (B). As the cells are passaged, the endothelial monolayers generated in culture become increasingly heterogeneous.

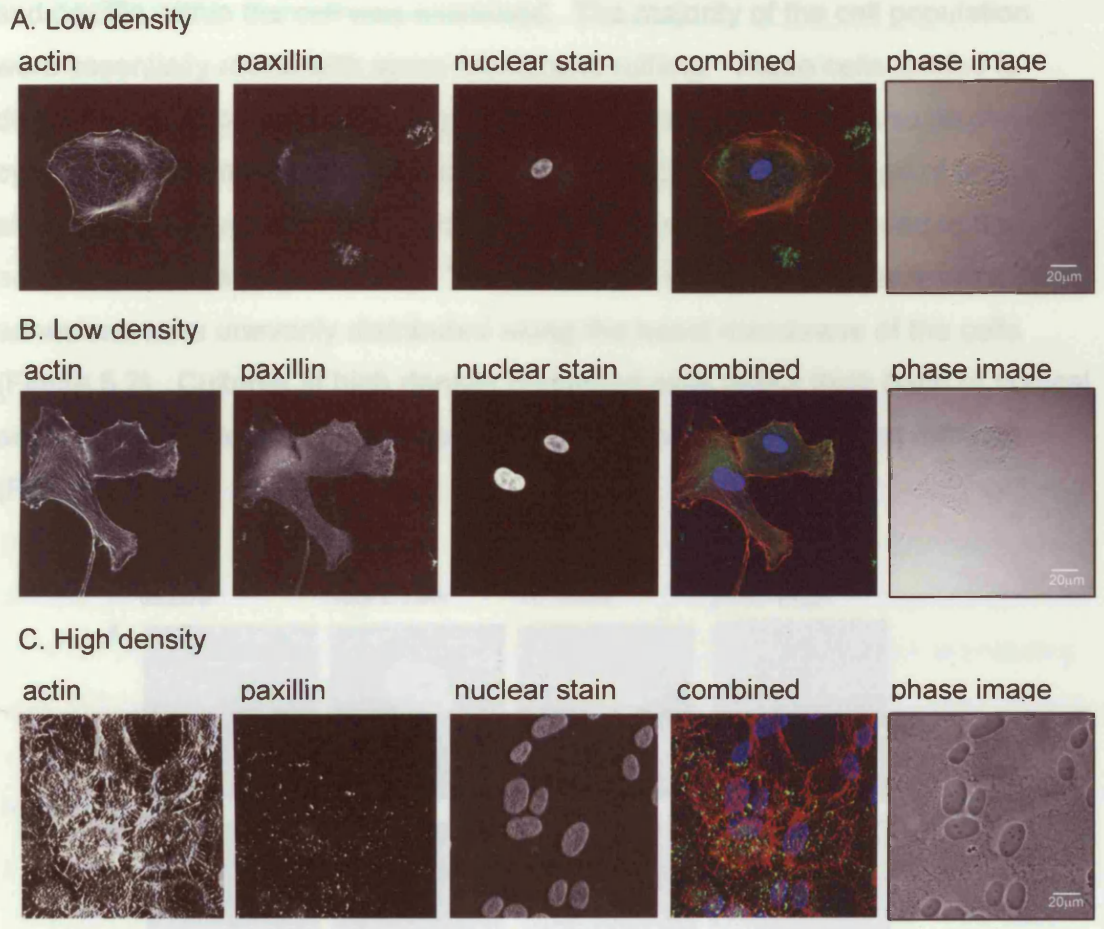

Figure 5.2 The F-actin phenotype of human corneal endothelial cells at high and low density. To examine the cytoskeletal morphology of human corneal endothelial cells at high and low density, cultures were fixed in paraformaldehyde for immunofluorescence staining of F-actin and paxillin. At low density, human corneal endothelial cells had a variable cell shape. The majority of cells showed cortical actin with a patchy distribution of paxillin (A). Low density cultures also contained a number of cells with actin stress fibres (B). Overall, very little paxillin was present in low density cultures. At higher density, cells consistently showed cortical actin and punctate paxillin along the basal membrane (C).

In order to further investigate the morphological differences between low and high density human corneal endothelial cell cultures, the expression of F-actin and paxillin within the cell was examined. The majority of the cell population were essentially round with some membrane ruffling. These cells tended to display a ring of cortical actin (Figure 5.2A). Occasionally, cells also displayed cytoplasmic extensions from the cell body. Membranes at the edge of the elongated area typically displayed ruffles and these cells also tended to have actin stress fibres (Figure 5.2B). The distribution of paxillin suggested that focal adhesions were unevenly distributed along the basal membrane of the cells (Figure 5.2). Cultures at high density contained cells with a thick band of cortical actin and a punctate distribution of focal adhesions along the basal membrane (Figure 5.2C).

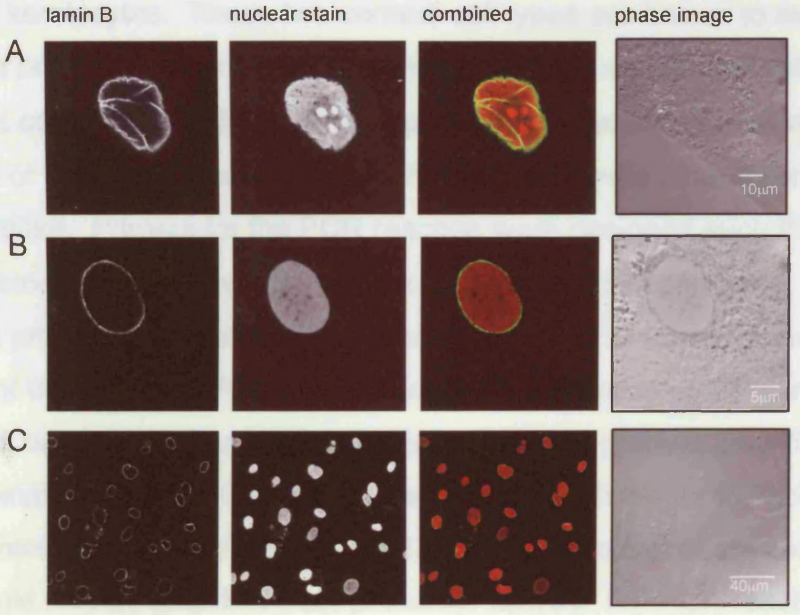

Figure 5.3 Nuclear morphology of human corneal endothelial cells. Primary human corneal endothelial cultures were fixed with cold methanol and stained using anti-lamin B antibodies. The majority of the cell population had an oval shaped nucleus (B,C), however, occasionally cells contained nuclei with large folds in the nuclear envelope (A). The nuclear envelope was identified by staining, lamin B.

The majority of cells in both low and high density primary human corneal endothelial cell cultures had oval shaped nuclei (Figure 5.3B&C), however, some low density cultures also contained cells with aberrations in nuclear morphology. The most frequent variation in nuclear morphology was manifest as folds in the nuclear envelope, which were visualized by immunofluorescence staining of lamin B (Figure 5.3A). The significance of these unusual folds in the nuclear envelope is unclear. However, as high density cultures did not contain these unusual shaped nuclei, it is likely that these cells alter their nuclear morphology to become oval shaped or die.

5.1.2 Verification of human corneal endothelial cell cultures

Despite displaying a typical endothelial phenotype, it was necessary to verify that primary cultures were indeed corneal endothelial cells and not contaminating corneal keratocytes. These two corneal cell types are known to express a different profile of matrix proteins, with only corneal endothelial cells expressing type VIII collagen. RT-PCR for α1 type VIII collagen was therefore used as one method of verification that cultures of human cells were indeed corneal endothelium. Primers for the PCR reaction were designed such that the forward primer-binding site lay in exon 1 of the α1 type VIII collagen gene, while the reverse primer-binding site was located in exon 2 of the same gene. The total length of the expected PCR product amplified from reverse transcribed mRNA was 478 base pairs. The length of a potential PCR product amplified from contaminating genomic DNA would have been much longer (5.7kb), as it would also contain the intron, thus ensuring that a PCR product of the correct predicted size could only be amplified from precursor mRNA. RT-PCR reactions from corneal keratocyte cultures and corneal endothelial cell cultures both showed mRNA expression of β-actin, demonstrating acceptable mRNA quality, however, only the corneal endothelial cell cultures demonstrated the 478bp band indicating mRNA expression of α1 type VIII collagen (Figure 5.4).

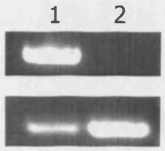

type VIII collagen

β-actin

1 primary human corneal endothelial cells

2 primary human corneal keratocytes

Figure 5.4 Primary human corneal endothelial cells express α1 type VIII collagen. Total RNA was extracted from primary cultures of human corneal endothelial cells and human corneal keratocytes. RT-PCR was used to generate cDNA and amplify α1 type VIII collagen expression in both cultures. Primary human corneal endothelial cell cultures were demonstrated to express α1 type VIII collagen mRNA, while primary human corneal keratocyte cultures do not. Expression of β-actin confirms the quality of mRNA preparations from both corneal endothelial and corneal keratocyte cultures.

In addition to demonstrating mRNA expression of type VIII collagen, a cell type specific antibody was used as a second determinant of corneal endothelial cells. In order to help identify corneal endothelial cultures, Engelmann et al. (2001) generated a monoclonal antibody, known as mab 9.3E, which recognizes a protein of 130kDa that is enriched along corneal endothelial cell membranes. While the protein targeted by the antibody is also present in a number of other cell types, including Schwann cells and adipocytes, only the corneal endothelium is identified in ocular tissue (Engelmann et al., 2001). Cells at confluence demonstrated distribution of this protein along the cell borders, while subconfluent cells showed a diffuse staining with occasional focal blebs within the cell (Engelmann et al., 2001). Human corneal endothelial cultures at a density similar to that in Figure 5.1B were stained with mab 9.3E, yielding a diffuse cytoplasmic immunoreactivity with occasional blebs or vesicular staining, as previously described by Engelmann et al. (2001) for subconfluent cultures (Figure 5.5A). In contrast, mab 9.3E staining of human corneal endothelial monolayers in situ, showed a distribution along the cell borders (Figure 5.5B). These results suggest that while cultures of human corneal endothelial cells may appear confluent when judged by phase microscopy, they do not exhibit the same degree of junctional integrity as endothelial monolayers in situ.

A. Primary human corneal endothelial cultures

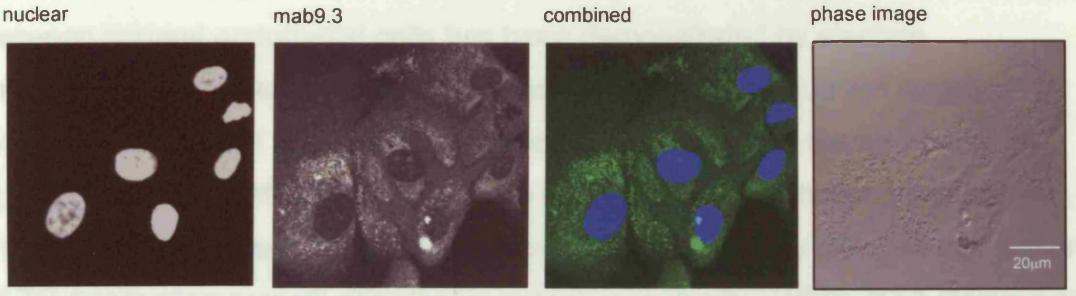

B. Human corneal endothelial monolayer

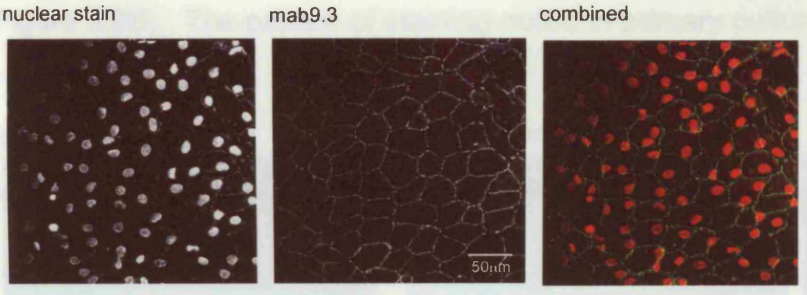

Figure 5.5 Antibody 9.3E stains primary human corneal endothelial cultures. Cultured human corneal endothelial cells and whole corneal tissue were fixed in cold methanol and stained with monoclonal antibody 9.3E. Images were captured on a Leica AOBS microscope with LCS (v.2) software. In ocular tissue, only the corneal endothelium is recognized by monoclonal antibody 9.3E, which targets a 130kDa protein. Both cultured cells and whole corneal tissue were fixed in methanol and stained with antibody 9.3E. Subconfluent cultures display a different pattern of staining to confluent cultures with antibody 9.3E. Immunofluorescence staining with antibody 9.3E shows a diffuse stain with occasional blebs in the cytoplasm in primary human corneal endothelial cultures (A). This pattern of antibody 9.3E staining is consistent with that noted for subconfluent cultures, despite human corneal endothelial cultures appearing confluent by phase microscopy. Immunofluorescence staining of human corneal endothelial monolayers in situ, however, shows the 130kDa protein to be distributed at the cell borders (B).

5.1.3 Junctional integrity of human corneal endothelial cells

Corneal hydration and transparency is maintained by the barrier of the corneal endothelium. The formation of tight junctions within the corneal endothelial monolayer is vital to its barrier function. While tight junction formation between corneal endothelial cells has been demonstrated by electron microscopy, the proteins that make up the tight junction plaque are largely unknown. Studies of the corneal endothelium generally use the distribution of tight junction associated protein ZO-1 as a marker of tight junction integrity. Primary human corneal endothelial cultures display a slightly different distribution of ZO-1 to human corneal endothelial monolayers in situ. While ZO-1 distribution in primary cultures is discontinuous around the cell borders (Figure 5.6A), ZO-1 is organised in a tight band surrounding the cells in endothelial monolayers in situ (Figure 5.6B). The pattern of staining noted in primary cultures is not

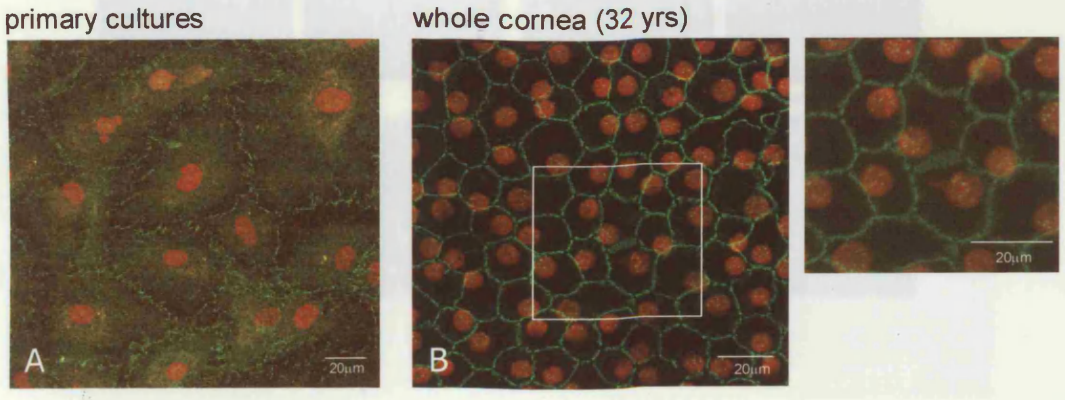

Figure 5.6 Distribution of ZO-1 in human corneal endothelial cells. Whole corneal tissue and confluent primary human corneal endothelial cultures were fixed in cold methanol and stained for tight junction protein ZO-1. Primary human corneal endothelial cultures were composed of larger, flatter cells than cells in corneal endothelial monolayers in situ. ZO-1 is distributed to cell borders in primary human corneal endothelial cultures, however, it does not appear as a tight band surrounding the cell, as expected during tight junction formation (A). The discontinuous staining at the cell borders noted in primary human corneal endothelial cultures (A) may represent ZO-1 distribution at adherens junctions or immature tight junctions. Human corneal endothelial monolayers in situ are known to form a tight junction barrier, which can be visualised in a strong band of ZO-1 staining around the cell borders (B). Distribution of ZO-1 on the corneal endothelial monolayer in situ also demonstrates the complex interdigitations between neighbouring cells (inset). The corneal button used to visualise ZO-1 distribution originated from a 32 year old keratoconus patient.

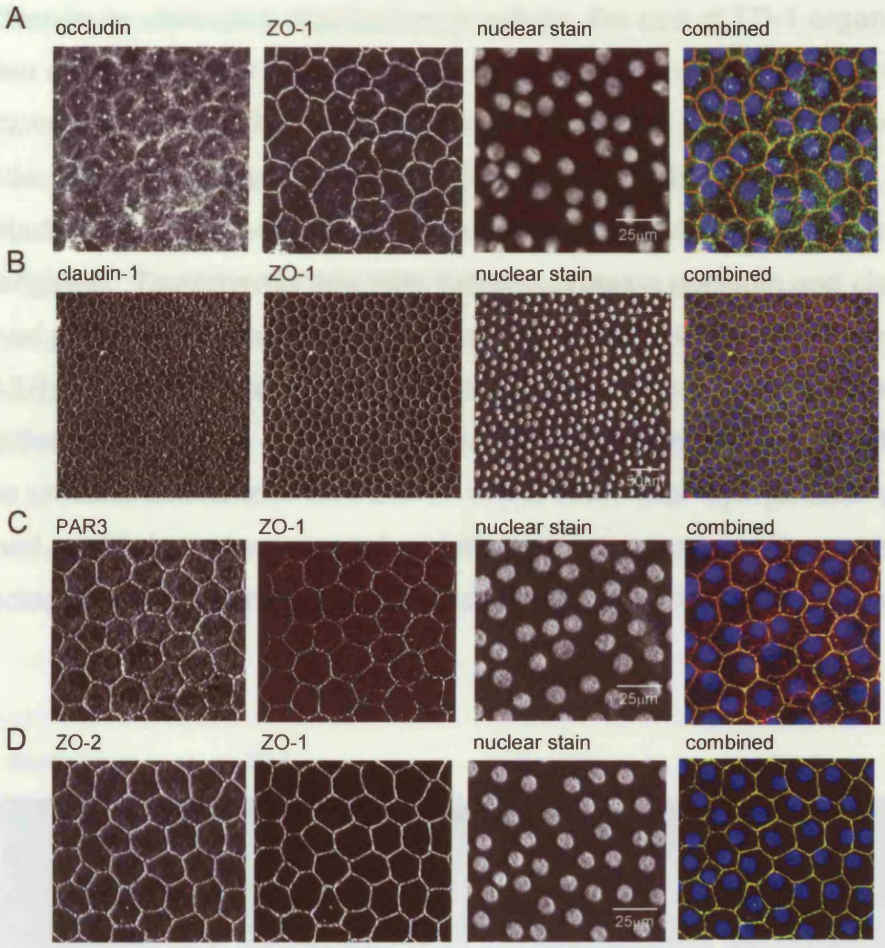

Figure 5.7 Distribution of tight junction proteins in human corneal endothelial monolayers. Corneal buttons from keratoconus patients were used to investigate the expression of tight junction proteins in the corneal endothelial monolayer. Corneal buttons were fixed in cold methanol and stained with antibodies to various tight junction proteins. Images were captured using a Leica AOBS microscope with LCS (v.2) software. Transmembrane tight junction proteins occludin (A) and claudin-1 (B) both co-localized with ZO-1 at the cell borders. Tight junction associated proteins PAR-3 (C) and ZO-2 (D) also co-localized with ZO-1 at the cell borders. Corneal tissue was received from patients of different ages; 20 years (C), 22 years (B), 36 years (A) and 37 years (D).

regarded as representative of mature tight junctions, but rather immature tight junctions or adherens junctions.

Despite its distinctive distribution in culture, the use of ZO-1 organisation as a marker of tight junction formation may be misrepresentative, as cells without tight junctions also exhibit ZO-1 enrichment at cell borders at the adherens junctions. In order to better assess the human corneal endothelial tight junction, the distribution of a number of other tight junction associated proteins was investigated. Transmembrane tight junction proteins occludin and claudin-1 both stained positively at the human corneal endothelial cell-cell contact points (Figure 5.7A&B). Similarly, adaptor tight junction proteins ZO-2 and PAR-3 were also identified at the human corneal endothelial cell borders (Figure 5.7C&D). All of these proteins colocalized with ZO-1. While these four tight junction proteins all stained readily in human corneal endothelial monolayers in situ, none were detected in primary human corneal endothelial cell cultures (not shown).

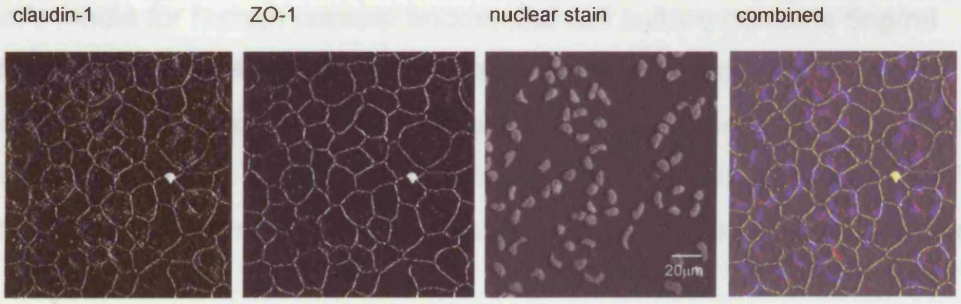

Figure 5.8 Distribution of tight junction proteins in the corneal endothelial monolayer of a patient with Fuchs' corneal endothelial dystrophy. The corneal button was fixed in cold methanol and stained with antibodies targeting tight junction proteins ZO-1 and claudin-1. Both tight junction proteins were found at the cell borders of corneal endothelial cells. Interestingly, some endothelial cells in the monolayer appeared to have no nuclei. It is likely that this is not the case, but rather the nuclei have shifted in position with alterations in Descemet's membrane, below the endothelial cell layer. The deposition of discrete excrescences of matrix by the corneal endothelium is one of the hallmarks of Fuchs' corneal endothelial dystrophy.

The distribution of tight junction proteins ZO-1 and claudin-1 was also assessed in the endothelial cell monolayer of a corneal button removed from a 55 year old patient with Fuchs' corneal endothelial dystrophy. Although ZO-1 and claudin-1 localized correctly to cell-cell contacts in corneal endothelial cells in the Fuchs' cornea (Figure 5.8), there was marked heterogeneity of cell size and shape, and the nuclei were highly disorganized, such that some cells appeared to lack a nucleus. This effect is likely the consequence of alterations in cell shape to accommodate discrete excrescences of matrix laid down by the diseased endothelium. The fact that corneal endothelial tight junctions remain intact indicates the importance of this feature to the function of the corneal endothelial monolayer.

5.2 Proliferation of human corneal endothelial cultures

Tissue culture media for human corneal endothelial cells is routinely supplemented with growth factors to enhance proliferation and assist survival. Chen's media for human corneal endothelial cell culture contains 5ng/ml epidermal growth factor (EGF), 20ng/ml nerve growth factor (NGF) and 100mg/ml pituitary extract, known to contain a high concentration of fibroblast growth factor (FGF). The proliferative effects of three growth factors, EGF, FGF-2 and PDGF BB, were thus investigated in primary human corneal endothelial cell cultures.

Human corneal endothelial cultures used for proliferation studies were passaged once and then maintained in serum and growth factor-free media for 24 hours prior to experimentation. Cultures were then treated for 24 or 48 hours with growth factor and BrdU, a reporter of cell proliferation as described in Chapter 4. Proliferating (BrdU positive) cells were identified as a percentage of the total cell population. Random samples of cells were counted from all areas of the primary cell monolayers, and at least 3000 cells were counted per treatment. Cultures maintained in base media, containing no serum or growth factors, were

used as a negative control, and treatment with 10% foetal calf serum was used as a positive control.

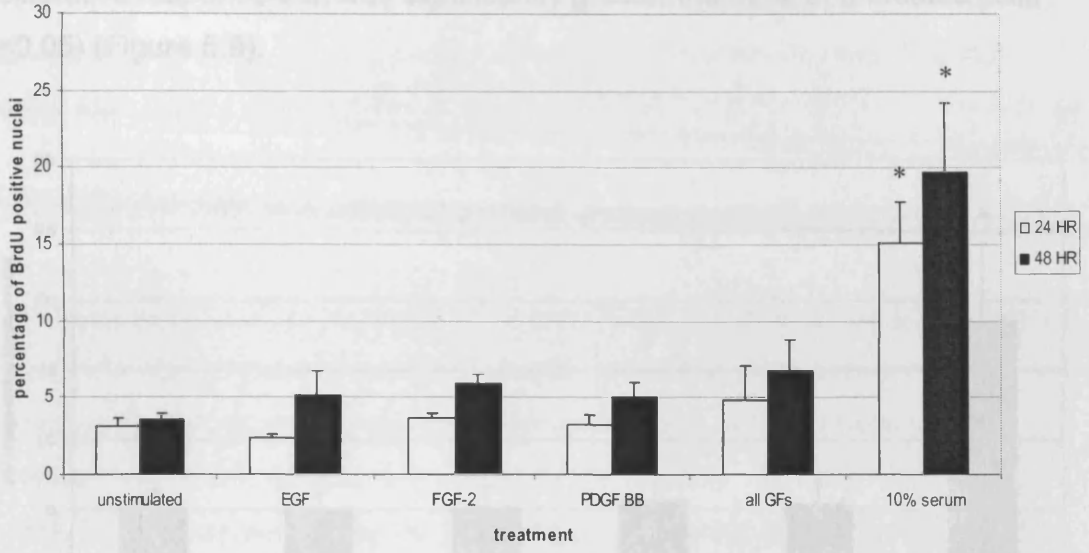

Figure 5.9 Proliferative response of human corneal endothelial cell cultures to growth factor stimulation. Human corneal endothelial cells were maintained in serum free media for 24 hours prior to treatment with growth factors. Cultures were concomitantly treated with BrdU and growth factors for a period of 24 or 48 hours. Proliferating cells were identified as a proportion of the total cell population with anti-BrdU antibody. Treatment with 100ng/ml EGF, 25ng/ml FGF-2 or 50ng/ml PDGF BB appeared to simulate a small amount of proliferation, however, this proliferative response were not significantly different compared to unstimulated cells. Similarly, a combination of all 3 growth factors stimulated a small amount of proliferation but this was also not significant with respect to that observed in unstimulated cultures. The proliferative response to treatment with 10% serum was significantly greater than that observed in unstimulated cultures, and was used as a positive control (*$p<0.05$). (n=4)

Surprisingly, unstimulated cells retained a low level of proliferation, with approximately 4% of the cell population staining BrdU positive. Supplementation of base media with individual growth factors did little to enhance this proliferation. Each growth factor was found to induce approximately 5% of the cell population to proliferate. While growth factor treatment consistently induced more proliferation than noted in unstimulated cultures, the increase was not significantly greater than in cells without growth factor stimulation. The

combination of all three growth factors also produced consistently greater proliferation than observed in unstimulated cells, however, this again was also not statistically significant. Stimulation with 10% serum, however, did induce a proliferative response that was significantly greater than that of untreated cells ($p<0.05$) (Figure 5.9).

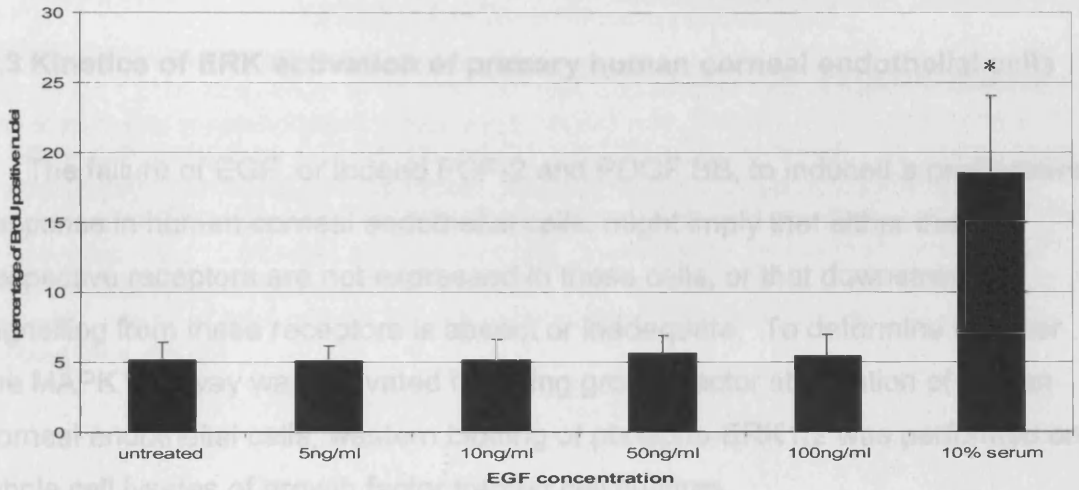

Figure 5.10 Proliferative response of human corneal endothelial cells to varying concentrations of epidermal growth factor, EGF. Confluent cultures of human corneal endothelial cells were maintained in serum free media for 24 hours prior to treatment with EGF. Cells were treated with both EGF and BrdU for 48 hours prior to fixation and staining with an anti-BrdU antibody to recognize proliferative cells. Concentrations of EGF ranging from 5ng/ml to 100ng/ml showed no difference in the proliferative effects on corneal endothelial cells. Unstimulated cells were used to determine the basal level of proliferation, while cells treated with 10% serum were used as a positive control. Only serum stimulation of primary cultures significantly increased human corneal endothelial cell proliferation above unstimulated cultures (*$p<0.05$). (n=4)

It has been suggested that different doses of EGF can produce opposing cellular responses, with low doses of EGF inducing proliferation and high doses of EGF inhibiting proliferation. Previous growth factor studies involved high doses of EGF, while human corneal endothelial growth media contains a low concentration of EGF. To test whether different doses of EGF might produce variable effects in human corneal endothelial cultures, the proliferative response

to 5ng/ml, 10ng/ml, 50ng/ml and 100ng/ml EGF was tested. Unstimulated cells were again used as a negative control and treatment with 10% serum as a positive control. At all concentrations tested, EGF failed to induce proliferation to an extent that was significantly different from proliferation noted in unstimulated cultures (Figure 5.10). Again, serum-induced proliferation was significantly greater than that of unstimulated cultures ($p<0.05$).

5.3 Kinetics of ERK activation of primary human corneal endothelial ceils

The failure of EGF, or indeed FGF-2 and PDGF BB, to induced a proliferative response in human corneal endothelial cells, might imply that either the respective receptors are not expressed in these cells, or that downstream signalling from these receptors is absent or inadequate. To determine whether the MAPK pathway was activated following growth factor stimulation of human corneal endothelial cells, western blotting of phospho-ERK1/2 was performed on whole cell lysates of growth factor treated cell cultures.

Primary human corneal endothelial cultures were serum starved overnight prior to growth factor stimulation. Cultures were treated with 100ng/ml EGF, 25ng/ml FGF-2 or 50ng/ml PDGF BB for 0, 5, 15, 30, 60, 90 or 120 minutes. Cell lysates were western blotted for the phosphorylated forms of ERK 1/2. All growth factors showed a similar pattern of ERK 1/2 phosphorylation. Phosphorylated ERK1/2 began to accumulate after 5 minutes of treatment with growth factor and peaked after 15 minutes of stimulation (Figure 5.11). The same blots were also probed for α-tubulin to ensure equal protein loading. Quantitative evaluation revealed little difference in the kinetics of ERK1/2 activation, irrespective of growth factor used.

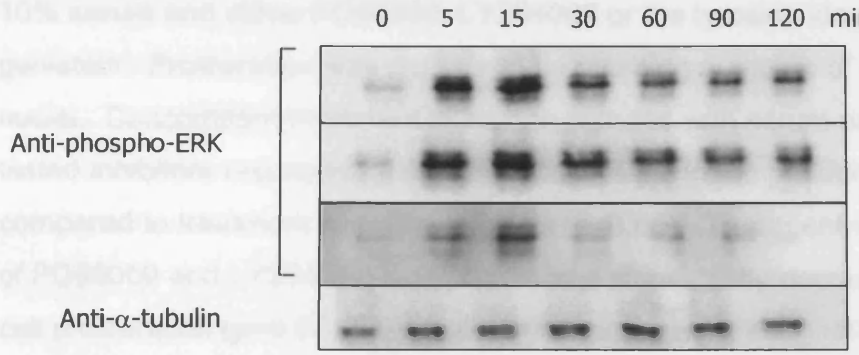

Figure 5.11 ERK activation in human corneal endothelial cell cultures following treatment with growth factor. Cells were treated with 25ng/ml FGF-2, 100ng/ml EGF or 50ng/ml PDGF BB for 0, 5, 15, 30, 60, 90 and 120 minutes. Whole cell lysates were made directly in reducing sample buffer. Western blotting for phosphorylated ERK demonstrated ERK activation after 5 minutes of treatment with growth factor, with a peak in activation after 15 minutes of treatment with growth factor. A low level of sustained ERK phosphorylation appeared to be present after 2 hours in FGF-2 and EGF treated cultures. Levels of total protein in samples was normalised and checked by western blotting for α-tubulin.

5.4 Inhibition of serum-induced proliferation in primary human corneal endothelial cultures

The PI3 kinase pathway has been shown to play a vital role in FGF-2 induced proliferation of rabbit corneal endothelium, with the PI3 kinase inhibitor, LY294002, able to abolish FGF-2 induced proliferation (Lee and Kay, 2003b). However, the intracellular pathways responsible for regulating proliferation of human corneal endothelium remain largely unknown. As growth factor stimulation of human corneal endothelial cultures did not produce significantly different proliferative responses to that observed in unstimulated cells, it would have been impossible to assess the actions of inhibitors of specific growth factors on proliferation of human corneal endothelial cultures. As treatment with 10% serum induced a significant amount of cell proliferation, inhibitors were used to investigate the intracellular pathways involved in serum-induced human corneal endothelial cell proliferation. Cultures were simultaneously treated with BrdU,

10% serum and either PD98059, LY294002 or the tyrosine kinase inhibitor genistein. Proliferation was measured by counting numbers of BrdU positive nuclei. Concomitant treatment of human cultures with serum and any of the tested inhibitors resulted in a significant decrease in the proliferative response as compared to treatment with serum alone ($p<0.05$). Treatment with a combination of PD98059 and LY294002 also produced a significantly decreased amount of cell proliferation ($p<0.05$) (Figure 5.12). These results suggest that the MAPK pathway, PI3 kinase pathway and tyrosine phosphorylation all play a critical role in serum-induced proliferation of human corneal endothelium.

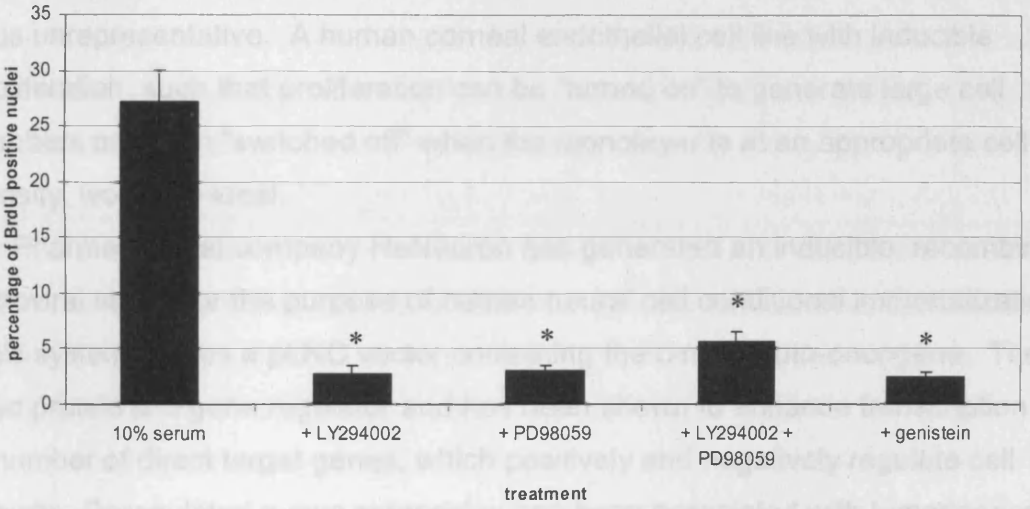

Figure 5.12 Effects of inhibitors on serum-induced proliferation of primary human corneal endothelial cultures. Confluent cultures were serum starved overnight prior to experimentation and then treated with BrdU, 10% serum and various inhibitors, including PI3 kinase inhibitor (LY294002), MAPK inhibitor (PD98059) and tyrosine kinase inhibitor (genistein). Anti-BrdU antibody was used to identify proliferating cells as a percentage of the total cell population. Each inhibitor significantly reduced serum stimulated proliferation to approximately basal levels (*$p<0.05$). The combination of inhibitors LY294002 and PD98059 also significantly reduced serum stimulated proliferation (*$p<0.05$). ($n<3$)

5.5 Development of a human corneal endothelial cell line

Because human corneal tissue is prioritised for transplantation, it is difficult to obtain material for research. One way to rectify this problem would be the development of a representative, high quality human corneal endothelial cell line, though the generation of such a line has yet to be achieved. A human corneal endothelial cell line was developed by Wilson et al. (1993) by transfection with SV40 large T antigen, however, this cell line is highly proliferative and, as was observed in the SV40 transformed mouse corneal endothelial cell line (Chapter 3), likely continues to proliferate beyond the monolayer to form multiple cell layers. As the corneal endothelium in vivo is contact inhibited, such a cell line is thus unrepresentative. A human corneal endothelial cell line with inducible proliferation, such that proliferation can be "turned on" to generate large cell numbers and then "switched off" when the monolayer is at an appropriate cell density, would be ideal.

Pharmaceutical company ReNeuron has generated an inducible, recombinant retroviral vector for the purpose of human neural cell conditional immortalization. This system utilizes a pLNC vector containing the c-myc proto-oncogene. The c-myc protein is a gene regulator and has been shown to enhance transcription of a number of direct target genes, which positively and negatively regulate cell growth. Deregulated c-myc expression has been associated with tumorigenesis and overexpression of c-myc induces telomerase expression, which is associated with extended lifespan. Within the specified vector, the c-myc protein is fused to a transcriptionally inactive mutant mouse oestrogen receptor, such that functional activity of c-myc is dependent upon the presence of exogenously applied 4-hydroxytamoxifen.

Aliquots of human and mouse corneal endothelial cell media containing replication incompetent retroviruses were obtained from ReNeuron. Primary human and mouse corneal endothelial cells were incubated in virus-containing media for a total of 48 hours, with media refreshed every 12 hours. Cells

transfected with the pLNC-cmycER^{TM} vector were selected with 600μg/ml geneticin. Selection resulted in cultures of very few, sparse corneal endothelial cells. These cells spread to become giant cells but did not proliferate. Treatment with 100nM 4-hydroxytamoxifen is known to induce transformed neural cells to proliferate but did not affect transformed corneal endothelial cells. Upon prolonged culture, transfected corneal endothelial cells failed to thrive, and it ultimately proved impossible to clone out a conditionally immortalized cell line.

5.6 Summary

Methods described for the isolation and culture of human corneal endothelial cells involve separation of the endothelial monolayer and its associated extracellular matrix (Descemet's membrane) from the cornea. Endothelial cells at low density spread by flattening and membrane ruffling, and proliferated to fill the tissue culture dish. Some cells showed cytoplasmic elongations, which contained stress fibres during cell spreading, though most showed a ring of cortical actin, similar to that observed in cells at confluence. Stress fibres have also been noted in rabbit corneal endothelial cultures upon prolonged treatment with FGF-2, and are thought to be involved in endothelial to mesenchymal transformation (EMT) (Lee et al., 2004; Lee and Kay, 2003a). Unlike rabbit corneal endothelial cells, primary human corneal endothelial cells which displayed stress fibres, did not alter their morphology to become elongated with mesenchymal characteristics, but instead grew to form a heterogeneous monolayer. Primary human corneal endothelial monolayers varied in density but all cells displayed cortical actin and focal adhesions along the basal cell membrane.

In order to confirm that established growing cells were endothelial, morphological characteristics noted by phase microscopy, α1 type VIII collagen expression and positive staining with corneal endothelial specific antibody 9.3E were used to assess the primary cultures. All three criteria indicated that primary cultures were indeed corneal endothelial. However, the distribution of

monoclonal antibody 9.3E was unexpected. Antibody 9.3E staining of subconfluent cultures displayed a diffuse staining with small focal blebs, while confluent cultures stained at the cell border with antibody 9.3E (Engelmann et al., 2001). Primary human corneal endothelial cultures, which appeared confluent by phase microscopy, were stained with monoclonal antibody 9.3E to reveal a staining pattern consistent with subconfluent cultures. Zhu & Joyce (2004) noted the same pattern of antibody 9.3E staining in primary human cultures. It is possible that the protein target of antibody 9.3E accumulates at the cell borders only in monolayers with proper junction formation. As the discontinuous distribution of ZO-1 at the cell borders noted in primary human cultures indicates improper junction formation, this may explain the unexpected results in staining with antibody 9.3E. While primary human corneal endothelial cultures form immature junctions, endothelial monolayers in situ form mature tight junctions as indicated by the distribution of ZO-1 in a tight band around the cell borders. While a number of studies have investigated the distribution of adherens junction proteins in the corneal endothelium, including catenins and cadherins, tight junction proteins have not been extensively studied. Transmembrane tight junction proteins occludin and claudin-1 were found to be present in endothelial monolayers in situ but not in primary cultures. Similarly, the tight junction adaptor proteins ZO-2 and PAR-3 were also expressed in endothelial monolayers in situ. PAR-3 has been demonstrated to form an active complex with PAR-6 and aPKC, which is important to tight junction formation and cell polarization (Lin, 2000). Its presence at the corneal endothelial tight junction reveals the cells of the monolayer to be polarized and contain functional tight junctions. The absence of PAR-3 in primary cultures suggests that tight junction formation is not complete and that cells are therefore unlikely to be fully polarized.

Incomplete junction formation may also help explain the surprising proliferative responses of primary human corneal endothelial cells to growth factor stimulation. While stimulation with EGF, FGF-2, PDGF BB or a combination of the three growth factors, consistently increased the rate of proliferation over that observed in unstimulated cells, these responses were not

significantly different. Corneal endothelial cells in vivo are known to be G1-phase arrested and cell contact inhibition is thought to play a vital role in the maintenance of G1-phase arrest (Senoo et al., 2000). Because human corneal endothelial cultures do not form mature junctions in the same manner as human corneal endothelial monolayers in situ, cultured cells are not properly contact inhibited, which is consistent with the observed low levels of proliferation. Zhu & Joyce (2004) also studied the proliferation of primary human corneal endothelial cell cultures treated with growth factors over a prolonged period of time and found a hierarchy of mitogenic action such that PDGF BB > FGF > EGF. The discrepancy between these results may be a factor of time, as differences in mitogenic effects of these growth factors were only noted after weeks of treatment, but not after 48 hours.

The intracellular signalling pathways induced by growth factor stimulation remain largely unknown in the human corneal endothelium. While the PI3 kinase pathway has been shown to be vital to FGF-2 induced proliferation in rabbit corneal endothelium (Lee and Kay, 2003b), inhibitor studies of serum-induced human corneal endothelial cell proliferation suggest that both the MAPK and PI3 kinase pathways are important. In addition, tyrosine phosphorylation appears to play a vital role in the human corneal endothelial proliferative response. Downstream targets of MAPK, ERK 1/2 were investigated following stimulation with EGF, FGF-2 and PDGF BB. Each growth factor elicited a similar response with a peak in ERK 1/2 activation following 15 minutes of growth factor stimulation. The failure of these growth factors to induce proliferation despite activating the MAPK pathway and in the absence of cell-cell contact inhibition, appears paradoxical. The fact that proliferation was observed with serum, indicates that further factor(s) must be present that provide additional stimuli or remove an unknown cellular block to cell cycle entry.

Because so little is known about the intracellular signalling of corneal endothelial cells, and corneal tissue available for research is rare, a representative model for the corneal endothelium would be ideal. Using the pLNC-cymcER construct from ReNeuron, attempts were made to generate an

inducible human corneal endothelial cell line. Unfortunately, a number of attempts to isolate an inducible cell line failed. The reasons for this are unclear, though there are a number of possibilities. First, viral titres in media used for infection (from ReNeuron) were not quantitated and may have been too low. Second, it has been suggested, by ReNeuron, that the virus incorporates readily into actively cycling cultures of cells but not into non-proliferative cultures. As the rate of proliferation in primary human corneal endothelial cultures is low, the chance of infection was reduced. Third, cells which appeared to have been infected with virus, after selection with G418, continued to die in normal growth media, after the selection process. The cells remaining at the end of the selection process were typically isolated cells spread around the tissue culture dish. These cells spread and flattened to form giant cells but then proceeded to die. It is unclear why treatment with 4-hydroxytamoxifen at this stage did not induce these cells to proliferate. Nevertheless, the generation of a representative cell line remains a much-needed objective for researchers in this area.

Chapter 6: Discussion

The primary goal of this work was to evaluate the utility of models of primary human corneal endothelial tissue. Bovine, rabbit and rat corneal endothelium are the most commonly used models for research on corneal endothelium, but while these tissues are readily available, they are not representative of the human corneal endothelial monolayer for the fundamental reason that they are highly proliferative. An alternative model, which has remained virtually unstudied, is the mouse corneal endothelium. Joo et al. (1994) described a complex methodology for the isolation and culture of mouse corneal endothelial cells, which were compared to a mouse corneal endothelial cell line generated by transformation with SV40 large T-antigen. Based on the cells' similar propensity to adhere to Descemet's membrane, and equivalent expression of EGF receptor and PDGF receptors α and β, it was concluded that the SV40 transformed mouse corneal endothelial cell line was indeed an appropriate model for primary mouse corneal endothelial cells (Joo et al., 1994). In this project, using a mechanistically simpler explant model of mouse corneal endothelium, it was found that there are in fact significant differences between primary mouse corneal endothelial cultures and SV40 transformed mouse corneal endothelial cells. The five major differences between primary and SV40 transformed mouse corneal endothelial cells are reviewed in detail below.

First, the propensity for SV40 transformed mouse corneal endothelial cultures to proliferate is unsurprisingly far greater than that of primary cultures. While primary cultures form a heterogeneous monolayer of cells, which cease to proliferate with time in culture, the SV40 transformed cell line forms a homogeneous monolayer of cells that continues to proliferate beyond the point of contact inhibition to form multiple cell layers. Additionally, whereas primary corneal endothelial cell proliferation is significantly increased by stimulation with growth factors FGF-2 or PDGF BB, the proliferative effects of growth factors on the SV40 transformed cell line are negligible due to the high levels of intrinsic proliferation. Schonthal et al. (1999) reported differences in the expression of

cell cycle proteins that might be responsible for differences in proliferation between primary and SV40 transformed human corneal endothelial cells. Elevated levels of cyclin A, and to a lesser extent cyclin D, CDK2 and CDK4, as well as a drop in the levels of cell cycle inhibitors p27Kip1 and p21Waf1, correlated with an increased proliferative potential of the SV40 transformed human corneal endothelial cells (Schonthal et al., 1999). Alterations in the expression levels of various cell cycle proteins may similarly account for the increased proliferation of SV40 transformed mouse corneal endothelial cells. However, the proliferative responses of the SV40 transformed cell line described in this thesis contradict those reported by Joo et al. (1994), who reported the SV40 transformed mouse corneal endothelial cells to be contact inhibited and require serum stimulation to induce proliferation. Additionally, Joo et al. (1994) suggested that serum stimulation of primary mouse corneal endothelial cells alone is insufficient to induce proliferation, but rather requires supplementation with growth factors. Discrepancies between these results may be explained either by different culture techniques, or differences between subclones of SV40 transformed cell lines.

Second, the kinetics of ERK 1/2 activation in response to growth factor stimulation were found to be different in primary cultures as compared to the SV40 transformed cell line. Overall, peak ERK 1/2 activation due to growth factor stimulation, occurred more rapidly in the SV40 transformed cell line than in primary cells, and FGF-2 stimulation elicited biphasic ERK 1/2 activation in primary mouse corneal endothelial cultures. This biphasic response was not noted in the SV40 transformed cell line, and the implications of this difference in corneal endothelial ERK 1/2 signalling remain unknown. A similar timeline of biphasic ERK activation was noted in the mitogenic response of hamster fibroblasts (CCL39), with the proliferative potential correlating to the second peak (1-2 hours) and further sustained (beyond 4 hours) activation of ERK (Meloche et al., 1992). Longer time points of FGF-2 stimulated ERK activation in mouse corneal endothelial cells should be investigated to determine whether sustained ERK activation is also a feature of these cells, and whether ablation of the

second peak in activation affects the mitogenic response to FGF-2. Interestingly, PDGF BB, which also showed a strong proliferative response, did not induce this second peak in ERK activation.

Third, differences in junctional integrity were noted between the SV40 transformed mouse corneal endothelial cells and primary mouse corneal endothelial cells. While SV40 transformed cells consistently show a discontinuous distribution of ZO-1 at the cell borders, typically associated with immature junction formation, the distribution of ZO-1 in primary cultures changed with time in culture. Primary cells that had been in culture for short periods of time showed a discontinuous distribution of ZO-1 at the cell borders, similar to the SV40 transformed cell line, but following culture for prolonged periods, ZO-1 localized in a band around the cell borders, typical of that associated with mature junction formation. As cell contact inhibition and junction formation play a major part in the maintenance of growth arrest in corneal endothelial cells (Senoo et al., 2000), these differences in junctional integrity may offer a partial explanation for the differences in proliferation between the SV40 transformed cell line and primary cells. Altered distributions of tight junction proteins have been described with proliferation in other cell types. In subconfluent cultures of MDCK cells, the Y-box transcription factor ZONAB does not bind to the tight junction plaque but instead is sequestered in the nucleus, where it binds promoter sequences of ErbB-2 and other cell cycle regulators that drive cell proliferation (Balda and Matter, 2000; Balda et al., 2003). Conversely, confluent cultures of MDCK cells sequester ZONAB at the tight junction, thus inhibiting cell proliferation (Balda et al., 2003). The localization of ZO-1 has also been observed to be transiently altered during EGF-induced proliferation in A431 cells (Van Itallie et al., 1995). Investigations of the distribution of ZONAB and ZO-1, following growth factor stimulation of mouse corneal endothelial cells, may provide additional insight into the involvement of these tight junction proteins in the corneal endothelial cell proliferative response.

Fourth, expression of apoptotic proteins differed in the SV40 transformed mouse corneal endothelial cells as compared to primary cultures. Overall, SV40

transformed cells expressed more anti-apoptotic proteins and fewer pro-apoptotic proteins than primary cultures. The Bcl family of proteins, members of which are expressed in both primary and SV40 transformed cultures, are known to form homo- or heterodimers of pro- and anti-apoptotic molecules and the ratios between these molecules determines the susceptibility of a cell to undergo apoptosis (Gross et al., 1999). Neutralising competition offered by the expression of more anti-apoptotic Bcl family members in SV40 transformed cells may offer greater protection against apoptotic stimuli, and therefore increased cell survival.

Finally, and consistent with the observations described above, SV40 transformed cultures were somewhat more resistant to staurosporine induced apoptosis than primary cultures, as they required a stronger dose of staurosporine over a longer time period to induce changes in mitochondrial morphology associated with apoptosis.

While Joo et al. (1994) suggest that the SV40 transformed mouse corneal endothelial cell line provides an appropriate model for primary mouse corneal endothelial cells, the five differences highlighted above clearly demonstrate that SV40 transformed cell line is a comparatively poor representative of the corneal endothelium. Not only do the five distinctions between the SV40 transformed mouse corneal endothelial cell line and primary cultures encompass differences in both the proliferative and apoptotic responses of the corneal endothelium, certain defining characteristics of the corneal endothelium are not fulfilled by the SV40 transformed cell line, including the formation of a G1-phase arrested monolayer. These findings indicate that caution is required when using the SV40 transformed mouse corneal endothelial cell line as a model for primary mouse corneal endothelial culture.

Nevertheless, a representative model of the human corneal endothelium would undoubtedly be of value to future research into human corneal endothelial cell biology. As previously mentioned, most current models of the corneal endothelium, namely rat, rabbit and bovine corneal endothelium, are unrepresentative as they are highly proliferative, in contrast to human corneal

endothelial monolayers in vivo. However, the explant model of mouse corneal endothelium, developed in this thesis, has proved to be relatively representative of human corneal endothelial cultures, with comparisons between the two cultures revealing a number of similarities. First, both mouse and human primary corneal endothelial cultures form heterogeneous monolayers with varying cell densities. The cells in the monolayer display cortical actin and focal adhesions on the basal membrane, that anchor the cell to underlying matrix proteins on the tissue culture dish. Second, the junctional maturity of both the primary cultures and endothelial monolayers in situ was similar in mouse and human. Most primary cultures showed a faint, discontinuous distribution of ZO-1 around cell borders suggesting the presence of immature junctions. This distribution of ZO-1 is different from that noted in endothelial monolayers in situ, which display a bright band of ZO-1 around the cell borders, a localization consistent with mature junction formation. This pattern of ZO-1 expression is consistent with changes noted during proliferation and junctional maturation in other cell types. Down-regulation of ZO-1 was observed in breast cancer tissues and during corneal wound repair, thus expression levels of ZO-1 have been suggested to be related to the proliferation state of epithelial cells (Hoover et al., 1998; Cao et al., 2002). These findings are supported by the observation that ZO-1 becomes stabilized in confluent cultures of MDCK cells and that expression levels increase with cell density (Balda and Matter, 2000; Balda et al., 2003). Additionally, endothelial monolayers in situ revealed localization of a number of other tight junction proteins at cell borders. These were not observed in primary endothelial cultures, though their presence may be a function of time in culture, since prolonged periods of culture appeared to yield cultures with more mature junctions. In developing foetuses, corneal endothelial cells begin to form proper tight junctions a month after proliferation has ceased (Waring, III et al., 1982). Because both primary mouse and human cells continued to exhibit very low levels of proliferation during culture ex vivo, it is possible that junction formation remains incomplete. Proper arrangement of the actin cytoskeleton has also been shown to be regulate the distribution of ZO-1 (Van Itallie et al., 1995). While the

F-actin phenotype of primary mouse and human corneal endothelial cells was similar, there may be differences between the F-actin phenotypes of primary cultures and corneal endothelial cells in situ that can account for the discrepancy in the distribution of ZO-1.

Despite the similarities noted between primary mouse and human corneal endothelial cultures, a number of species-specific differences were also observed. First, the migrating phenotype and nuclear morphology of primary mouse corneal endothelial cells was found to be different from those of human cells. Migrating primary mouse corneal endothelial cells showed a number of projections from the cell body with focal adhesions localized at their ends, while migrating primary human cells were more rounded in shape. Additionally, prolonged culture of primary mouse corneal endothelial cultures resulted in a larger proportion of bean-shaped nuclei, as compared to oval shaped nuclei. Similar nuclear morphology has been described for corneal keratocytes near Descemet's membrane in situ (Lwigale, 1999). Conversely, prolonged culture of primary human corneal endothelial cultures resulted in a larger proportion of smooth, oval shaped nuclei, as compared to nuclei with large folds in the nuclear envelope. Both primary mouse and human corneal endothelial cultures demonstrated a correlation between time in culture and numbers of binucleate cells.

Second, the proliferative response to growth factor stimulation was found to be readily detectable in primary mouse corneal endothelial cultures but not in primary human cultures. Indeed, the mitotic response of primary mouse corneal endothelial cultures to all stimuli was greater than that of primary human cultures, whereas the basal level of proliferation exhibited by unstimulated cells was more rapid in primary human cultures than in primary mouse cultures (Figure 6.1). Both FGF-2 and PDGF BB induced a significantly greater amount of proliferation in mouse corneal endothelial cultures as compared to unstimulated cells. While these growth factors also modestly induced human corneal endothelial cell proliferation, the response was not significantly different from that of unstimulated cells. A similar study of growth factor induced proliferation in primary human

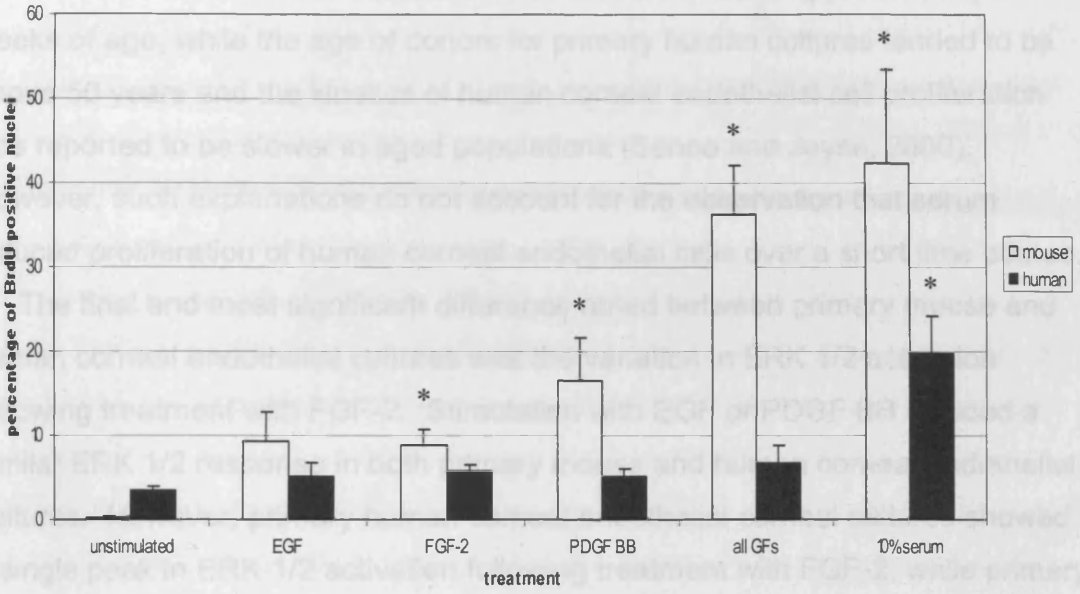

Figure 6.1 Proliferative responses of primary mouse and human corneal endothelial cultures to 48 hour growth factor stimulation. Primary cultures of mouse and human corneal endothelial cells were simultaneously treated with BrdU and growth factors. Proliferative cells were measured as a proportion of the total cell population. Unstimulated cells were used as a negative control and 10% serum as a positive control. Primary mouse corneal endothelial cultures treated with growth factors (white bars) showed a significant amount of proliferation compared to unstimulated cells (* $p<0.05$). However, growth factor treatment of primary human corneal endothelial cultures (black bars) did not. Levels of proliferation in unstimulated cells were higher in primary human cultures as compared to primary mouse cultures.

corneal endothelial cultures, however, revealed a hierarchy of mitogenic potential akin to that of primary mouse corneal endothelial cultures; PDGF BB > FGF > EGF (Zhu and Joyce, 2004). The apparent discrepancy between these results may reflect differences in the duration of the experiment, since the mitogenic potential of factors used by these authors were noticeable only after a few weeks, not 48 hours. Therefore, it is possible that the species-differences between the primary mouse and human corneal endothelial cell proliferative response may also be a factor of time, with primary mouse corneal endothelial cells responding to growth factor simulation faster than primary human cultures.

These results may also reflect differences in the age of the tissue, as primary mouse corneal endothelial tissues were taken from mice at approximately 3 weeks of age, while the age of donors for primary human cultures tended to be above 50 years and the kinetics of human corneal endothelial cell proliferation was reported to be slower in aged populations (Senoo and Joyce, 2000). However, such explanations do not account for the observation that serum induced proliferation of human corneal endothelial cells over a short time course.

The final and most significant difference noted between primary mouse and human corneal endothelial cultures was the variation in ERK 1/2 activation following treatment with FGF-2. Stimulation with EGF or PDGF BB induced a similar ERK 1/2 response in both primary mouse and human corneal endothelial cultures. However, primary human corneal endothelial corneal cultures showed a single peak in ERK 1/2 activation following treatment with FGF-2, while primary mouse cultures showed biphasic ERK 1/2 activation, with a second peak in activation after 90 minutes of stimulation. As previously mentioned, the implications of this difference in ERK 1/2 activation remain unclear, though the effects of the second peak in activation, which has been suggested to affect mitogenic activity in CCL39 cells (Meloche et al., 1992), warrants further investigation.

Overall, work in this thesis has shown that primary mouse corneal endothelial cultures are relatively similar to human corneal endothelial cultures, with only two major differences between the two; namely, the kinetics of the proliferative response to growth factor stimulation and FGF-2 induced ERK 1/2 activation. While these variations are significant, primary mouse corneal endothelial cultures are more similar to primary human corneal endothelium than many other currently available models. The corneal endothelial model most often used for cell biology studies is the highly proliferative rabbit corneal endothelium. In addition to being highly proliferative, investigations into the intracellular signalling pathways illustrate further differences between the rabbit, mouse and human corneal endothelium. Both mouse and human corneal endothelial cells were demonstrated to utilize the MAPK and PI3 kinase pathways during growth factor

induced proliferation, while studies in rabbit corneal endothelium have suggested FGF-2 induced proliferation to be wholly reliant on the PI3 kinase pathway (Lee and Kay, 2003b). Additionally, stimulation of rabbit corneal endothelial cells with FGF-2 was shown to induces changes in cell shape associated with cell motility and a transformation to a mesenchymal phenotype (Lee et al., 2004). These changes are associated with rearrangement of the actin cytoskeleton and were shown to be mediated by the PI3 kinase pathway, but not the MAPK pathway (Lee and Kay, 2003a). Effects of the PI3 kinase inhibitor on FGF-2 induced mouse corneal endothelial cell proliferation may therefore be tied to changes in cell shape and the endothelial to mesenchymal transformation, with decreased cell proliferation being a secondary effect of other changes. Treatment of primary mouse corneal endothelial cells with PDGF BB did not induce changes in cell shape associated with transformation to a mesenchymal phenotype, and inhibitor studies of PDGF BB-induced proliferation indicated a greater role for the MAPK pathway than the PI3 kinase pathway in this proliferative response. This reveals that the rabbit corneal endothelium is not only more proliferative than mouse and human corneal endothelial cultures, but also that the intracellular signals which underlie this response are different. This provides further justification for the preferential use of a mouse corneal endothelial model. Primary mouse corneal endothelial cells have the additional advantage of the possibility for research using genetically modified animals.

Although primary mouse corneal endothelial cultures comprise a reasonable model for primary human corneal endothelial cultures, the reliability of all primary corneal endothelial cell cultures as a model for corneal endothelial monolayers in vivo is questionable. For example, investigations into junctional integrity suggest that primary human corneal endothelial cultures are not truly representative of corneal endothelial monolayers in vivo. The broken distribution of ZO-1 observed at the cell borders of primary cultures is dissimilar from the tight band of ZO-1 staining seen in endothelial monolayers in situ. These patterns of ZO-1 localization suggest that junctions in forming monolayers are at different stages of maturity, and that primary cultures generally only form immature junctions. As

previously suggested, the pattern of expression of ZO-1 may be related to the arrangement of the actin cytoskeleton (Van Itallie et al., 1995). As proliferation is known to be affected by junctional integrity (Senoo et al., 2000), differences in junctional organisation may be functionally tied into differences in proliferative potential, as is highlighted by the proliferation observed in unstimulated human corneal endothelial cultures. With even primary human corneal endothelial cultures being unrepresentative of corneal endothelial monolayers in vivo, the creation of a representative corneal endothelial cell line would provide a valuable tool for future research. Ideally, a corneal endothelial cell line should contain an inducible vector, which could stimulate proliferation to form an intact monolayer. With formation of the monolayer, removal of the growth stimulus would allow the cells to return to G1-phase arrest and form an authentic barrier with mature tight junctions. With further understanding of the intracellular processes involved in regulating cell viability, such a cell line may also be able to repopulate denuded portions of Descemet's membrane to be used as a treatment to corneal endothelial disease. However, attempts at generating such a cell line have not been fruitful with either the pLNC-cmycER construct used in this thesis or a dexamethasone-inducible version of large T-antigen used by Wilson et al. (1995).

While initial investigations have begun to define the proliferative and apoptotic response to a number of factors, there remains one major aspect of corneal endothelial cell biology that merits further attention; namely the interactions between corneal endothelial cells and Descemet's membrane. Studies of matrix effects on corneal endothelial cell proliferation and cellular organisation have been conducted previously (Blake et al., 1997; Gordon, 1990; Gospodarowicz and Ill, 1980). Similar studies were also performed using vascular endothelial cells cultured on extracellular matrix generated by corneal endothelial cells (cECM), which demonstrated increased vascular endothelial cell proliferation and the formation of a closely apposed, non-overlapping and contact-inhibited endothelial cell monolayer (Fridman et al., 1985). Cultures of vascular endothelial cells on extracellular matrix generated by fibroblasts did not elicit the same response, indicating that specific components of extracellular matrix may

have a role in shaping the characteristic morphological appearance of these cells (Fridman et al., 1985). While cultures of primary mouse corneal endothelial cells on various matrices (type I and IV collagen, laminin and fibronectin) did not produce any noticeable phenotypic effects (not shown), different combinations of matrix components of Descemet's membrane may influence endothelial cell gene expression and hence function. Type VIII collagen is a matrix component unique to Descemet's membrane and other specialized membranes (Shuttleworth, 1997), but which is unfortunately unavailable from commercial or other sources. Homo- or heterotrimers of two distinct α-chains make type VIII collagen a non-fibrillar, short-chain collagen (Greenhill et al., 2000; Illidge et al., 1998). In Descemet's membrane, type VIII collagen exists as a heterotrimer with two α1(VIII) chains for every α2(VIII) chain (Mann et al., 1990). In addition to its structural function, type VIII collagen may also play a role in the mediation of cellular responses. During vascular injury, increased proliferation of vascular smooth muscle cells (VSMC) has been shown to coincide with increased expression of type VIII collagen (MacBeath et al., 1996; Sibinga et al., 1997). A similar increase in proliferation and type VIII collagen expression is noted in VSMC treated with PDGF BB (Bendeck et al., 1996). As PDGF BB also induced a significant proliferative response in corneal endothelial cultures, it would be interesting to know whether type VIII collagen is also upregulated by PDGF BB treatment in corneal endothelial cultures, and whether this upregulation of type VIII collagen plays a role in the proliferative response to PDGF BB.

By contrast, cleavage of type VIII collagen has been shown to play a role in cell survival. The NC1 (non-triple-helical domain) of type VIII collagen, known as vastatin, has been shown to inhibit FGF-2 induced proliferation, arrest cells at G0/G1 phase of the cell cycle and induce apoptosis (Xu et al., 2001). Thus, expression of matrix metalloproteinases responsible for the cleavage of type VIII collagen, may affect corneal endothelial cell survival.

In addition to type VIII collagen, a number of other components of Descemet's membrane may influence corneal endothelial cell viability. Proteoglycans, which are common constituents of Descemet's membrane, are thought to be more than

inert structural molecules and may modulate cellular responses to external stimuli (Yamada and Kemler, 2002). Additionally, the pericellular matrix is a compartment of the extracellular matrix (ECM) containing growth factors, cytokines, proteases and other bioactive molecules that interact at the cell surface (Bornstein and Sage, 2002). The combination of these factors, matrix molecules and other soluble proteins have been shown to influence cell motility, proliferation, differentiation and predisposition to apoptosis (Bornstein and Sage, 2002). This portion of ECM also contains the matricellular proteins, which modulate cell function but do not appear to contribute directly to the organization or physical properties of structures such as fibrils or basal laminae. One such protein, SPARC (secreted protein, acidic and rich in cysteine), which influences cell adhesion and proliferation, is known to be upregulated during corneal wound repair (Berryhill et al., 2003). A host of factors present in Descemet's membrane and their effects on the corneal endothelium have yet to be adequately described and may largely influence the response of corneal endothelial cells to various stimuli in vivo.

At present, difficulties in obtaining human corneal endothelial tissue and isolation and maintenance of human corneal endothelial cultures mean that little is known about the cell biology of the corneal endothelium. By establishing animal models of the human corneal endothelium, the constraints of tissue supply are relieved, and the field can advance. Work in this thesis has shown that an explant model of the mouse corneal endothelium is more representative of human corneal endothelium than other current models and may therefore provide more useful information with respect to the proliferative response. The use of such a model to gain new insight into corneal endothelial cell biology may aid in the identification of potential candidate molecules that may be targeted in the treatment of corneal endothelial disease. At present, the only available treatment for primary corneal endothelial disease involves corneal transplantation. A better understanding of corneal endothelial cell biology may reveal factors which can initiate corneal endothelial cell proliferation or enhance

corneal endothelial cell survival. Such factors may supplement corneal organ culture media, allowing prolonged storage of donor organ corneas both for transplantation and for research. Additionally, identification of intracellular targets to enhance corneal endothelial cell viability may, in future, eliminate the need for corneal transplantation and give rise to less invasive treatments for primary corneal endothelial disease.

Reference List

Adamis,A.P., Molnar,M.L., Tripathi,B.J., Emmerson,M.S., Stefansson,K., and Tripathi,R.C. (1985). Neuronal-specific enolase in human corneal endothelium and posterior keratocytes. Exp. Eye Res. *41*, 665-668.

Adams,J.M. and Cory,S. (1998). The Bcl-2 protein family: Arbiters of cell survival. Science *281*, 1322-1326.

Albon,J., Armstong,M., and Tullo,A.B. (2001). Bacterial contamination of human organ-cultured corneas. Cornea *20*, 260-263.

Albon,J., Tullo,A.B., Aktar,S., and Boulton,M.E. (2000). Apoptosis in the endothelium of human corneas for transplantation. Invest Ophthalmol. Vis. Sci. *41*, 2887-2893.

Anderson,N.J., Badawi,D.Y., Grossniklaus,H.E., and Stulting,R.D. (2001). Posterior polymorphous membranous dystrophy with overlapping features of iridocorneal endothelial syndrome. Arch. Ophthalmol. *119*, 624-625.

Arffa, R. C. Grayson's Diseases of the Cornea; fourth edition. 4. 1997. USA, Mosby.
Ref Type: Serial (Book,Monograph)

Armitage,W.J. and Easty,D.L. (1997). Factors influencing the suitability of organ-cultured corneas for transplantation. Invest Ophthalmol. Vis. Sci. *38*, 16-24.

Armitage,W.J., Hall,S.C., and Routledge,C. (2002). Recovery of endothelial function after vitrification of cornea at -110 degrees C. Invest Ophthalmol. Vis. Sci. *43*, 2160-2164.

Ashkenazi,A. and Dixit,V.M. (1998). Death receptors: Signalling and modulation. Science *281*, 1305-1308.

Balda,M.S., Garrett,M.D., and Matter,K. (2003). The ZO-1 associated Y-box factor XONAB regulates epithelial cell proliferation and cell density. J Cell Biol *160*, 423-432.

Balda,M.S. and Matter,K. (2000). The tight junction protein ZO-1 and an interactin transcription factor regulate ErbB-2 expression. EMBO J *19*, 2024-2033.

Ban,Y., Dota,A., Cooper,L.J., Fullwood,N.J., Nakamura,T., Tsuzuki,M., Mochida,C., and Kinoshita,S. (2003). Tight junction-related protein expression and distribution in human corneal epithelium. Exp. Eye Res. *76*, 663-669.

Baum,J.M., Niedra,R., Davis,C., and Yue,B.Y. (1984). Mass culture of human corneal endothelial cells. Arch. Ophthalmol. *97*, 1136-1140.

Bazzoni,G. and Dejana,E. (2004). Endothelial cell-to-cell junctions: molecular organization and role in vascular homeostasis. Physiol Rev. *84*, 869-901.

Bednarz,J., Rodokanaki-von Schrenck,A., and Engelmann,K. (1998). Different characteristics of endothelial cells from central and peripeheral human cornea in primary culture and after subculture. In Vitro Cell Dev. Biol. *34*, 149-153.

Bednarz,J., Teifel,M., Friedl,P., and Engelmann,K. (2000). Immortalization of human corneal endothelial cells using electroporation protocol optimized for human corneal endothelial and human retinal pigment epithelial cells. Acta Ophthalmol. Scand. *78*, 130-136.

Beebe,D.C. and Coats,J.M. (2000). The lens organizes the anterior segment: specification of neural crest cell differentiation in the avian eye. Dev. Biol. *220*, 424-431.

Behndig,A., Karlsson,K., Brannstrom,T., Sentman,M.L., and Marklund,S.L. (2001). Corneal endothelial integrity in mice lacking extracellular superoxide dismutase. Invest Ophthalmol. Vis. Sci. *42*, 2784-2788.

Ben-Ze'ev,A. and Geiger,B. (1998). Differential molecular interactions of beta-catenin and plakoglobin in adhesion, signalling and cancer. Curr Opin Cell Biol *10*, 629-639.

Bendeck,M.P., Regenass,S., Tom,W.D., Giachelli,C.M., Schwartz,S.M., Hart,C., and Reidy,M.A. (1996). Differential Expression of α1 Type VIII Collagen in Injured Platelet-Derived Growth Factor-BB Stimulated Rat Carotid Arteries. Circ Res *79*, 524.

Bergmanson,J.P.G., Sheldon,T.M., and Goosey,J.D. (1999). Fuchs' endothelial dystrophy: a fresh look at an aging disease. Opthal. Physiol. Opt. *19*, 210-222.

Berryhill,B.L., Kane,B., Stramer,B., Fini,E.M., and Hassel,J.R. (2003). Increased SPARC accumulation during corneal repair. Exp. Eye Res *77*, 85-92.

Biswas,S., Munier,F.L., Yardley,J., Hart-Holden,N., Perveen,R., Cousin,P., Sutphin,J.E., Noble,B., Batterbury,M., Kielty,C., Hackett,A., Bonshek,R., Ridgway,A., McLeod,D., Sheffield,V.C., Stone,E.M., Schorderet,D.F., and Black,G.C. (2001). Missense mutations in COL8A2, the gene encoding the alpha2 chain of type VIII collagen, cause two forms of corneal endothelial dystrophy. Hum. Mol. Genet. *10*, 2415-2423.

Blake,D.A., Yu,H., Young,D.L., and Caldwell,D.R. (1997). Matrix stimulates the proliferation of human corneal endothelial cells in culture. Invest Ophthalmol. Vis. Sci. *38*, 1119-1129.

Borderie,V.M., Baudrimont,M., Vallee,A., Ereau,T.L., Gray,F., and Laroche,L. (2000). Corneal endothelial cell apoptosis in patients with Fuchs' dystrophy. Invest Ophthalmol. Vis. Sci. *41*, 2501-2505.

Bornstein,P. and Sage,E.H. (2002). Matricellular proteins: extracellular modulators of cell function. Curr Opin Cell Biol *14*, 608-616.

Bourges,J.L., Valamanesh,F., Torriglia,A., Jeanny,J.C., Savoldelli,M., Renard,G., BenEzra,D., de Kozak,Y., and Behar-Cohen,F. (2004). Cornea graft endothelial cells undergo apoptosis by way of an alternate (caspase-independent) pathway. Transplantation *78*, 316-323.

Bourne,W.M. (2003). Biology of the corneal endothelium in health and disease. Eye *17*, 912-918.

Brogdon,J.D., McLaughlin,S.A., Brightman,A.H., and Helper,L.C. (1989). Effect of epidermal growth factor on healing of corneal endothelial cells in cats. Am. J. Vet. Res. *50*, 1237-1243.

Bron, A. J., Tripathi, R. C., and Tripathi, B. J. Wolff's Anatomy of the Eye and Orbit; eighth edition. 8. 2001. London, Hodder Headline Group.
Ref Type: Serial (Book,Monograph)

Brunette,I., Le François,M., Tremblay,M.-C., and Guertin,M.C. (2001). Corneal transplant tolerance of cryopreservation. Cornea *20*, 590-596.

Callaghan,M., Hand,C.K., Kennedy,S.M., FitzSimon,J.S., Collum,L.M., and Parfrey,N.A. (1999). Homozygosity mapping and linkage analysis demonstrate that autosomal recessive congenital hereditary endohtelial dystrophy (CHED) and autosomal dominant CHED are genetically distinct. Br. J. Ophthalmol. *83*, 115-119.

Cao,Z., Wu,H.K., Bruce,A., Wollenberg,K., and Panjwant,N. (2002). Detection of differentially expressed genes in healing mouse corneas using cDNA microarrays. Invest Ophthalmol. Vis. Sci. *43*, 2897-2904.

Chao,D.T. and Korsmeyer,S.J. (1998). BCL-2 Family: Regulators of cell death. Annu. Rev. Immunol. *16*, 395-419.

Charrasse,S., Meriane,M., Comunale,F., Blangy,A., and Gauthier-Rouvier,E.C. (2002). N-cadherin-dependent cell-cell contact regulates Rho GTPsaes and beta-catenin localization in mouse C2C12 myoblasts. J Cell Biol *158*, 953-965.

Chen,K.H., Harris,D.L., and Joyce,N.C. (1999). TGF-beta2 in aqueous humor suppresses S-phase entry in cultured corneal endothelial cells. Invest Ophthalmol. Vis. Sci. *40*, 2513-2519.

Chen,K.H., Hsu,W.M., and Lee,S.M. (2002). Differential Effects of Transforming Growth Factor-beta2 on Corneal Endothelial Cell Proliferation - A Role of Serum Factors. Exp. Eye Res. *75*, 61-67.

Cho,K.S., Lee,E.H., Choi,J.S., and Joo,C.K. (1999). Reactive oxygen species-induced apoptosis and necrosis in bovine corneal endothelial cells. Invest Ophthalmol. Vis. Sci. *40*, 911-919.

Choi,J., Ko,M.K., and Kay,E.P. (2000). Subcellular localization of the expressed 18 kDa FGF-2 isoform in corneal endothelial cells. Mol. Vis. *6:222-31.*, 222-231.

Choi,S.H., Kay,E.P., Oh,D.S., Gu,X., and Smith,R.E. (1995). Insulin-like growth factor-I promotes cell proliferation in the absence of modulation of collagen phenotypes and utilizes IRS-1, not PLC-gamma 1, in corneal endothelial cells. Curr. Eye Res. *14*, 669-676.

Chung,E.-H., Hutcheon,A.E.K., Joyce,N.C., and Zieske,J.D. (1999). Synchronization of the G1/S transition in response to conreal debridement. Invest Ophthalmol. Vis. Sci. *40*, 1952-1958.

Cockerham,G.C., Laver,N.V., Hidayat,A.A., and McCoy,D.L. (2002). An immunohistochemical analysis and comparison of posterior polymorphous dystrophy with congenital hereditary endohteilal dystrophy. Cornea *21*, 787-791.

Collin,S.P. and Barry Collin,H. (2004). Primary cilia in vertebrate corneal endothelial cells. Cell Biol. Int. *28*, 125-130.

Cordenonsi,M., D'atri,F., Hammar,E., Parry,D.A., Kendrick-Jones,J., Shore,D., and Citi,S. (1999). Cingulin contains globuerular and coiled-coil domains and interacts with ZO-1, ZO-2, ZO-3 and myosin. J Cell Biol *147*, 1569-1582.

Couch,J.M., Cullen,P., Casey,T.A., and Fabre,J.W. (1987). Mitotic activity of corneal endothelial cells in organ culture with recombinant human epidermal growth factor. Ophthalmology *94*, 1-6.

Cousins,S.W., McCabe,M.M., Danielpour,D., and Streilein,J.W. (1991). Identification of transforming growth factor-beta as an immunosuppressive factor in aqueous humor. Invest Ophthalmol. Vis. Sci. *32*, 2201-2211.

Crawford,K.M., Ernst,S.A., Meyer,R.F., and MacCallum,D.K. (1995). NaK-ATPase pump sites in cultured bovine corneal endothelium of varying cell density at confluence. Invest Ophthalmol. Vis. Sci. *36*, 1317-1326.

Crewe,J.M. and Armitage,W.J. (2001). Integrity of epithelium and endothelium in organ-cultured human corneas. Invest Ophthalmol. Vis. Sci. *42*, 1757-1761.

Dabin,I. and Courtois,Y. (1991). In vitro kinetics of basic fibroblast growth factor diffusion across a reconstituted corneal endothelium. J. Cell Physiol *147*, 396-402.

Danielson,K.G., Baribault,H., Holmes,D.F., Graham,H., Kadler,K.E., and Iozzo,R.V. (1997). Targeted disruption of decorin leads to abnormal collagen fibril morphology and skin fragility. J Cell Biol *136*, 729-743.

Donepudi,M. and Grutter,M.G. (2002). Structure and zymogen activation of caspases. Biophys. Chem. *101-102*, 145-153.

Dudek,H., Datta,S.R., Franke,T.F., Birnbaum,M.J., Yao,R., Cooper,G.M., Segal,R.A., Kaplan,D.R., and Greenberg,M.E. (1997). Regulation of neuronal survival by the serine-threonine protein kinase Akt. Science *275*, 661-665.

Egan,C.A., Savre-Train,I., Shay,J.W., Wilson,S.E., and Bourne,W.M. (1998). Analysis of telomere lengths in human corneal endothelial cells from donors of different ages. Invest Ophthalmol. Vis. Sci. *39*, 648-653.

Engelmann,K., Bednarz,J., Schafer,H.J., and Friedl,P. (2001). Isolation and characterization of a mouse monoclonal antibody against human corneal endothelial cells. Exp. Eye Res. *73*, 9-16.

Engelmann,K., Bohnke,M., and Friedl,P. (1988). Isolation and long-term cultivation of human corneal endothelial cells. Invest Ophthalmol. Vis. Sci. *29*, 1656-1662.

Engelmann,K. and Friedl,P. (1989). Optimization of culture conditions for human corneal endothelial cells. In Vitro Cell Dev. Biol. *25*, 1065-1072.

Faragher,R.G.A., Mulholland,B., Tuft,S.J., Sandeman,S., and Khaw,P.T. (1997). Aging and the cornea. Br. J. Ophthalmol. *81*, 814-817.

Feldman,S.T., Gately,D., Schonthal,A., and Feramisco,J.R. (1992). Fos expression and growth regulation in bovine corneal endothelial cells. Invest Ophthalmol. Vis. Sci. *33*, 3307-3314.

Feldman,S.T., Gjerset,R., Gately,D., Chien,K.R., and Feramisco,J.R. (1993). Expression of SV40 virus large T antigen by recombinant adenoviruses activates proliferation of corneal endothelium in vitro. J. Clin. Invest. *91*, 1713-1720.

Fischbarg,J. and Maurice,D.M. (2004). An update on corneal hydration control. Exp. Eye Res *78*, 537-541.

Fridman,R., Alon,Y., Doljanski,F., Fuks,Z., and Vlodavsky,I. (1985). Cell interaction with the extracellular matrices produced by endothelial cells and fibroblasts. Exp. Cell Res. *158*, 461-476.

Furuse,M., Hata,M., Furuse,K., Yoshida,Y., Haratake,A., Sugitani,Y., Noda,T., Kubo,A., and Tsukita,S. (2002). Claudin-based tight junctions are crucial for the mammalian epidermal barrier: a lesson from claudin-1-deficient mice. J Cell Biol *156*, 1099-1111.

Furuse,M., Itoh,M., Hirase,T., Nagasuchi,A., Yonemura,S., and Tsukita,S. (1994). Direct association of occludin with ZO-1 and its possible involvement in the localization of occluind at tight junction. J Cell Biol *127*, 1617-1626.

Furuse,M., Sasaki,H., Fujimoto,K., and Tsukita,S. (1998). A single gene product, claudin-1 or -2, reconstitutes tight junction strands and recruits occludin in fibroblasts. J Cell Biol *143*, 391-401.

Gain,P., Thuret,G., Chiquet,C., Dumollard,J.M., Mosnier,J.F., and Campos,L. (2001). In situ immunohistochemical study of Bcl-2 and heat shock proteins in human corneal endothelial cells during corneal storage. Br. J. Ophthalmol. *85*, 996-1000.

Gilbertson-Beadling,S.K. and Fischer,C. (1993). A potential role for N-cadherin in mediating endothelial cell-smooth muscle cell interactions in the vasculature. Lab Invest. *69*, 203-209.

Gipson,I.K. and Inatomi,T. (1995). Extracellular matrix and growth factors in corneal wound healing. Curr. Opin. Ophthalmol. *6*, 3-10.

Gordon,S.R. (1990). Changes in extracellular matrix proteins and actin during corneal endothelial growth. Invest Ophthalmol. Vis. Sci. *31*, 94-101.

Gordon,S.R. (2002). Microfilament disruption in a noncycling organized tissue, the corneal endothelium, intiates mitosis. Exp. Cell Res. *272*, 127-134.

Gospodarowicz,D. and III,C. (1980). The extracellular matrix and the control of proliferation of corneal endothelial and lens epithelial cells. Exp. Eye Res. *31*, 181-199.

Gospodarowicz,D., Mescher,A.L., and Birdwell,C.R. (1977). Stimulation of corneal endothelial cell proliferations in vitro by fibroblast and epidermal growth factors. Exp. Eye Res *25*, 75-89.

Graham,M.A., Rawe,I., Dartt,D.A., and Joyce,N.C. (2000). Protein kinase C regulation of corneal endothelial cell proliferation and cell cycle. Invest Ophthalmol. Vis. Sci. *41*, 4124-4132.

Grant,M.B., Khaw,P.T., Schultz,G.S., Adams,J.L., and Shimizu,R.W. (1992). Effects of epidermal growth factor, fibroblast growth factor, and transforming growth factor-beta on corneal cell chemotaxis. Invest Ophthalmol. Vis. Sci. *33*, 3292-3301.

Greenhill,N.S., Rüger,B.M., Hasan,Q., and Davis,P.F. (2000). The α1(VIII) and α2(VIII) collagen chains form two distinct homotrimeric proteins in vivo. Matrix Biol *19*, 19-28.

Gross,A., McDonnell,J.M., and Korsmeyer,S.J. (1999). Bcl-2 family members and the mitochondria in apoptosis. Genes Dev. *13*, 1899-1911.

Gross,A., McDonnell,J.M., and Korsmeyer,S.J. (1999). Bcl-2 family members and the mitochondria in apoptosis. Genes Dev. *13*, 1899-1911.

Grupcheva,C.N., McGhee,C.N.J., Dean,S., and Craig,J.P. (2004). In vivo confocal microscopic characteristics of iridocorneal endothelial syndrome. Clin. Exp. Ophthalmol. *32*, 275-283.

Gu,X. and Kay,E.P. (1998). Distribution and putative roles of fibroblast growth factor-2 isoforms in corneal endothelial modulation. Invest Ophthalmol. Vis. Sci. *39*, 2252-2258.

Gu,X., Seong,G.J., Lee,Y.G., and Kay,E.P. (1996). Fibroblast growth factor 2 uses distinct signaling pathways for cell proliferation and cell shape changes in corneal endothelial cells. Invest Ophthalmol. Vis. Sci. *37*, 2326-2334.

Gualandris,A., Rusnati,M., Belleri,M., Nelli,E.E., Bastaki,M., Molinari-Tosatti,M.P., Bonardi,F., Parolini,S., Albini,A., Morbidelli,L., Ziche,M., Corallini,A., Possati,L., Vacca,A., Ribatti,D., and Presta,M. (1996). Basic fibroblast growth factor overexpression in endothelial cells: an autocrine mechanism for angiogenesis and angioproliferative diseases. Cell Growth Differ. *7*, 147-160.

Hamrah,P., Liu,Y., Zhang,Q., and Dana,M.R. (2003). Alterations in corneal stromal dendritic cell phenotype and distribution in inflammation. Arch. Ophthalmol. *12*, 1132-1140.

Harris,D.L. and Joyce,N.C. (1999). Transforming growth factor-beta suppresses proliferation of rabbit corneal endothelial cells in vitro. J. Interferon Cytokine Res. *19*, 327-334.

Hempel,B., Bednarz,J., and Engelmann,K. (2001). Use of a serum-free medium for long-term storage of human corneas. Influence on endothelial cell density and corneal metabolism. Graefes Arch. Clin. Exp. Ophthalmol. *239*, 801-805.

Hirase,T., Staddon,J.M., Saitou,M., Ando-Akatsuka,Y., Itoh,M., Furuse,M., Fujimoto,K., Tsukita,S., and Rubin,L.L. (1997). Occludin as a possible determinant of tight junction permeability in endothelial cells. J Cell Sci *110*, 1603-1613.

Holley,G.P., Sugerman,P.E., Purohit,A.R., and Edelhauser,H.F. (2000). Endothelial cell density is significantly increased in the far peripheral (limbal) region of the human cornea. Invest Ophthalmol. Vis. Sci. *ARVO abstract*, 3176.

Honda,H., Ogita,Y., Higuchi,S., and Kani,K. (1982). Cell movements in a living mammalian tissue: long-term observation of individual cells in wounded corneal endothelia of cats. J. Morphol. *174*, 25-39.

Hoover,K.B., Liao,S.Y., and Bryant,P.J. (1998). Loss of the tight junction MAGUK ZO-1 in breast cancer: relationship to glandular differentiation and loss of heterozygosity. Am. J. Pathol. *153*, 1767-1773.

Hoppenreijs,V.P., Pels,E., Vrensen,G.F., Oosting,J., and Treffers,W.F. (1992). Effects of human epidermal growth factor on endothelial wound healing of human corneas. Invest Ophthalmol. Vis. Sci. *33*, 1946-1957.

Hoppenreijs,V.P., Pels,E., Vrensen,G.F., Felten,P.C., and Treffers,W.F. (1993). Platelet-derived growth factor: receptor expression in corneas and effects on corneal cells. Invest Ophthalmol. Vis. Sci. *34*, 637-649.

Hoppenreijs,V.P., Pels,E., Vrensen,G.F., and Treffers,W.F. (1994). Basic fibroblast growth factor stimulates corneal endothelial cell growth and endothelial wound healing of human corneas. Invest Ophthalmol. Vis. Sci. *35*, 931-944.

Hoppenreijs,V.P., Pels,E., Vrensen,G.F., and Treffers,W.F. (1996). Corneal endothelium and growth factors. Surv. Ophthalmol. *41*, 155-164.

Hoppenreijs,V.P., Pels,E., Vrensen,G.F., and Treffers,W.F. (1996). Corneal endothelium and growth factors. Surv. Ophthalmol. *41*, 155-164.

Hoppenreijs,V.P., Pels,E., Vrensen,G.F., and Treffers,W.F. (1994b). Effects of platelet-derived growth factor on endothelial wound healing of human corneas. Invest Ophthalmol. Vis. Sci. *35*, 150-161.

Hoppenreijs,V.P., Pels,E., Vrensen,G.F., and Treffers,W.F. (1994a). Basic fibroblast growth factor stimulates corneal endothelial cell growth and endothelial wound healing of human corneas. Invest Ophthalmol. Vis. Sci. *35*, 931-944.

Hsu,J.K., Cavanagh,H.D., Jester,J.V., Ma,L., and Petroll,W.M. (1999). Changes in corneal endothelial apical junctional protein organization after corneal cold storage. Cornea *18*, 712-720.

Huang,P.T., Nelson,L.R., and Bourne,W.M. (1989). The morphology and function of healing cat corneal endothelium. Invest Ophthalmol. Vis. Sci. *30*, 1794-1801.

Hudde,T., Comer,R.M., Kinsella,M.T., Buttery,L., Luthert,P.J., Polak,J.M., George,A.J., and Larkin,D.F. (2002). Modulation of hydrogen peroxide induced injury to corneal endothelium by virus mediated catalase gene transfer. Br. J. Ophthalmol. *86*, 1058-1062.

Hull,D.S., Green,K., Thomas,L., and Alderman,N. (1984). Hydrogen peroxide-mediated corneal endothelial damage. Induction by oxygen free radical. Invest Ophthalmol. Vis. Sci. *25*, 1246-1253.

Hulleman,E. and Boonstra,J. (2001). Regulation of G1 phase progression by growth factors and the extracellular matrix. Cell Mol. Life Sci. *58*, 80-93.

Ickes,R., Harris,D.L., and Joyce,N.C. (2002). Classical cadherin expression in corneal endothelium. Invest Ophthalmol. Vis. Sci. *ARVO abstract*, 3190.

Ikebe,H., Takamatsu,T., Itoi,M., and Fujita,S. (1988). Changes in nuclear DNA content and cell size of injured human corneal endothelium. Exp. Eye Res. *47*, 205-215.

Illidge,C., Kielty,C., and Shuttleworth,C.A. (1998). The α1(VIII) and α2(VIII) chains of type VIII collagen can form stable homotrimeric molecules. J. Biol. Chem. *273*, 22091-22095.

Imanishi,J., Kamiyama,K., Iguchi,I., Kita,M., Sotozono,C., and Kinoshita,S. (2000). Growth factors: importance in wound healing and maintenance of transparency of the cornea. Prog. Retin. Eye Res. *19*, 113-129.

Ing,J.J., Ing,H.H., Nelson,L.R., Hodge,D.O., and Bourne,W.M. (1998). Ten-year postoperative results of penetrating keratoplasty. Ophthalmology *105*, 1855-1865.

Itoh,M., Nagafuchi,A., Moroi,S., and Tsukita,S. (1997). Involvement of ZO-1 in cadherin-based cell adhesion through its direct binding to alpha catenin and actin filaments. J. Cell Biol. *138*, 181-192.

Jacobsen,I.E., Jensen,O.A., and Prause,J.U. (1984). Structure and composition of Bowman's membrane. Study by frozen resin crackin. Acta Ophthalmol. (Copenh) *62*, 39-53.

Johnston,M.C., Noden,D.M., Hazelton,R.D., Coulombre,J.L., and Coulombre,A.J. (1979). Origins of avian ocular and periocular tissues. Exp. Eye Res. *29*, 27-43.

Joo,C., Cho,K., Kim,H., Choi,J.S., and Oh,Y.J. (1999). Protective role for bcl-2 in experimentally induced cell death of bovine corneal endothelial cells. Ophthalmic Res. *31*, 287-296.

Joo,C.K., Pepose,J.S., and Fleming,T.P. (1994). In vitro propagation of primary and extended life span murine corneal endothelial cells. Invest Ophthalmol. Vis. Sci. *35*, 3952-3957.

Joyce,N.C. (2003). Proliferative capacity of the corneal endothelium. Prog. Retin. Eye Res *22*, 359-389.

Joyce,N.C., Harris,D.L., and Mello,D.M. (2002). Mechanisms of mitotic inhibition in corneal endothelium: contact inhibition and TGF-beta2. Invest Ophthalmol. Vis. Sci. *43*, 2152-2159.

Joyce,N.C., Harris,D.L., and Zieske,J.D. (1998). Mitotic inhibition of corneal endothelium in neonatal rats. Invest Ophthalmol. Vis. Sci. *39*, 2572-2583.

Joyce,N.C., Joyce,S.J., Powell,S.M., and Meklir,B. (1995). EGF and PGE2: effects on corneal endothelial cell migration and monolayer spreading during wound repair in vitro. Curr. Eye Res. *14*, 601-609.

Joyce,N.C., Meklir,B., Joyce,S.J., and Zieske,J.D. (1996a). Cell cycle protein expression and proliferative status in human corneal cells. Invest Ophthalmol. Vis. Sci. *37*, 645-655.

Joyce,N.C., Meklir,B., and Neufeld,A.H. (1990). In vitro pharmacologic separation of corneal endothelial migration and spreading responses. Invest Ophthalmol. Vis. Sci. *31*, 1816-1826.

Joyce,N.C., Navon,S.E., Roy,S., and Zieske,J.D. (1996b). Expression of cell cycle-associated proteins in human and rabbit corneal endothelium in situ. Invest Ophthalmol. Vis. Sci. *37*, 1566-1575.

Joyce,N.C. and Zieske,J.D. (1997). Transforming growth factor-beta receptor expression in human cornea. Invest Ophthalmol. Vis. Sci. *38*, 1922-1928.

Kaji,Y., Amano,S., Usui,T., Oshika,T., Yamashiro,K., Ishida,S., Suzuki,K., Tanaka,S., Adamis,A.P., Nagai,R., and Horiuchi,S. (2003). Expression and function of receptros for advanced glycation end products in bovine corneal endothelial cells. Invest Ophthalmol. Vis. Sci. *44*, 521-528.

Kaji,Y., Amano,S., Usui,T., Suzuki,K., Tanaka,S., Oshika,T., Nagai,R., and Horiuchi,S. (2001). Advanced glycation end products in Descemet's membrane and their effect on corneal endothelial cell. Curr. Eye Res. *23*, 469-477.

Kaji,Y., Usui,T., Oshika,T., Matsubara,M., Yamashita,H., Araie,M., Murata,T., Ishibashi,T., Nagai,R., Horiuchi,S., and Amano,S. (2000). Advanced glycation end products in diabetic corneas. Invest Ophthalmol. Vis. Sci. *41*, 362-368.

Kamiyama,K., Iguchi,I., Wang,X., Kita,M., Imanishi,J., Yamaguchi,N., Hongo,M., Sotozono,C., and Kinoshita,S. (1995). Enhancement of growth of rabbit corneal endothelial cells by PDGF. Cornea *14*, 187-195.

Kapoor,R., Sakai,L.Y., Funk,S., Roux,E., Bornstein,P., and Sage,E.H. (1988). Type VIII collagen has a restricted distribution in specialized extracellular matrices. J. Cell Biol. *107*, 721-730.

Kato,A., Takahashi,H., Takahashi,Y., and Matsushime,H. (1997). Inactivation of the cyclin D-dependent kinase in the rat fibroblast cell line, 3Y1, induced by contact inhibition. J Biol Chem *272*, 8065-8070.

Kay,E.P., Gu,X., Ninomiya,Y., and Smith,R.E. (1993). Corneal endothelial modulation: a factor released by leukocytes induces basic fibroblast growth factor that modulates cell shape and collagen. Invest Ophthalmol. Vis. Sci. *34*, 663-672.

Kay,E.P., Gu,X., and Smith,R.E. (1994). Corneal endothelial modulation: bFGF as direct mediator and corneal endothelium modulation factor as inducer. Invest Ophthalmol. Vis. Sci. *35*, 2427-2435.

Kay,E.P. and Oh,S. (1988). Modulation of type III collagen synthesis in bovine corneal endothelial cells. Invest Ophthalmol. Vis. Sci. *29*, 200-207.

Kay,E.P., Park,S.Y., Ko,M.K., and Lee,S.C. (1998). Fibroblast growth factor 2 uses PLC-gamma1 for cell proliferation and PI3-kinase for alteration of cell shape and cell proliferation in corneal endothelial cells. Mol. Vis. *4:22.*, 22.

Kay,E.P., Smith,R.E., and Nimni,M.E. (1985). Type I collagen synthesis by corneal endothelial cells modulated by polymorphonuclear leukocytes. J. Biol. Chem. *260*, 5139-5146.

Kenney,M.C., Lewis,W., Redding,J., and Waring,G.O. (1986). Decreased fibronectin levels in aqueous humor after corneal injury. Ophthalmic Res. *18*, 165-171.

Kikuchi,M., Harris,D.L., Obara,Y., Senoo,T., and Joyce,N.C. (2004). p27kip1 Antisense-induced proliferative activity of rat corneal endothelial cells. Invest Ophthalmol. Vis. Sci. *45*, 1763-1770.

Kim,T.Y., Kim,W.I., Smith,R.E., and Kay,E.D. (2001a). Role of p27(Kip1) in cAMP- and TGF-beta2-mediated antiproliferation in rabbit corneal endothelial cells. Invest Ophthalmol. Vis. Sci. *42*, 3142-3149.

Kim,T.Y., Kim,W.I., Smith,R.E., and Kay,E.P. (2001b). Differential activity of TGF-beta2 on the expression of p27Kip1 and Cdk4 in actively cycling and contact inhibited rabbit corneal endothelial cells. Mol. Vis. *%20;7:261-70.*, 261-270.

Koh,S.W. and Waschek,J.A. (2000). Corneal endothelial cell survival in organ cultures under acute oxidative stress: effect of VIP. Invest Ophthalmol. Vis. Sci. *41*, 4085-4092.

Komuro,A., Hodge,D.O., Gores,G.J., and Bourne,W.M. (1999). Cell death during corneal storage at 4 degrees C. Invest Ophthalmol. Vis. Sci. *40*, 2827-2832.

Kuang, K., Zuniga, F. A., Ma, L., and Fischbarg, J. Expression of Claudins in Cultured Mice Corneal Endothelial Cells. Invest Ophthalmol.Vis.Sci. ARVO abstract, 3454/B157. 2003.
Ref Type: Generic

Landshman,N., Belkin,M., Ben Hanan,I., Ben Chaim,O., Assia,E., and Savion,N. (1987). Regeneration of cat corneal endothelium induced in vivo by fibroblast growth factor. Exp. Eye Res. *45*, 805-811.

Landshman,N., Solomon,A., and Belkin,M. (1989). Cell division in the healing of the corneal endothelium of cats. Arch. Ophthalmol. *107*, 1804-1808.

Lee,H.J., Lin,C.P., and Chen,C.W. (1991). The effects of epidermal growth factor and chondroitin sulfate on the animal corneal endothelial cell culture. Gaoxiong. Yi. Xue. Ke. Xue. Za Zhi. *7*, 614-621.

Lee,H.T. and Kay,E.P. (2003b). Regulatory role of PI 3-kinase on expression of Cdk4 and p27, nuclear localization of Cdk4, and phosphorylation of p27 in corneal endothelial cells. Invest Ophthalmol. Vis. Sci. *44*, 1521-1528.

Lee,H.T. and Kay,E.P. (2003a). FGF-2 induced reorganization and disruption of actin cytoskeleton through PI 3-kinase, Rho, and Cdc42 in corneal endothelial cells. Mol. Vis. *9:624-34.*, 624-634.

Lee,H.T., Lee,J.G., Na,M., and Kay,E.P. (2004). FGF-2 induced by interleukin-1 beta through the action of phosphatidylinositol 3-kinase mediates endothelial mesenchymal transformation in corneal endothelial cells. J. Biol. Chem. *279*, 32325-32332.

Levy,S.G., Kirkness,C.M., Ficker,L., and McCartney,A.C.E. (1996). The histopathology of the iridocorneal-endothelial syndrome. Cornea *15*, 46-54.

Levy,S.G., McCartney,A.C.E., Baghai,M.H., Barrett,M.C., and Moss,J. (1995). Pathology of the iridocorneal-endothelial syndrome. Invest Ophthalmol. Vis. Sci. *36*, 2592-2601.

Li,X.Y., De Marco,B.M., Mayhew,E.S., and Niederkorn,J.Y. (1998). Aqueous humor-borne factor upregulates Bcl-2 expression in corneal endothelial cells. Curr. Eye Res. *17*, 970-978.

Liang,R.A., Neubauer,L., Leibowitz,H.M., and Oak,S.S. (1983). Coalescence of endothelial cells in the traumatized cornea. II. Clinical observations. Arch. Ophthalmol. *101*, 1712-1715.

Lin,D. (2000). A mammalian PAR-3-PAR-6 complex implicated in Cdc42/Rac1 and aPKC signalling and cell polarity. Naure Cell Biol. *2*, 540-547.

Lwigale,P.Y. (1999). Nuclear morphologies of bovine corneal cells as visualized by confocal microscopy. Cells Tissues Organs *165*, 104-112.

MacBeath,J.R.E., Kielty,C., and Shuttleworth,C.A. (1996). Type VIII collagen is a product of vascular smooth-muscle cells in development and disease. Biochem. J. *319*, 993-998.

Mann,K., Jander,R., Korsching,E., Kuhn,K., and Rauterberg,J. (1990). The primary structure of a triple-helical domain of collagen type VIII form bovine Descemet's membrane. FEBS Lett. *273*, 168-172.

Martinou,J.C., Desagher,S., and Antonsson,B. (2000). Cytochrome c release from mitochondria: all or nothing. Nat. Cell Biol. *2*, E41-E43.

Mason,I.J. (1994). The ins and outs of fibroblast growth factor. Cell *78*, 547-552.

Matter,K. and Balda,M.S. (2003). Signalling to and from tight junctions. Nat. Rev. Mol. Cell Biol. *4*, 225-236.

Medina,R., Rahmer,C., Mitic,L.L., Anderson,J.M., and Van Itallie,C.M. (2000). Occludin localization at the tight junction requires the second extracellular loop. J. Membr. Biol. *178*, 235-247.

Meek,K.M. and Boote,C. (2004). The organization of collagen in the corneal stroma. Exp. Eye Res *78*, 503-512.

Meloche,S., Seuwen,K., Pages,G., and Pouyssegur,J. (1992). Biphasic and synergistic activation of p44mapk (ERK1) by growth factors; correlation between late phase activation and mitogenicity. Mol. Endocrinol *6*, 845-854.

Mitsumoto,T., Nishimura,T., Toda,S., Okinami,S., Oono,S., and Sugihara,H. (2001). Combined effect of extracellular matrices and growth factors on bovine corneal endothelial cells in culture. Jpn. J. Ophthalmol. *45*, 115-124.

Mohan,R.R., Liang,Q., Kim,W.J., Helena,M.C., Baerveldt,F., and Wilson,S.E. (1997). Apoptosis in the cornea: further characterization of Fas/Fas ligand system. Exp. Eye Res. *65*, 575-589.

Moller-Pedersen,T. and Ehlers,N. (1995). A three-dimensional study of the human corneal keratocyte density. Curr. Eye Res *14*, 459-464.

Moller-Pedersen,T., Hartmann,U., Ehlers,N., and Engelmann,K. (2001). Evaluation of potential organ culture media for eye banking using a human corneal endothelial cell growth assay. Graefes Arch. Clin. Exp. Ophthalmol. *239*, 778-782.

Morisaki,H., Fujimoto,A., Ando,A., Nagata,Y., Ikeda,K., and Nakanishi,M. (1997). Cell cycle-dependent phosphorylation of p27 cyclin-dependent kinase (Cdk) inhibitor by cyclin E/Cdk2. Biochem. Biophys. Res. Commun. *240*, 386-390.

Morita,K., Sasaki,H., Furuse,M., and Tsukita,S. (1999). Endothelial claudin: claudin-5/MVCF constitutes tight junction strands in endothelial cells. J Cell Biol *147*, 185-194.

Muller,L.J., Pels,E., Schurmans,L.R.H.M., and Vrensen,G.F. (2004). The new three-dimensional model of the organization of proteoglycans and collagen fibrils in the human corneal stroma. Exp. Eye Res *78*, 493-501.

Murphy,C., Alvarado,J., Juster,R., and Maglio,M. (1984). Prenatal and postnatal cellularity of the human corneal endothelium. A quantitative histologic study. Invest Ophthalmol. Vis. Sci. *25*, 312-322.

Murphy,L.O., Smith,S., Chen,R.H., Fingar,D.C., and Blenis,J. (2002). Molecular interpretation of ERK signal duration by immediate early gene products. Nat. Cell Biol. *4*, 556-564.

Nakagawa,M., Fukata,M., Yamaga,M., Itoh,M., and Kaibuchi,K. (2001). Recruitment and activation of Rac1 by the formation of E-cadherin-mediated cell-cell adhesion sites. J Cell Sci *114*, 1829-1838.

Neubauer,L., Baratz,R.S., Liang,R.A., Oak,S.S., and Leibowitz,H.M. (1984). Coalescence of endothelial cells in the traumatized cornea. III. Correlation between specular and scanning electron microscopy. Arch. Ophthalmol. *102*, 921-922.

Neubauer,L., Liang,R.A., Leibowitz,H.M., and Oak,S.S. (1983). Coalescence of endothelial cells in the traumatized cornea. I. Experimental observations in cryopreserved tissue. Arch. Ophthalmol. *101*, 1787-1790.

Nguyen,V., Schonthal,A., and Feldman,S.T. (1994). Expression of c-jun proto-oncogene in corneal endothelium. Exp. Eye Res. *59*, 335-341.

Ohkoshi,K., Ishida,N., Yamaguchi,T., and Kanki,K. (1989). Corneal endothelium in a case of mitochondrial encephalomyopathy (Kearns-Sayre syndrome). Cornea *8*, 210-214.

Pagano,M., Tam,S.W., Theodoras,A.M., Beer-Romero,P., Del Sal,G., Chau,V., Yew,P.R., Draetta,G.F., and Rolfe,M. (1995). Role of the ubiquitin-proteasome pathway in regulating abundance of the cyclin-dependent kinase inhibitor p27. Science *269*, 682-685.

Petroll,W.M., Hsu,J.K., Bean,J., Cavanagh,H.D., and Jester,J.V. (1999). The spatial organization of apical junctional complex-associated proteins in feline and human corneal endothelium. Curr. Eye Res. *18*, 10-19.

Petroll,W.M., Jester,J.V., Barry-Lane,P.A., and Cavanagh,H.D. (1995). Assessment of f-actin organization and apical-basal polarity during in vivo cat endothelial wound healing. Invest Ophthalmol. Vis. Sci. *36*, 2492-2502.

Pfister,R.R. and Burnstein,N.L. (1977). The normal and abnormal human corneal epithelial surface: a scanning electron microscope study. Invest Ophthalmol. Vis. Sci. *16*, 614-622.

Polyak,K., Kato,J.Y., Solomon,M.J., Sherr,C.J., Massague,J., Roberts,J.M., and Koff,A. (1994). $p27^{Kip1}$, a cyclin-Cdk inhibitor, links transforming growth factor-β and contact inhibition to cell cycle arrest. Genes Dev. *8*, 9-22.

Raphael,B., Kerr,N.C., Shimizu,R.W., Lass,J.H., Crouthamel,K.C., Glaser,S.R., Stern,G.A., McLaughlin,B.J., Musch,D.C., Duzman,E., and . (1993). Enhanced healing of cat corneal endothelial wounds by epidermal growth factor. Invest Ophthalmol. Vis. Sci. *34*, 2305-2312.

Raymond,G.M., Jumblatt,M.M., Bartels,S.P., and Neufeld,A.H. (1986). Rabbit corneal endothelial cells in vitro: effects of EGF. Invest Ophthalmol. Vis. Sci. *27*, 474-479.

Reed,J.C. (2000). Mechanisms of apoptosis. Am. J. Pathol. *157*, 1415-1430.

Rieck,P., Hartmann,C., Jacob,C., Pouliquen,Y., and Courtois,Y. (1992). Human recombinant bFGF stimulates corneal endothelial wound healing in rabbits. Curr. Eye Res. *11*, 1161-1172.

Rieck,P., Oliver,L., Engelmann,K., Fuhrmann,G., Hartmann,C., and Courtois,Y. (1995). The role of exogenous/endogenous basic fibroblast growth factor (FGF2) and transforming growth factor beta (TGF beta-1) on human corneal endothelial cells proliferation in vitro. Exp. Cell Res. *220*, 36-46.

Rieck,P.W., Cholidis,S., and Hartmann,C. (2001). Intracellular signaling pathway of FGF-2-modulated corneal endothelial cell migration during wound healing in vitro. Exp. Eye Res. *73*, 639-650.

Sagoo,P., Chan,G., Larkin,D.F., and George,A.J. (2004). Inflammatory cytokines induce apoptosis of corneal endothelium through nitric oxide. Invest Ophthalmol. Vis. Sci. *45*, 3964-3973.

Saitou,M., Fujimoto,K., Doi,Y., Itoh,M., Fujimoto,T., Furuse,M., Takano,H., Noda,T., and Tsukita,S. (1998). Occludin-deficient embryonic stem cells can differentiate into polarized epithelial cells bearing tight junctions. J Cell Biol *141*, 397-408.

Saitou,M., Furuse,M., Sasaki,H., Schulzke,J.D., Fromm,M., Takano,H., Noda,T., and Tsukita,S. (2000). Complex phenotype of mice lacking occludin, a component of tight junctions strands. Mol. Biol. Cell *11*, 4131-4142.

Samples,J.R., Binder,P.S., and Nayak,S.K. (1991). Propagation of human corneal endothelium in vitro effect of growth factors. Exp. Eye Res. *52*, 121-128.

Schilling-Schon,A., Pleyer,U., Hartmann,C., and Rieck,P.W. (2000). The role of endogenous growth factors to support corneal endothelial migration after wounding in vitro. Exp. Eye Res. *71*, 583-589.

Schimmelpfennig,B.H. (1984). Direct and indirect determination of nonuniform cell density distribution in human corneal endothelium. Invest Ophthalmol. Vis. Sci. *25*, 223-229.

Schmidt,A., Utepbergenov,D.I., Krause,G., and Blasig,I.E. (2001). Use of surface plasmon resonance for real-time analysis of the interaction of ZO-1 and occludin. Biochem. Biophys. Res. Commun. 1194-1199.

Schonthal,A.H., Hwang,J.J., Stevenson,D., and Trousdale,M.D. (1999). Expression and activity of cell cycle-regulatory proteins in normal and transformed corneal endothelial cells. Exp. Eye Res. *68*, 531-539.

Schultz,G., Cipolla,L., Whitehouse,A., Eiferman,R., Woost,P., and Jumblatt,M. (1992). Growth factors and corneal endothelial cells: III. Stimulation of adult human corneal endothelial cell mitosis in vitro by defined mitogenic agents. Cornea *11*, 20-27.

Sellheyer,K. and Spitznas,M. (1988). Surface differentiation of the human corneal epithelium during prenatal development. Graefes Arch. Clin. Exp. Ophthalmol. *226*, 482-488.

Senoo,T. and Joyce,N.C. (2000). Cell cycle kinetics in corneal endothelium from old and young donors. Invest Ophthalmol. Vis. Sci. *41*, 660-667.

Senoo,T., Obara,Y., and Joyce,N.C. (2000). EDTA: a promoter of proliferation in human corneal endothelium. Invest Ophthalmol. Vis. Sci. *41*, 2930-2935.

Sherrard,E.S. (1976). The corneal endothelium in vivo: its response to mild trauma. Exp. Eye Res. *22*, 347-357.

Shimizu,S., Krafchak,C., Fuse,N., Epstein,M.P., Schteingart,M.T., Sugar,A., Eibschitz-Tsimhoni,M., Downs,C.A., Rozsa,F., Trager,E.H., Reed,D.M., Bohnke,M., Moroi,S., and Richards,J.E. (2004). A locus for posterior polymorphous corneal dystrophy (PPCD3) maps to chromosome 10. Am. J. Med. Genet. *130A*, 372-377.

Shuttleworth,C.A. (1997). Type VIII collagen. Int. J. Biochem. Cell Biol. *29*, 1145-1148.

Sibinga,N.E.S., Foster,L.C., Hsieh,C.M., Perrella,M.A., Lee,W.S., Endege,W.O., Sage,E.H., Lee,M.E., and Haber,E. (1997). Collagen VIII is expressed by

vascular smooth muscle cells in response to vascular injury. Circ Res *80*, 532-541.

Simon,A.M. and Goodenough,D.A. (1998). Diverse functions of vertebrate gap junctions. Trends Cell Biol. *8*, 477-483.

Simonsen,A.H., Sorensen,K.E., and Sperling,S. (1981). Thymidine incorporation by human corneal endothelium during organ culture. Acta Ophthalmol. (Copenh) *59*, 110-118.

Sobottka Ventura,A.C. and Böhnke,M. (2001). Pentoxifylline influences the autocrine function of organ cultured donor corneas and enhances endothelial cell survival. Br. J. Ophthalmol. *85*, 1110-1114.

Sobottka Ventura,A.C., Engelmann,K., Dahinden,C., and Bohnke,M. (1997). Endotoxins modulate the autocrine funciton of organ cultured donor corneas and increase the incidence of endothelial cell death. Br. J. Ophthalmol. *81*, 1093-1098.

Song,J., Lee,Y.G., Houston,J., Petroll,W.M., Chakravarti,S., Cavanagh,H.D., and Jester,J.V. (2003). Neonatal corneal stromal development in the normal and lumican-deficient mouse. Invest Ophthalmol. Vis. Sci. *44*, 548-557.

Sosnowski,R.G., Feldman,S., and Feramisco,J.R. (1993). Interference with endogenous ras function inhibits cellular response to wounding. J. Cell Biol. *121*, 113-119.

Stevenson,B.R., Siliciano,J.D., Mooseker,M.S., and Goodenough,D.A. (1986). Identification of ZO-1: a high molecular weight polypeptide associated with the tight junction (zonula occludens) in a variety of epithelia. J. Cell Biol. *103*, 755-766.

Stiemke,M.M., Edelhauser,H.F., and Geroski,D.H. (1991a). The developing corneal endothelium: correlation of morphology, hydration and Na/K ATPase pump site density. Curr. Eye Res. *10*, 145-156.

Stiemke,M.M., McCartney,M.D., Cantu-Crouch,D., and Edelhauser,H.F. (1991b). Maturation of the corneal endothelial tight junction. Invest Ophthalmol. Vis. Sci. *32*, 2757-2765.

Thuret,G., Chiquet,C., Bernal,F., Acquart,S., Romanet,J.P., Mouillon,M., Hegelhoffer,H., Burillon,C., Damour,O., Maugery,J., Armitage,W.J., and Gain,P. (2003a). Prospective, randomized clinical and endothelial evaluation of 2 storage times for cornea donor tissue in organ culture at 31 degrees C. Arch. Ophthalmol. *121*, 442-450.

Thuret,G., Chiquet,C., Herrag,S., Dumollard,J.M., Boudard,D., Bednarz,J., Campos,L., and Gain,P. (2003b). Mechanisms of staurosporine induced

apoptosis in a human corneal endothelial cell line. Br. J. Ophthalmol. *87*, 346-352.

Tuberville,A.W., McCartney,M.D., Boykins,L.G., and McLaughlin,B.J. (1989). A correlative electron microscopic and freeze-fracture examination of cat corneal endothelial wound repair. Curr. Eye Res. *8*, 365-377.

Tuft,S.J. and Coster,D.J. (1990). The corneal endothelium. Eye *4*, 389-424.

Usui,T., Takase,M., Kaji,Y., Suzuki,K., Ishida,K., Tsuru,T., Miyata,K., Kawabata,M., and Yamashita,H. (1998). Extracellular matrix production regulation by TGF-beta in corneal endothelial cells. Invest Ophthalmol. Vis. Sci. *39*, 1981-1989.

Van Itallie,C.M., Balda,M.S., and Anderson,J.M. (1995). Epidermal growth factor induces tyrosine phosphorylation and reorganization of the tight junction protein ZO-1 in A431 cells. J. Cell Sci. *108*, 1735-1742.

Waring,G.O., III, Bourne,W.M., Edelhauser,H.F., and Kenyon,K.R. (1982). The corneal endothelium. Normal and pathologic structure and function. Ophthalmology *89*, 531-590.

Watsky,M.A. (1995). Keratocyte gap junctional communcation in normal and wounded rabbit corneas and human corneas. Invest Ophthalmol. Vis. Sci. *36*, 2568-2576.

Weiss,E.E., Kroemker,M., Rudiger,A.H., Jockusch,B.M., and Rudiger,M. (1998). Vinculin is part of the cadherin-catenin junctional complex: complex formation between alpha-catenin and vinculin. J Cell Biol *41*, 755-764.

Whikehart,D.R., Vaughn,A.C., Holley,G.P., and Edelhauser,H.F. (2002). Telomerase activity in the human corneal endothelial limbus. Invest Ophthalmol. Vis. Sci. *ARVO abstract*, 1627.

Williams,E.J., Williams,G., Howell,F.V., Skaper,S.D., Walsh,F.S., and Doherty,P. (2001). Identification of an N-cadherin motif that can interact with the fibroblast growth factor receptor and is required for axonal growth. J. Biol. Chem. *276*, 43879-43886.

Williams,K. and Watsky,M. (2002). Gap junctional communication in the human corneal endothelium and epithelium. Curr. Eye Res *25*, 29-36.

Wilson,S.E., Li,Q., Weng,J., Barry-Lane,P.A., Jester,J.V., Liang,Q., and Wordinger,R.J. (1996). The Fas-Fas ligand system and other modulators of apoptosis in the cornea. Invest Ophthalmol. Vis. Sci. *37*, 1582-1592.

Wilson,S.E. and Lloyd,S.A. (1991). Epidermal growth factor and its receptor, basic fibroblast growth factor, transforming growth factor beta-1, and interleukin-1

alpha messenger RNA production in human corneal endothelial cells. Invest Ophthalmol. Vis. Sci. *32*, 2747-2756.

Wilson,S.E., Weng,J., Blair,S., He,Y.G., and Lloyd,S. (1995). Expression of E6/E7 or SV40 large T antigen-coding oncogenes in human corneal endothelial cells indicates regulated high-proliferative capacity. Invest Ophthalmol. Vis. Sci. *36*, 32-40.

Woost,P.G., Jumblatt,M.M., Eiferman,R.A., and Schultz,G.S. (1992). Growth factors and corneal endothelial cells: I. Stimulation of bovine corneal endothelial cell DNA synthesis by defined growth factors. Cornea *11*, 1-10.

Wrana,J.L., Attisano,L., Wieser,R., Ventura,F., and Massague,J. (1994). Mechanism of activation of the TGF-β receptor. Nature *370*, 341-347.

Xu,R., Yao,Z.-Y., Xin,L., Zhang,Q., Li,T.-P., and Gan,R.-B. (2001). NC1 domain of human type VIII collagen (α1) inhibits bovine aortic endothelial cell proliferaion and causes cell apoptosis. Biochem. Biophys. Res. Commun. *289*, 264-268.

Yamada,K.M. and Kemler,R. (2002). Cell-to-cell contact and extracellular matrix. Curr Opin Cell Biol *14*, 527-530.

Yamamoto,K., Ladage,P.M., Ren,D.H., Li,L., Petroll,W.M., Jester,J.V., and Cavanagh,H.D. (2001). Bcl-2 expression in the human cornea. Exp. Eye Res. *73*, 247-255.

Zieske,J.D., Francesconi,C.M., and Guo,X. (2004). Cell cycle regulators at the ocular surface. Exp. Eye Res. *78*, 447-456.

Zhu,C. and Joyce,N.C. (2004). Proliferative response of corneal endothelial cells from young and older donors. Invest Ophthalmol. Vis. Sci. *45*, 1743-1751.